Study of Discrete Biological Models with Nonstandard Finite Difference Method

Thesis submitted for the award of the degree of

Doctor of Philosophy

by

Priyanka Saha

Under the supervision of

Prof. Nandadulal Bairagi

Center for Mathematical Biology and Ecology
Department of Mathematics
Jadavpur University
Kolkata-700032, India

April 2024

Declaration

I, Priyanka Saha, solemnly declare that this thesis represents my own work which has been done after registration for the degree of Ph.D at Jadavpur University and has not been previously included in any thesis or dissertation for the purpose of earning a degree, diploma, or any other credential.

Priyanka Saha

DEPARTMENT OF MATHEMATICS
FACULTY OF SCIENCE
JADAVPUR UNIVERSITY
Kolkata – 700032, India
Telephone: 91 (33) 2414 6717

Dr. Nandadulal Bairagi
Professor and Coordinator
CENTRE FOR MATHEMATICAL BIOLOGY AND ECOLOGY
Mail: nbairagi.math@jadavpuruniversity.in

Date: 09/04/2024

CERTIFICATE FROM THE SUPERVISOR

This is to certify that the thesis entitled "**Study of Discrete Biological Models with Nonstandard Finite Difference Method**" submitted by **Miss Priyanka Saha**, who got her name registered **(Index No.: 163/18/Maths./26)** on 12/09/18 for the award of Ph.D. (Science) degree of Jadavpur University, is based upon her work under the supervision of myself and that neither this thesis nor any part of it has been submitted for either any degree/diploma or any other academic award anywhere before.

09/04/24

Nandadulal Bairagi

Nandadulal Bairagi (Ph. D.)
Professor, Dept. of Mathematics
Jadavpur University
Kolkata-700032

This thesis is dedicated to

all my family members

for their unlimited love, support and encouragement.

Acknowledgement

Hereby, I would like to take this opportunity to express my heartfelt thanks and gratitude to my supervisor, **Prof. Nandadulal Bairagi**, Department of Mathematics, Jadavpur University, Kolkata, for his guidance, motivation and perennial support throughout my Ph.D tenure. Also it wouldn't have been possible for me to complete this thesis without him spending time on discussing and reviewing complex aspects of my Ph.D work.

My sincere gratitude also goes out to the Center for Mathematical Biology and Ecology, Department of Mathematics, Jadavpur University, Bio-Mathematical Society of India, and all my respected teachers at the Department of Mathematics, Jadavpur University, Kolkata.

I am grateful to the Council of Scientific and Industrial Research (CSIR), Govt. of India for supporting me financially through a Research Fellowship.

I also thank Dr. Suman Saha, Dr. Santu Ghorai, Dr. Shuvojit Mondal, Dr. Bhaskar Chakraborty, Dr. Abhijit Majumder and Dr. Chittaranjan Mondal for their kind help.

Further I would like to thank my fellow researchers Dr. Santanu Bhattacharya, Mr. Sounov Marick, Mr. Chirodeep Mondal, Mr. Ayanava Basak, and Mr. Debjit Pal who have been a constant source of encouragement and help.

Finally, I must express my very profound gratitude to my entire family for providing me unfailing support and continuous encouragement throughout my years of study.

Contents

1 Introduction **1**

1.1 Nonstandard finite difference scheme 1

1.2 Some definitions 5

1.3 Linear stability criteria for first-order two-dimensional discrete system 7

1.4 Stability criteria for first-order higher-dimensional discrete system 9

1.5 Stability of difference scheme by the Fourier series method or Von Neumann stability analysis 11

1.6 A brief review of NSFD scheme 12

1.7 Objectives of the Thesis 13

1.8 Thesis overview 14

2 On the dynamics of a discrete predator-prey model **17**

2.1 Introduction 17

2.2 Properties of the continuous-time model 18

2.3 Nonstandard finite difference (NSFD) model 19

2.3.1 Existence of fixed points 20

2.3.2 Stability analysis of fixed points 20

2.4 The Euler forward method 22

2.4.1 Existence and stability of fixed points 22

2.5 Numerical simulations 23

2.6 Summary 26

3 Dynamics of vertically and horizontally transmitted parasites: Continuous vs discrete models 27

3.1 Introduction 27

3.2 Analysis of continuous-time models 28

3.2.1 Model with horizontal and imperfect vertical transmission 29

3.2.2 Model with horizontal and perfect vertical transmissions 31

3.2.3 Model with perfect vertical transmission and no horizontal transmission 31

3.3 Discrete Models 32

3.3.1 Discrete model for horizontal and imperfect vertical transmission . . . 32

3.3.2 Discrete model for horizontal and perfect vertical transmissions 35

3.3.3 Discrete model for perfect vertical and no horizontal transmission . . . 36

3.4 Numerical simulations 37

3.5 Summary 40

4 Positivity and dynamics preserving discretization schemes for nonlinear evolution equations 41

4.1 Introduction 41

4.2 Nonlocal discretization techniques 43

4.3 Example 1: Continuous-time epidemic model 44

4.3.1 NSFD model and its analysis 45

4.3.2 Numerical experiments 47

4.4 Example 2: Continuous-time epidemic model 48

4.4.1 Stability results of the continuous-time epidemic model 49

4.4.2 Construction of NSFD model and its analysis 49

4.4.3 Euler discrete-time epidemic model 53

4.4.4 Numerical experiments 53

4.5 Example 3: Continuous-time ecological model 54

4.5.1 NSFD model and its analysis 55

4.5.2 Numerical experiments 59
4.6 Summary 60

5 Nonstandard finite difference scheme for diffusion-induced ratio-dependent predator-prey model 61
5.1 Introduction 61
5.2 Properties of the predator-prey continuous system 63
5.3 NSFD model construction 63
5.3.1 Accuracy 64
5.3.2 Consistency 65
5.3.3 Positivity 66
5.3.4 Stability of the proposed NSFD scheme 67
5.4 Numerical analysis 68
5.5 Summary 71

6 Positivity preserving nonstandard finite difference scheme for an in-host HIV reaction-diffusion model 73
6.1 Introduction 73
6.2 Properties of the continuous system 75
6.3 NSFD model construction 75
6.3.1 Accuracy 76
6.3.2 Consistency 77
6.3.3 Positivity 79
6.3.4 Stability of the suggested NSFD scheme 79
6.4 Numerical analysis 80
6.5 Summary 84

7 Discussions and future work 87

Bibliography 89

List of Publications 97

1

Introduction

1.1 Nonstandard finite difference scheme

In order to understand the fundamental dynamics of physical, chemical, and biological events, nonlinear systems of ordinary differential equations are widely employed. Finding the system's analytical solution in a compact form becomes unfeasible in most circumstances. This necessitates a numerical solution, which requires discretization of the continuous-time model. For numerical solutions of both ordinary and partial differential equations, standard finite difference schemes, such the Euler method, Runge-Kutta method, etc., are the frequently used discretization approaches [1, 2, 3]. Nevertheless, these popular discretization techniques have a number of serious shortcomings. First, typical finite difference schemes display step-size dependent instability because their behaviors are tightly reliant on the step-size [4]. For example, the simple logistic equation in the continuous system and its corresponding Euler discrete equation are represented, respectively, by

$$\dot{x} = x(1-x), \;\; x(0) = x_0 > 0, \tag{1.1}$$

$$x_{t+1} = x_t + hx_t(1-x_t), \;\; x_0 > 0, \tag{1.2}$$

where $h > 0$ is the step-size. It is easy to show that the nontrivial fixed point $x = 1$ of the continuous system (1.1) is always stable. However, for the discrete system (1.2), stability holds for $h < 2$ only and unstable if $h > 2$. The bifurcation diagram (Figure 1.1) of the system (1.2) with step-size h as the bifurcation parameter shows period-doubling bifurcation, leading to chaos [5]. Thus, the dynamics of the Euler discrete model (1.2) depend on the step-size and exhibits spurious behaviours which are not observed in the corresponding continuous system (1.1).

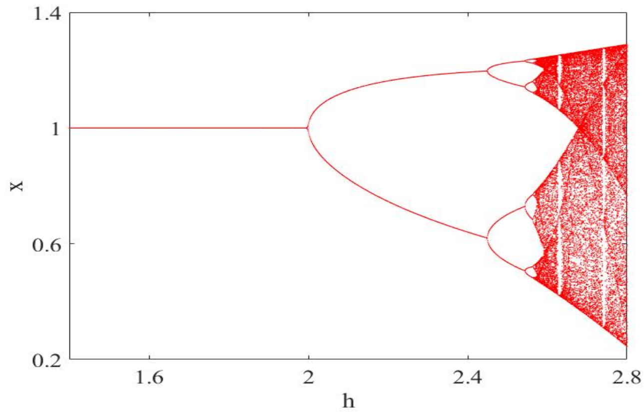

Figure 1.1: Bifurcation diagram of the discrete model (1.2) with respect to the step-size (h). The fixed point $x = 1$ is stable for $h < 2$ and unstable for $h > 2$. Chaos exists through period-doubling bifurcation for higher values of h, indicating a strong dependency on the step-size.

Secondly, the positivity of the solutions of the corresponding Euler discrete system of a continuous system may not be preserved for all step-size. For example, consider the continuous system

$$\dot{x} = -x, \;\; x(0) = x_0 > 0. \tag{1.3}$$

The solution of this equation $x(t) = x_0 e^{-t}$ is always positive and monotonically converges to zero. However, the solution $x_t = (1-h)^t x_0$ of the corresponding Euler discrete system

$$x_{t+1} = (1-h)x_t, \, h > 0, \, h \neq 1, \tag{1.4}$$

is not always positive but may be negative also depending on the step-size. In fact, the solution remains positive for $0 < h < 1$, $\forall t \geq 0$ and becomes alternatively positive and negative for $h > 1$ and $t \geq 0$ (see Figure 1.2). In the latter case, all solutions having positive initial value converge to the fixed point $x = 0$ for any positive step-size $h < 2$. More precisely, solutions show oscillatory (taking positive and negative values in consecutive iterations) convergence for $1 < h < 2$ and oscillatory divergence for $h > 2$. Thus, huge differences exist in the dynamic behaviour between a continuous system and its corresponding discrete system. Any discrete system that permits negative solutions is supposed to show spurious dynamics, like bifurcation and chaos [2, 6, 7].

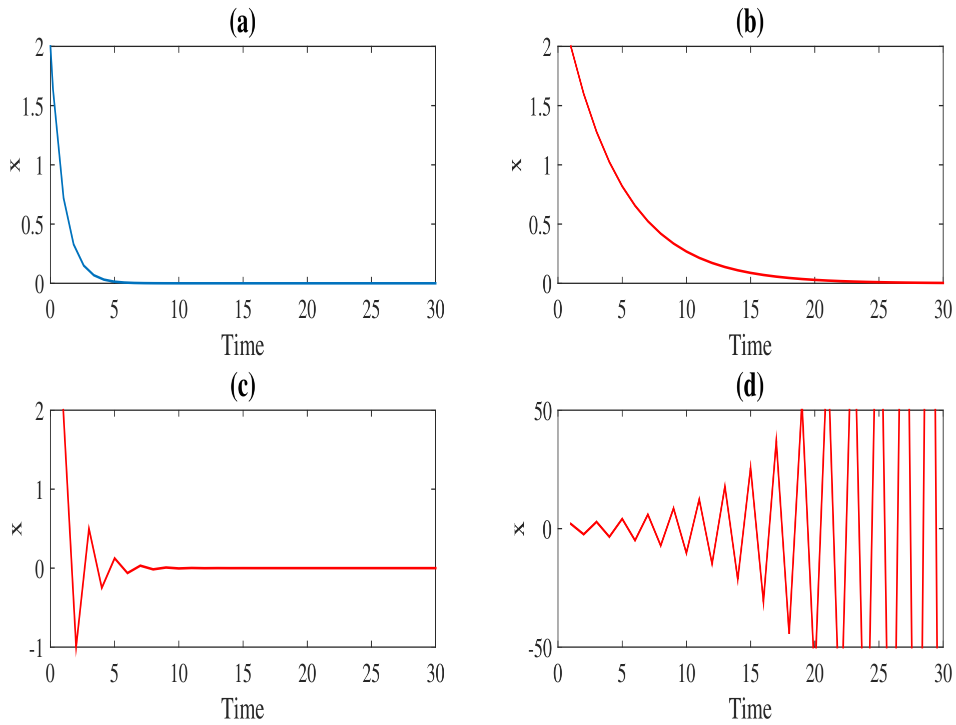

Figure 1.2: (**a**) Solution of the continuous model (1.3) converges exponentially to zero. Similar solutions of the Euler discrete system (1.4) are presented in Figure 1.2b-Figure 1.2d for different values of step-size. It shows: (**b**) monotonic convergence for $h = 0.2$, (**c**) oscillatory convergence for $h = 1.5$ and (**d**) oscillatory divergence for $h = 2.2$.

Thirdly, in case of partial differential equations, the absolute value of the error of the solutions of the Euler discrete system with the solutions of its corresponding continuous system may increase for some value of step-sizes Δt and Δx. By the absolute value of the error we mean the modulus value of the difference between the solutions of the continuous system and the solutions of the corresponding Euler discrete system [8]. As an example, we use the dimensionless version of Stokes' first problem, which is given by

$$\frac{\partial u}{\partial t} = \frac{\partial^2 u}{\partial x^2}, \tag{1.5}$$

with initial condition $u(x,0) = 0$ and boundary conditions $u(0,t) = 1$ and $u(x,t) \to 0$ as $x \to \infty$. The corresponding Euler discrete system, obtained by applying the Euler forward difference scheme and the second-order central difference technique, is

$$u_i^{n+1} = u_i^n + h(u_{i+1}^n - 2u_i^n + u_{i-1}^n), \tag{1.6}$$

where $h = \frac{\Delta t}{(\Delta x)^2}$. For $0 < h \leq \frac{1}{2}$, the discrete system (1.6) will be positive and also Von Neumann stable (see Section 1.5 of Chapter 1).

We provide the absolute value of the error of the solutions of (1.6) with the solutions of (1.5) in Figure 1.3 to illustrate accuracy (see Definition 1.9) of the Euler difference scheme. The number of time grid points and the number of space grid points were set to $n_t = 100$ and $n_x = 40$, respectively, with the end time being $t_f = 1$.

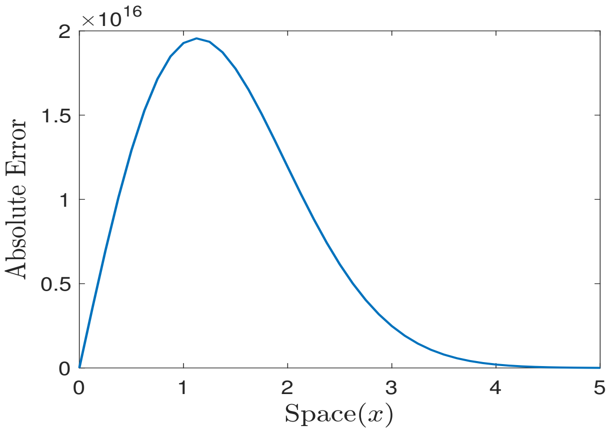

Figure 1.3: Absolute error of the corresponding Euler discrete system (1.6) for $t_f = 1$ with $\Delta t = 0.01$ and $\Delta x = 0.125$.

These examples demonstrate that the discrete systems constructed by standard finite difference scheme is unable to preserve some properties of its corresponding continuous systems. Dynamic behaviors of the discrete model depend strongly on the step-size. However, on principles, the corresponding discrete system should have same properties to that of the original continuous system. It is therefore of immense importance to construct discrete model which will preserve the properties of its constituent continuous models. In the recent past, a considerable effort has been given in the construction of discrete-time model to preserve dynamic consistency of the corresponding continuous-time model without any limitation on the step-size. Also it becomes necessary to build a discrete scheme for system of PDEs in order to ensure that the recommended discrete system is accurate in both time and space and maintains solution consistency as well as Von Neumann stable. Mickens first proved that corresponding to any ODE, there exists an exact difference equation which has zero local truncation error [4, 9] and proposed a non-standard finite difference scheme (NSFD) in 1989 [10]. Later in 1994, he introduced the concept of elementary stability, the property which brings correspondence between the local stability at equilibria of the differential equation and the numerical method [5]. Anguelov and Lubuma [11] formalized some of the foundations of Micken's rules, including convergence properties of non-standard finite difference schemes. They defined qualitative stability, which means that the constructed discrete system satisfies some properties like positivity of solutions, conservation laws and equilibria for any step-size. In 2005, Micken coined the term dynamic consistency, which means that a numerical method is qualitatively stable with respect to all desired properties of the solutions to the differential equation [12]. NSFD scheme has gained lot of attentions in the last few years because it generally does not show spurious behavior as compared to other standard finite difference methods. NSFD scheme has been successfully used in different fields like economics [13], physiology [14], epidemic [15, 16, 17, 18, 19], ecology [20, 21, 22, 23, 24] and physics [25, 26, 27, 28].

1.2 Some definitions

Consider the differential equation

$$\frac{dx}{dt} = f(x,t,\gamma), \tag{1.7}$$

where γ represents the parameter defining the system (1.7). Assume that a finite difference scheme corresponding to the continuous system (1.7) is described by

$$x_{m+1} = F(x_m, t_m, h, \gamma). \tag{1.8}$$

We assume that $F(.,.,.,.)$ is such that the proper uniqueness and existence properties hold; the step-size is $h = \Delta t$ with $t_m = hm$, $m =$ integer; and x_m is an approximation to $x(t_m)$.

Definition 1.1. *[12] Let the differential equation* (1.7) *and/or its solutions have a property Q. The discrete model* (1.8) *is said to be dynamically consistent with the equation* (1.7) *if it and/or its solutions also have the property Q.*

Definition 1.2. *[12, 29, 30] The NSFD procedures are based on just two fundamental rules:*

(i) the discrete first-derivative has the representation

$$\frac{dx}{dt} \rightarrow \frac{x_{m+1} - \psi(h)x_m}{\phi(h)}, \quad h = \triangle t,$$

where $\psi(h)$, $\phi(h)$ satisfy the conditions $\psi(h) = 1 + O(h^2)$, $\phi(h) = h + O(h^2)$;

(ii) both linear and nonlinear terms may require a nonlocal representation on the discrete computational lattice. For example,

$$x \rightarrow 2x_m - x_{m+1}, \qquad x^2 \rightarrow \left(\tfrac{x_{m+1}+x_m+x_{m-1}}{3}\right)x_m,$$
$$x^3 \rightarrow 2x_m^3 - x_m^2 x_{m+1}, \qquad x^3 \rightarrow \left(\tfrac{x_{m+1}+x_{m-1}}{2}\right)x_m^2.$$

While no general principles currently exist for selecting the functions $\psi(h)$ and $\phi(h)$, particular forms for a specific equation can easily be determined. Functional forms commonly used for $\psi(h)$ and $\phi(h)$ are

$$\psi(h) = cos(\lambda h), \ \phi(h) = \frac{1-e^{-\lambda h}}{\lambda},$$

where λ is some parameter appearing in the differential equation.

Definition 1.3. *[31] The finite difference method* (1.8) *is called positive if for any value of the step-size h, solution of the discrete system remains positive for all positive initial values.*

Definition 1.4. *[31] The finite difference method* (1.8) *is called elementary stable if for any value of the step-size h, the fixed points of the difference equation are those of the differential system and the linear stability properties of each fixed point being the same for both the differential system and the discrete system.*

Definition 1.5. *[31] A method that follows the Mickens rules (given in the Definition 1.2) and preserves the positivity of the solutions is called positive and elementary stable nonstandard (PESN) method.*

Definition 1.6. *[32] A fixed point X^* of a map $f:\mathbb{R}^2\to\mathbb{R}^2$ is said to be*

(a) stable if given $\varepsilon>0$ there exists $\delta>0$ such $|X-X^*|<\delta$ implies $|f^n(X)-X^*|<\varepsilon$ for all $n\in\mathbb{Z}^+$.

(b) attracting (sink) if there exists $N>0$ such that $|X-X^*|<N$ implies $\lim_{n\to\infty} f^n(X)=X^*$. It is globally attracting if $N\to\infty$.

(c) asymptotically stable if it is both stable and attracting and it is globally asymptotically stable if it is both stable and globally attracting.

(d) unstable if it is not stable.

Definition 1.7. *[33] A one-step finite difference approximating a partial differential equation is a convergent scheme if for any solution of the partial differential equation, $w(t,x)$, and solutions to the finite difference scheme, u_n^m, such that u_n^0 converges to $w_0(x)$ as nh converges to x, then u_n^m converges to $w(t,x)$ as (mk,nh) converges to (t,x) as k, h converges to zero.*

Definition 1.8. *[33] Given a partial differential equation, $Pw=f$, and a finite difference scheme, $P_{k,h}u=f$, we say that the finite difference scheme is consistent with the partial differential equation if for any smooth function $\phi(t,x)$*

$$P\phi - P_{k,h}\phi \to 0 \text{ as } k,h\to 0,$$

the convergence being pointwise convergence at each point (t,x).

Definition 1.9. *[33] A scheme $P_{k,h}u=R_{k,h}f$ that is consistent with the differential equation $Pw=f$ is accurate of order p in time and order r in space if for any smooth function $\psi(t,x)$,*

$$P_{k,h}\psi - R_{k,h}P\psi = O(k^p)+O(h^r).$$

Such a scheme is called accurate of order (p,r).

Definition 1.10. *[33] A finite difference scheme $P_{k,h}u^n = 0$ for a first-order equation is stable in a stability region Δ if there is an integer M such that for any positive time T, there is a constant A_T such that*

$$h\sum_{n=-\infty}^{\infty}|u_n^m|^2 \leq A_T h\sum_{q=0}^{M}\sum_{n=-\infty}^{\infty}|u_n^q|^2$$

for $0 \leq mk \leq T$, with $(k,h) \in \Delta$.

Definition 1.11. *[34] Let M be a $p \times p$ matrix and $M = (m_{ij})$, where $m_{ij} \leq 0$ for all $i \neq j$, $1 \leq i, j \leq p$. If M can be expressed as $M = cI - N$, where I is $p \times p$ identity matrix and $N = (n_{ij})_{p\times p}$ with $n_{ij} \geq 0$, for all $1 \leq i, j \leq p$ and $c \geq \rho(N)$, where $\rho(N)$ is the spectral radius of N, i.e., maximum of the modulus value of the eigenvalues of N, then the matrix M is called a M-matrix. Also M is inverse-positive, i.e., M^{-1} exists and each entry of M is nonnegative.*

1.3 Linear stability criteria for first-order two-dimensional discrete system

We consider the following system of two-dimensional first-order difference equations:

$$\begin{aligned} x_{m+1} &= f(x_m, y_m), \\ y_{m+1} &= g(x_m, y_m), \end{aligned} \tag{1.9}$$

where f and g both are nonlinear functions and have continuous second-order partial derivatives in an open set that contains the equilibrium $(\bar{x},\bar{y})$.

For the stability of the equilibrium point $(\bar{x},\bar{y})$, linearize the system (1.9) about the equilibrium point $(\bar{x},\bar{y})$. To do this, we expand the function f at an arbitrary point (x,y) about the equilibrium point $(\bar{x},\bar{y})$ by using Taylor series expansion, giving

$$f(x,y) = f(\bar{x},\bar{y}) - \frac{\partial f(\bar{x},\bar{y})}{\partial x}(x-\bar{x}) + \frac{\partial f(\bar{x},\bar{y})}{\partial y}(y-\bar{y}) + \frac{\partial^2 f(\bar{x},\bar{y})}{\partial x^2}\frac{(x-\bar{x})^2}{2!} + \frac{\partial^2 f(\bar{x},\bar{y})}{\partial xy}\frac{(x-\bar{x})(y-\bar{y})}{2!} + \frac{\partial^2 f(\bar{x},\bar{y})}{\partial y^2}\frac{(y-\bar{y})^2}{2!} + \dots,$$

where $\frac{\partial f(\bar{x},\bar{y})}{\partial x} = \left.\frac{\partial f(x,y)}{\partial x}\right|_{(x,y)=(\bar{x},\bar{y})}$.

Neglecting second and higher order terms, we get

$$f(x,y) = f(\bar{x},\bar{y}) - \frac{\partial f(\bar{x},\bar{y})}{\partial x}(x-\bar{x}) + \frac{\partial f(\bar{x},\bar{y})}{\partial y}(y-\bar{y}).$$

Similarly, for the function $g(x,y)$, we get

$$g(x,y) = g(\bar{x},\bar{y}) - \frac{\partial g(\bar{x},\bar{y})}{\partial x}(x-\bar{x}) + \frac{\partial g(\bar{x},\bar{y})}{\partial y}(y-\bar{y}).$$

Now, if perturbations $u_m = x_m - \bar{x}$ and $v_m = y_m - \bar{y}$ are given to the system (1.9), then the first equation of the system (1.9) gives

$$\begin{aligned} u_{m+1} + \bar{x} &= f(\bar{x},\bar{y}) + \frac{\partial f(\bar{x},\bar{y})}{\partial x}u_m + \frac{\partial f(\bar{x},\bar{y})}{\partial y}v_m \\ &= \bar{x} + \frac{\partial f(\bar{x},\bar{y})}{\partial x}u_m + \frac{\partial f(\bar{x},\bar{y})}{\partial y}v_m \end{aligned}$$

and thus we have

$$u_{m+1} = \frac{\partial f(\bar{x},\bar{y})}{\partial x}u_m + \frac{\partial f(\bar{x},\bar{y})}{\partial y}v_m. \tag{1.10}$$

Similarly, second equation of the system (1.9) gives

$$v_{m+1} = \frac{\partial g(\bar{x},\bar{y})}{\partial x}u_m + \frac{\partial g(\bar{x},\bar{y})}{\partial y}v_m. \tag{1.11}$$

The equations (1.10) and (1.11) can be written in the matrix form as

$$X_{m+1} = J(\bar{x},\bar{y})X_m,$$

where $X_m = (u_m, v_m)^T$ and J represents the Jacobian matrix of $(f,g)^T$ evaluated at the fixed point $(\bar{x},\bar{y})$, which is given by

$$J(\bar{x},\bar{y}) = \begin{pmatrix} \frac{\partial f(\bar{x},\bar{y})}{\partial x} & \frac{\partial f(\bar{x},\bar{y})}{\partial y} \\ \frac{\partial g(\bar{x},\bar{y})}{\partial x} & \frac{\partial g(\bar{x},\bar{y})}{\partial y} \end{pmatrix}. \tag{1.12}$$

It is known that $\lim_{n\to\infty} J^n = \mathbf{0}$ if and only if the spectral radius $\rho(J) < 1$, so that the eigenvalues of J satisfies $|\lambda_i| < 1$, $i = 1,2$, where $\rho(J) = \max\{|\lambda_1|, |\lambda_2|\}$ [32, 35].
The eigenvalues of the Jacobian matrix $J(\bar{x},\bar{y})$ will determine the local stability of the discrete system (1.9) around the equilibrium point $(\bar{x},\bar{y})$. Regarding the characterization of an equilibrium point of a two-dimensional discrete system, we have the following theorem.

Theorem 1.12. *[32] Consider the map $f : \mathbb{R}^2 \to \mathbb{R}^2$ and let $\bar{X} = (\bar{x},\bar{y})^T$ be a fixed point of f, i.e., $f(\bar{X}) = \bar{X}$. Let λ_1 and λ_2 be the eigenvalues of the variational matrix*

$$J(x,y) = \begin{pmatrix} a_{11} & a_{12} \\ a_{21} & a_{22} \end{pmatrix}$$

evaluated at the fixed point $\bar{X}$. The fixed point $\bar{X}$ of the map f is stable if $|\lambda_1| < 1$, $|\lambda_2| < 1$ and a source if $|\lambda_1| > 1$, $|\lambda_2| > 1$. It is a saddle if $|\lambda_1| < 1$, $|\lambda_2| > 1$ or $|\lambda_1| > 1$, $|\lambda_2| < 1$ and a non-hyperbolic fixed point if either $|\lambda_1| = 1$ or $|\lambda_2| = 1$. It is a spiral sink if $\lambda_{1,2} = \alpha \pm i\beta$, $\beta \neq 0$, $\alpha, \beta \in \mathbb{R}$ and $|\lambda_{1,2}| < 1$ and a spiral source if $|\lambda_{1,2}| > 1$.

Theorem 1.13. *[32, 35] Assume the functions $f(x,y)$ and $g(x,y)$ have continuous first-order partial derivatives in x and y on some open set in $\mathbb{R}^2$ that contains the equilibrium point $(\bar{x},\bar{y})$. Then the equilibrium point $(\bar{x},\bar{y})$ of the nonlinear system*

$$x_{m+1} = f(x_m, y_m),$$
$$y_{m+1} = g(x_m, y_m),$$

is locally asymptotically stable if the eigenvalues of the Jacobian matrix J evaluated at the equilibrium satisfy $|\lambda_i| < 1$ if and only if

$$|Tr(J)| < 1 + \det(J) < 2.$$

The equilibrium is unstable if some $|\lambda_i| > 1$, that is, if any one of the following three inequalities is satisfied:

$$Tr(J) > 1 + \det(J),\ Tr(J) < -1 - \det(J),\ or\ \det(J) > 1.$$

Lemma 1.14. *[20, 32, 35] Let λ_1 and λ_2 be the eigenvalues of the jacobian matrix*

$$J(x,y) = \begin{pmatrix} a_{11} & a_{12} \\ a_{21} & a_{22} \end{pmatrix}$$

evaluated at the equilibrium point. Then $|\lambda_1| < 1$ and $|\lambda_2| < 1$ if and only if

$$(i)\ 1 - \det(J) > 0,\ (ii)\ 1 - Tr(J) + \det(J) > 0\ and\ (iii)\ 1 + Tr(J) + \det(J) > 0.$$

1.4 Stability criteria for first-order higher-dimensional discrete system

Consider a first-order system consisting of n equations, $X(t) = (x_1(t), x_2(t), \ldots, x_n(t))^T$,

$$X(t+1) = F(X(t)), \tag{1.13}$$

where $F = (f_1, f_2, \ldots, f_n)^T$ and $f_i = f_i(x_1, x_2, \ldots, x_n)$, $i = 1, 2, \ldots, n$. Suppose system (1.13) has an equilibrium point at $\bar{X}$. Then if $U_t = X_t - \bar{X}$, linearization of system (1.13) about $\bar{X}$ leads to the system

$$U_{t+1} = JU_t,$$

where J is the Jacobian matrix evaluated at $\bar{X}$,

$$J = \begin{pmatrix} \frac{\partial f_1(\bar{X})}{\partial x_1} & \frac{\partial f_1(\bar{X})}{\partial x_2} & \dots & \frac{\partial f_1(\bar{X})}{\partial x_n} \\ \frac{\partial f_2(\bar{X})}{\partial x_1} & \frac{\partial f_2(\bar{X})}{\partial x_2} & \dots & \frac{\partial f_2(\bar{X})}{\partial x_n} \\ \vdots & \vdots & \dots & \vdots \\ \frac{\partial f_n(\bar{X})}{\partial x_1} & \frac{\partial f_n(\bar{X})}{\partial x_2} & \dots & \frac{\partial f_n(\bar{X})}{\partial x_n} \end{pmatrix}.$$

Local asymptotic stability of $\bar{X}$ depends on the eigenvalues of the Jacobian matrix, which in turn depend on the existence of the partial derivatives in a region containing $\bar{X}$. Therefore, for local asymptotic stability of $\bar{X}$, we require that the partial derivatives of f_i be continuous in an open set containing $\bar{X}$.
The eigenvalues of the Jacobian matrix are the solutions of the characteristic equation

$$\det(J - \lambda I) = 0.$$

The eigenvalues are the zeros of the following nth-degree polynomial:

$$p(\lambda) = \lambda^n + a_1\lambda^{n-1} + a_2\lambda^{n-2} + \cdots + a_n. \tag{1.14}$$

The coefficients in (1.14) are real because f_i are the real valued functions.

Theorem 1.15. *[35] If the solutions λ_i, $i = 1,2,\dots,n$, of (1.11), $p(\lambda) = 0$, satisfy $|\lambda_i| < 1$, then*

(a) $p(1) = 1 + a_1 + a_2 + \cdots + a_n > 0$,

(b) $(-1)^n p(-1) = 1 - a_1 + a_2 - \cdots + (-1)^n a_n > O$ *(alternate in sign),*

(c) $|a_n| < 1$.

Lemma 1.16. *[35, 20]* ***(Jury conditions, Schur-Cohn criteria, n = 3)*** *Suppose the characteristic polynomial $p(\lambda)$ is given by*

$$p(\lambda) = \lambda^3 + a_1\lambda^2 + a_2\lambda + a_3.$$

The solutions λ_i, $i = 1,2,3$, of $p(\lambda) = 0$ satisfy $|\lambda_i| < 1$ if and only if the following three conditions hold:

(a) $p(1) = 1 + a_1 + a_2 + a_3 > 0$,

(b) $(-1)^3 p(-1) = 1 - a_1 + a_2 - a_3 > 0$,

(c) $1 - (a_3)^2 > |a_2 - a_3 a_1|$.

1.5 Stability of difference scheme by the Fourier series method or Von Neumann stability analysis

A finite difference scheme is stable if the errors made during one computing time step do not result in more errors as the calculations proceed. A difference scheme is said to be neutrally stable if errors in that scheme stay constant as the computations go. A difference scheme is deemed to be stable if the inaccuracies gradually diminish and become less. Conversely, if the errors increase with time, the numerical system is considered unstable [36]. The Von Neumann stability analysis is based on the decomposition of numerical error into Fourier series [37, 38]. We are concerned about the stability of a linear difference equation in $w(x,t)$ in the time interval $0 \leq t \leq t_f$, where $t_f = M\Delta t$ is finite, as $\Delta x \to 0$ and $\Delta t \to 0$, i.e., $M \to \infty$. In terms of the exponential form, the Fourier series expansion of $w(x,t)$ can be expressed as $\sum A_m e^{\frac{im\pi x}{l}}$, where $i = \sqrt{-1}$ and l represents the x-interval that the function is defined throughout. We can write the function $w(x,t)$ as $w(p\Delta x, \Delta t) = w_{p,q}$ and in terms of this notation,

$$A_m e^{\frac{im\pi x}{l}} = A_m e^{\frac{im\pi p\Delta x}{N\Delta x}} = A_m e^{i\beta_m p\Delta x},$$

where $\beta_m = \frac{m\pi}{N\Delta x}$ and $N\Delta x = l$.
At $t = 0$, the initial values at the pivotal points are denoted by $w(p\Delta x, 0) = w_{p,0}$, $p = 0, 1, 2, \ldots, N$. Then the following $(N+1)$ equations

$$w_{p,0} = \sum_{m=0}^{N} A_m e^{i\beta_m p\Delta x}, \ p = 0, 1, 2, \ldots, N,$$

are sufficient to determine the $(N+1)$ unknowns $A_0, A_1, \ldots, A_N$ uniquely, showing that the initial mesh values can be expressed in this complex exponential form. As only linear-difference equations are considered, we need to investigate the propagation of only one initial value, such as $e^{i\beta p\Delta x}$, because separate solutions are additive. The coefficients A_m, $m = 0, 1, 2, \ldots, N$ are constants and can be neglected.
To investigate the propagation of this term as t increases, substitute

$$w_{p,q} = e^{i\beta x} e^{\alpha t} = e^{i\beta p\Delta x} e^{\alpha q\Delta t} = e^{i\beta p\Delta x} \xi^q,$$

where $\eta = e^{\alpha\Delta t}$ and in general α is a complex constant. The term η is known as the amplification factor.
By the Lax-Richtmyer definition [39, 40, 41], the finite-difference equations will be stable if for all $q \leq M$, $|w_{p,q}|$ remains bounded as $\Delta x \to 0$ and $\Delta t \to 0$ and the initial conditions will be satisfied for all vales of β.
If the exact solution of the difference equations does not increase exponentially with time, then a necessary and sufficient condition for stability is that $|\eta| \leq 1$, i.e., $-1 \leq \eta \leq 1$.

If, however, $w_{p,q}$ increases with time t, then the necessary and sufficient condition for stability is $|\eta| \leq 1 + D\Delta t = 1 + O(\Delta t)$, where the positive number D is independent of Δx, Δt and β [37].

1.6 A brief review of NSFD scheme

In domains as diverse as ecology, physiology, epidemics, economics, physics, chemistry, and engineering, Non-Standard Finite Deference (NSFD) techniques have proven effective. Mickens [42] shows how to apply an NSFD scheme to a structured unstable planner dynamical system in order to get numerical solutions that behave correctly. He demonstrated that the discrete system suggested by NSFD method is dynamically consistent by taking into account the well-known Lotka-Volterra predarator-prey system. Gumel et al. [43] investigated a kind of finite difference method created by NSFD scheme for solving systems of differential equations that arise in population biology. A continuous time SI epidemic model was taken into consideration, and its results were compared with those of the corresponding Euler discrete system, second order Runge-Kutta discrete system, and NSFD discrete system. It is demonstrated that, in contrast to other approaches, the NSFD discrete system maintains all of the dynamic aspects of the continuous model. Additionally, they examined an HIV model and demonstrated how all of the dynamic features present in the continuous system are preserved in the matching NSFD discrete system. Anguelov et al. [44] discretized an HIV-induced MSEIR system using the NSFD scheme, and they demonstrated that the discrete system adheres to the continuous model's dynamic consistency. This includes the dissipation of the system, its inherent conservation law, the positivity of the solution, the global asymptotic stability of the disease-free equilibrium, and the linear stability of the endemic equilibrium.

Anguelov et al. [45] presented the notion of topological dynamic consistency in their work. It is precisely defined as the topological equivalency of maps. By doing this, it is guaranteed that all topological characteristics will be retained, including solutions, invariant sets, fixed points their stabilities, etc. They showed how to construct the topological dynamic consistency utilizing the NSFD scheme using the examples of the logistic equation and combustion equation. In 2011, Anguelov et al. [46] demonstrated that the NSFD scheme is topologically dynamically consistent for one-dimensional dynamical systems. They also provided numerical simulations in support of this conclusion. In addition, they presented a two-dimensional epidemiological system discretized by the NSFD scheme, and demonstrated numerical simulations for topological dynamic consistency of the discrete system.

Cole [47] has developed algorithms for computational electromagnetics using the NSFD scheme and provided several examples to demonstrate the method. It is shown that the standard finite difference scheme is not as good as the NSFD scheme. Verma and Kayenat [48] employed the NSFD technique on the Lane Emden equations in their work. They graphically contrasted the discrete system solutions, as well as the errors, produced by the NSFD and FD schemes. It was demonstrated that near singular point that the NSFD approximate solution is efficient, where FD is not that much efficient, and that the qualitative behaviour of the NSFD discrete system is the same as that of the original one.

Mickens [42] investigated a nonlinear diffusion system for Fisher partial differential equations. The two-dimensional parabolic system, with temperature-dependent thermal characteristics in a double-layered metal thin film exposed to picosecond thermal pulses, has also been successfully solved using the NSFD approach [49]. It is demonstrated that this approach meets an energy estimate discrete analogous. In order to solve a one-dimensional advection-diffusion equation, Appadu [50] took into consideration the Lax-Wendroff scheme, Crank-Nicolson scheme, and an NSFD scheme. His comparative study demonstrated that the NSFD scheme and Lax-Wendroff are both very effective approaches than the other. Tadmon and Foko [51] discretized a mathematical model of hepatitis B virus (HBV) infection using the NSFD scheme. The suggested NSFD scheme is demonstrated to be unconditionally positive and shown global asymptotic stability of the HBV-free equilibrium. They show that there are benefits to the suggested NSFD method over the conventional finite difference method.

1.7 Objectives of the Thesis

Nonstandard finite difference scheme plays a major role in discretizing continuous systems to know their exact dynamics numerically. However, for systems of ODEs, there are no universal rules that how to discretize a continuous system using an NSFD scheme and how to choose the denominator functions, and for systems of PDEs this scheme is not much developed till now. This thesis aims to comprehensively explore the NSFD scheme for continuous systems of ODEs and also for systems of partial differential equations. The primary objectives of this thesis are as follows:

- Investigate the dynamic consistency of the NSFD discrete systems with their corresponding ecological and epidemiological continuous systems.
- Investigate the superiority of the NSFD scheme over other standard finite difference schemes.
- For the NSFD scheme, are there any universal rules to give the nonlocal transformations to all the linear and nonlinear terms of the continuous system of ODEs?
- Do the predetermined denominator functions always permit the dynamic consistency of the NSFD discrete systems? If not, then how to choose the denominator functions?

- In the case of PDE systems, how to discretize the second-order partial derivative terms using the NSFD scheme?
- For the system of PDEs, how to choose the denominator functions so that the positivity of the NSFD discrete systems does not depend on the step-sizes or any other parameter values.

The study will also show that for the system of PDEs, the NSFD scheme proposed by us guarantees the discrete systems' accuracy, consistency, and stability. Also, the proposed NSFD discrete system produces a comparatively very small absolute value of error than other schemes. Throughout the thesis, we provide both analytical and numerical results.

1.8 Thesis overview

In **Chapter 2**, we discretize a predator-prey model by standard Euler forward method and non-standard finite difference method and then compare their dynamic properties with the corresponding continuous-time model. We show that NSFD model preserves positivity of the solutions and is completely consistent with the dynamics of the corresponding continuous-time model. On the other hand, the discrete model formulated by forward Euler method does not show dynamic consistency with its continuous counterpart. Rather it shows scheme–dependent instability when step-size restriction is violated.

In **Chapter 3**, we analyze a continuous-time epidemic model and its discrete counterpart, where infection spreads both horizontally and vertically. We consider three cases: model with horizontal and imperfect vertical transmissions, model with horizontal and perfect vertical transmissions, and model with perfect vertical and no horizontal transmissions. Stability of different equilibrium points of both the continuous and discrete systems in all cases are determined. It is shown that the stability criteria are identical for continuous and discrete systems. The dynamics of the discrete system have also shown to be independent of the step-size. Numerical computations are presented to illustrate analytical results of both the systems and their subsystems.

In a nonstandard finite difference (NSFD) scheme, there are two fundamental issues regarding the construction of NSFD models. First, how to construct the denominator function of the discrete first-order derivative? Second, how to discretize the nonlinear terms of a given differential equation with nonlocal terms? In **Chapter 4**, we define a uniform technique for nonlocal discretization and construction of denominator function for NSFD models. We have discretized a couple of highly nonlinear continuous-time population models using these rules. We give analytical proof in each case to show that the proposed NSFD model has identical dynamic properties to the continuous-time model. It is also shown that each NSFD system is positively invariant, and its dynamics do not depend on the step-size. Numerical experiments have also been performed in favour of such claims.

Most of the cases, discretization becomes essential to obtain the numerical solutions of continuous system. But numerical instability occurs in case of standard finite discretization schemes. Thus, to get minimum error, the NSFD scheme becomes essential. A continuous system of differential equations must eventually be discretized in order to obtain the numerical solutions. However, while conventional finite discretization schemes suffer from numerical instability, the NSFD scheme is dynamically consistent. The recently developed NSFD techniques for partial differential equations do not provide consistency or first-order accuracy in time, or else they fail to retain positivity in the absence of step-size requirements. Our first proposal in **Chapter 5** is an NSFD scheme that ensures consistency of the suggested NSFD scheme as well as first-order accuracy in time and second-order accuracy in space, while maintaining the positivity of solutions undiminished. Additionally, we show the stability of the proposed scheme. In order to illustrate the effectiveness of the proposed NSFD scheme, we present a comparison with two other well-known NSFD approaches, which demonstrates the proposed scheme's excellency over the others.

In **Chapter 6**, we consider a three-dimensional HIV reaction-diffusion system. We discretized the continuous-time system of partial differential equations using the NSFD scheme. Then it is shown that the proposed NSFD scheme is consistent with respect to time and space step-sizes, first-order accurate in time and second-order accurate in space. Also, the suggested NSFD scheme guarantees the positivity of solutions for all feasible initial values without any other limitations and assures that the NSFD scheme is Von Neumann stable. We compared the dynamics of the solutions of the discrete system following our suggested NSFD scheme with the solutions of other two systems discretized by the previously defined NSFD scheme and Crank-Nicolson scheme. It is shown that our suggested NSFD scheme for three-dimensional system of PDE is more efficient and accurate than the others.

The thesis ends with the discussions and future work in **Chapter 7**.

2

On the dynamics of a discrete predator-prey model[1]

2.1 Introduction

Nonlinear systems of ordinary differential equations are frequently used to unveil the underlying dynamics of physical, chemical and biological phenomena. In most cases, it becomes impossible to find the analytical solution of the system in a compact form. For this, the need for a numerical solution arises for which discretization of the continuous-time model is essential.

We consider the following Holling-Tanner predator-prey system with ratio-dependent functional response investigated by Celik [52]:

$$\begin{aligned} \frac{dx}{dT} &= rx\left(1-\frac{x}{K}\right)-\frac{mxy}{x+Ay}, \\ \frac{dy}{dT} &= sy\left(1-\frac{hy}{x}\right), \end{aligned} \tag{2.1}$$

where x and y represents the numbers of prey and predator individuals at time T, and $x(T) > 0$, $y(T) \geq 0$ for all $T \geq 0$. The parameters r and K represent, respectively, the intrinsic growth

[1] *The bulk of this chapter has been published in Trends in Biomathematics: Modeling, Optimization and Computational Problems, R. P. Mondaini (ed.), Springer Nature, Moscow, pp. 219-232, 2018.*

rate and carrying capacity of prey population in the absence of predator. In the functional response term $\frac{mxy}{x+Ay}$, m denotes maximum rate of predation and A is the half-saturation constant. The parameter s represents the intrinsic growth rate of predator and h represents the required number of prey to support one predator.

After giving the following transformations:

$$N=\frac{x}{K},\ P=\frac{my}{rK},\ t=\frac{T}{r},\ \alpha=\frac{rA}{m},\ \beta=\frac{sh}{m} \text{ and } \delta=\frac{m}{hr}$$

in the continuous system (2.1), the dimensionless form of (2.1) becomes

$$\begin{aligned}\frac{dN}{dt}&=N(1-N)-\frac{NP}{N+\alpha P},\\ \frac{dP}{dt}&=\beta P(\delta-\frac{P}{N}).\end{aligned} \tag{2.2}$$

Our objective here is to propose a discrete model of the continuous system (2.2) following Micken's NSFD scheme [10], which will show dynamic consistency with its continuous counterpart and dynamics of this NSFD discrete system doesn't depend on the step-size. Also, we will discretize the continuous system (2.2) using the Euler forward method. Our motive is to compare the dynamics of these two discrete systems.

The chapter is arranged in the following sequence. In the next section, we describe the properties of the considered continuous-time model. Section 2.3 contains technique of constructing a NSFD discrete system and the analysis of NSFD and Section 2.4 contains the analysis of the Euler discrete system. Extensive simulations are presented in Section 2.5. The paper ends with the summary in Section 2.6.

2.2 Properties of the continuous-time model

We are interested only on the interior equilibrium point, where both populations coexist. The interior equilibrium is given by $E^*=(N^*,P^*)$, where

$$N^*=\frac{1+\alpha\delta-\delta}{1+\alpha\delta},\quad P^*=\delta N^*,\quad (1+\alpha\delta)>\delta.$$

The following results are known [52].

Theorem 2.1. *The interior equilibrium point E^* of the system* (2.2) *exists and becomes stable if*

$$(i) 1+\alpha\delta>\delta,\ (ii) \delta(2+\alpha\delta)<(1+\alpha\delta)^2(1+\beta\delta).$$

Here we seek to construct a discrete model of the corresponding continuous model (2.2) that preserves the qualitative properties of the continuous system and maintains dynamic consistency. We also construct the corresponding Euler discrete model and compare its results with the results of NSFD model.

2.3 Nonstandard finite difference (NSFD) model

For convenience, we write the continuous system (2.2) as

$$\begin{aligned}\frac{dN}{dt} &= N - N^2 - \frac{NP}{(N+\alpha P)} + (N-N)(N+\alpha P),\\ \frac{dP}{dt} &= \beta\delta P - \frac{\beta P^2}{N}.\end{aligned} \tag{2.3}$$

The above system can be expressed as follows:

$$\begin{aligned}\frac{dN}{dt} &= N - N^2 - NA(N,P) + (N-N)B(N,P),\\ \frac{dP}{dt} &= \beta\delta P - \beta PC(N,P),\end{aligned} \tag{2.4}$$

where

$$A(N,P) = \frac{P}{N+\alpha P},\ B(N,P) = (N+\alpha P) \text{ and } C(N,P) = \frac{P}{N}.$$

We employ the following non-local approximations term-wise for the system (2.4):

$$\begin{cases} \frac{dN}{dt} \to \frac{N_{n+1}-N_n}{h}, & \frac{dP}{dt} \to \frac{P_{n+1}-P_n}{h},\\ N \to N_n, & P \to P_n,\\ N^2 \to N_nN_{n+1}, & PC(N,P) \to P_{n+1}C(N_n,P_n),\\ NA(N,P) \to N_{n+1}A(N_n,P_n), & \\ (N-N)B(N,P) \to (N_n-N_{n+1})B(N_n,P_n), & \end{cases} \tag{2.5}$$

where h (>0) is the step-size.
By these transformations, the continuous-time system (2.3) is converted to

$$\begin{aligned}\frac{N_{n+1}-N_n}{h} &= N_n - N_nN_{n+1} - \frac{N_{n+1}P_n}{N_n+\alpha P_n} + (N_n - N_{n+1})(N_n+\alpha P_n),\\ \frac{P_{n+1}-P_n}{h} &= \beta\delta P_n - \frac{\beta P_{n+1}P_n}{N_n}.\end{aligned} \tag{2.6}$$

System (2.6) can be simplified to

$$\begin{aligned} N_{n+1} &= \frac{N_n\{1+h+h(N_n+\alpha P_n)\}(N_n+\alpha P_n)}{(1+2hN_n+\alpha hP_n)(N_n+\alpha P_n)+hP_n}, \\ P_{n+1} &= \frac{P_nN_n(1+\beta\delta h)}{N_n+\beta hP_n}. \end{aligned} \tag{2.7}$$

Note that all solutions of the discrete-time system (2.7) remains positive for any step-size if they start with positive initial values. Therefore, the system (2.7) is positive.

2.3.1 Existence of fixed points

Fixed points of the system (2.7) are the solutions of the coupled algebraic equations obtained by putting $N_{n+1} = N_n = N$ and $P_{n+1} = P_n = P$ in (2.7). However, the fixed points can be obtained more easily from (2.6) with the same substitutions. Thus, fixed points are the solutions of the following nonlinear algebraic equations:

$$\begin{aligned} N - N^2 - \frac{NP}{N+\alpha P} &= 0, \\ \beta\delta P - \frac{\beta P^2}{N} &= 0. \end{aligned} \tag{2.8}$$

It is easy to observe that $E_1 = (1,0)$ is the predator-free fixed point. The interior fixed point $E^* = (N^*, P^*)$ satisfies

$$1 - N^* - \frac{P^*}{N^*+\alpha P^*} = 0 \text{ and } \delta - \frac{P^*}{N^*} = 0. \tag{2.9}$$

From the second equation of (2.9), we have $P^* = \delta N^*$. Substituting P^* in the first equation of (2.9), we find $N^* = \frac{1+\alpha\delta-\delta}{1+\alpha\delta}$, which is always positive if $1+\alpha\delta > \delta$. Thus, the positive fixed point E^* exists if $1+\alpha\delta > \delta$.

2.3.2 Stability analysis of fixed points

The variational matrix of system (2.7) evaluated at an arbitrary fixed point (N,P) is given by

$$J(N,P) = \begin{pmatrix} a_{11} & a_{12} \\ a_{21} & a_{22} \end{pmatrix}, \tag{2.10}$$

where

$$\begin{aligned} a_{11} = &\frac{\{1+h+h(N_n+\alpha P_n)\}(N_n+\alpha P_n)}{(1+2hN_n+\alpha hP_n)(N_n+\alpha P_n)+hP_n} + \frac{hN_n(N_n+\alpha P_n)}{(1+2hN_n+\alpha hP_n)(N_n+\alpha P_n)+hP_n} \\ &+ \frac{N_n\{1+h+h(N_n+\alpha P_n)\}}{(1+2hN_n+\alpha hP_n)(N_n+\alpha P_n)+hP_n} \\ &- \frac{N_n\{1+h+h(N_n+\alpha P_n)\}(N_n+\alpha P_n)\{2h(N_n+\alpha P_n)+(1+2hN_n+\alpha hP_n)\}}{\{(1+2hN_n+\alpha hP_n)(N_n+\alpha P_n)+hP_n\}^2}, \end{aligned}$$

$$a_{12} = \frac{\alpha h N_n(N_n+\alpha P_n)}{(1+2hN_n+\alpha hP_n)(N_n+\alpha P_n)+hP_n} + \frac{\alpha N_n\{1+h+h(N_n+\alpha P_n)\}}{(1+2hN_n+\alpha hP_n)(N_n+\alpha P_n)+hP_n} - \frac{N_n\{1+h+h(N_n+\alpha P_n)\}(N_n+\alpha P_n)\{\alpha h(N_n+\alpha P_n)+\alpha(1+2hN_n+\alpha hP_n)+h\}}{\{(1+2hN_n+\alpha hP_n)(N_n+\alpha P_n)+hP_n\}^2},$$

$$a_{21} = \frac{P_n(1+\beta\delta h)}{N_n+\beta hP_n} - \frac{P_nN_n(1+\beta\delta h)}{(N_n+\beta hP_n)^2},$$

$$a_{22} = \frac{(1+\beta\delta h)N_n}{N_n+\beta hP_n} - \frac{\beta hP_nN_n(1+\beta\delta h)}{(N_n+\beta hP_n)^2}.$$

Theorem 2.2. *Suppose that conditions of Theorem 2.1 hold. Then the fixed point E^* of the system* (2.7) *is locally asymptotically stable.*

Proof. At the interior fixed point E^*, the variational matrix reads

$$J(N^*,P^*) = \begin{pmatrix} a_{11}^* & a_{12}^* \\ a_{21}^* & a_{22}^* \end{pmatrix},$$

where

$$\begin{cases} a_{11}^* = 1 + \frac{N^*h(1-2N^*-\alpha P^*)}{G}, \\ a_{12}^* = \frac{N^*h(\alpha-\alpha N^*-1)}{G}, \\ a_{21}^* = \frac{\beta\delta hP^*}{H}, \\ a_{22}^* = 1 - \frac{\beta hP^*}{H}, \end{cases} \tag{2.11}$$

with $G = \{1+h+h(N^*+\alpha P^*)\}(N^*+\alpha P^*)$ and $H = (1+\beta\delta h)N^*$.
Using $P^* = \delta N^*$ in (2.11), we have

$$\begin{cases} a_{11}^* = 1 + \frac{N^*h(1-2N^*-\alpha\delta N^*)}{G}, \\ a_{12}^* = \frac{N^*h(\alpha-\alpha N^*-1)}{G}, \\ a_{21}^* = \frac{\beta\delta^2hN^*}{H}, \\ a_{22}^* = 1 - \frac{\beta\delta hN^*}{H}. \end{cases} \tag{2.12}$$

One can compute that $1-det(J) = -\frac{(N^*)^2h\{(1-\beta\delta-\alpha\beta\delta^2)-(2+\alpha\delta)N^*\}}{GH} + \frac{\beta\delta h^2(N^*)^3(1+\alpha\delta)(2+\alpha\delta)}{GH} + \frac{\alpha\beta\delta^3(N^*)^2}{(1+\alpha\delta)GH} > 0$, provided $-(1-\beta\delta-\alpha\beta\delta^2)+(2+\alpha\delta)N^* > 0$, i.e. $\delta(2+\alpha\delta) < (1+\alpha\delta)^2(1+\beta\delta)$. Note that $trace(J) = \frac{(N^*)^2}{GH}[(1+\alpha\delta)\{2+h(2+\beta\delta+2N^*\alpha\delta)\}+h(1+N^*\alpha\delta)+h^2\beta\delta\{\frac{2\delta}{1+\alpha\delta}+\alpha\delta(1+N^*+N^*\alpha\delta)+N^*\}] > 0$ and $1-trace(J)+det(J) = \frac{\beta\delta h^2(N^*)^2(1+\alpha\delta-\delta)}{GH} > 0$, following the existing condition of E^*. Therefore, the positive fixed point E^* is locally asymptotically stable provided conditions of Theorem 2.1 hold. Hence the theorem is proven. □

2.4 The Euler forward method

By Euler's forward method, we transform the continuous model (2.2) in the following discrete model:

$$\begin{aligned} \frac{N_{n+1}-N_n}{h} &= N_n\left[1-N_n-\frac{P_n}{N_n+\alpha P_n}\right], \\ \frac{P_{n+1}-P_n}{h} &= \beta P_n\left[\delta-\frac{P_n}{P_n}\right], \end{aligned} \tag{2.13}$$

where $h>0$ is the step-size.
Rearranging the above equations, we have

$$\begin{aligned} N_{n+1} &= N_n+hN_n\left[1-N_n-\frac{P_n}{N_n+\alpha P_n}\right], \\ P_{n+1} &= P_n+h\beta P_n\left[\delta-\frac{P_n}{N_n}\right]. \end{aligned} \tag{2.14}$$

It is to be noticed that the system (2.14) with positive initial values is not unconditionally positive due to the presence of negative terms. The system may therefore exhibit spurious behaviors and numerical instabilities [5].

2.4.1 Existence and stability of fixed points

At the fixed point, we substitute $N_{n+1}=N_n=N$ and $P_{n+1}=P_n=P$. One can easily compute that (2.14) has the same interior fixed points as in the previous case. The fixed point $E_1=(1,0)$ always exist and the fixed point $E^*=(N^*,P^*)$ exists if $1+\alpha\delta>\delta$, where $N^*=\frac{1+\alpha\delta-\delta}{1+\alpha\delta}$, $P^*=\delta N^*$. We are interested for interior equilibrium only.
The variational matrix of the system (2.14) at any arbitrary fixed point (N,P) is given by

$$J(x,y)=\begin{pmatrix} a_{11} & a_{12} \\ a_{21} & a_{22} \end{pmatrix},$$

where

$$\begin{cases} a_{11}=1+h\left[1-N_n-\frac{P_n}{N_n+\alpha P_n}\right]+hN_n\left[-1+\frac{P_n}{(N_n+\alpha P_n)^2}\right], \\ a_{12}=-h\left(\frac{N_n}{N_n+\alpha P_n}\right)^2, \\ a_{21}=h\beta\left(\frac{P_n}{N_n}\right)^2, \\ a_{22}=1+h\left[\beta\delta-\frac{\beta P_n}{N_n}-\beta\frac{P_n}{N_n}\right]. \end{cases}$$

Theorem 2.3. *Suppose that the conditions of Theorem 2.1 hold. The interior fixed point E^* of the system* (2.14) *is then locally asymptotically stable if* $h < \min\left\{\frac{G}{H}, \frac{2(1+\alpha\delta)^2}{G}\right\}$, *where* $G = (1+\alpha\delta)^2(1+\beta\delta) - \delta(2+\alpha\delta)$, $H = \beta\delta(1+\alpha\delta-\delta)(1+\alpha\delta)$.

Proof. At the interior equilibrium point E^*, the Jacobian matrix is evaluated as

$$J(N^*, P^*) = \begin{pmatrix} a_{11} & a_{12} \\ a_{21} & a_{22} \end{pmatrix},$$

where

$$a_{11} = 1 - hN^*\left[1 - \frac{P^*}{(N^*+\alpha P^*)^2}\right], a_{12} = -h\left(\frac{N^*}{N^*+\alpha P^*}\right)^2,$$
$$a_{21} = h\beta\left(\frac{P^*}{N^*}\right)^2, a_{22} = 1 - h\beta\frac{P^*}{N^*}.$$

Note that $1 - trace(J) + det(J) = h^2\beta P^*$ is always positive, following the existence conditions of E^*. Thus, condition (ii) of Lemma 1.14 is satisfied. One can compute that $det(J) = 1 - hN^*\left\{\frac{G}{H} - h\right\}$. Here H is positive following the existence condition of E^* and $G > 0$ if $(1+\alpha\delta)^2(1+\beta\delta) > \delta(2+\alpha\delta)$. Thus, condition (i) of Lemma 1.14 is satisfied if $h > \frac{G}{H}$. Simple computations give $1 + trace(J) + det(J) = 2\left(2 - h\frac{G}{(1+\alpha\delta)^2}\right) + h^2 H$. This expression will be positive if $0 < h < \frac{2(1+\alpha\delta)^2}{G}$. Therefore, coexistence equilibrium point E^* exists and becomes stable if $1+\alpha\delta > \delta$, $\delta(2+\alpha\delta) < (1+\alpha\delta)^2(1+\beta\delta)$ and $h < \min\left\{\frac{G}{H}, \frac{2(1+\alpha\delta)^2}{G}\right\}$. Hence the theorem. □

Remark 2.4. *Note that if $h > \frac{G}{H}$ then E^* is unstable even when the other two conditions are satisfied.*

2.5 Numerical simulations

In this section, we present some numerical simulations to validate our analytical results of the NSFD discrete system (2.7) and the Euler system (2.14) with their continuous counterpart (2.2). For this experiment, we consider the parameters set as in Celik [52]: $\alpha = 0.7, \beta = 0.9, \delta = 0.6$. The step-size is kept fixed at $h = 0.1$ in all simulations, if not stated otherwise. We consider the initial value $I_1 = (0.2, 0.2)$ as in Celik [52] for all simulations. For the above parameter set, the interior fixed point is evaluated as $E^* = (N^*, P^*) = (0.5775, 0.3465)$. We first reproduce the phase plane diagrams (Fig. 2.1) of the continuous system (2.2), the NSFD discrete system (2.7) and the Euler discrete system (2.14) by using ODE45 of the software Matlab 7.11. Following the analytical results stated in the Sect. 3, the phase plane diagrams show that the equilibrium E^* is stable for all three cases.

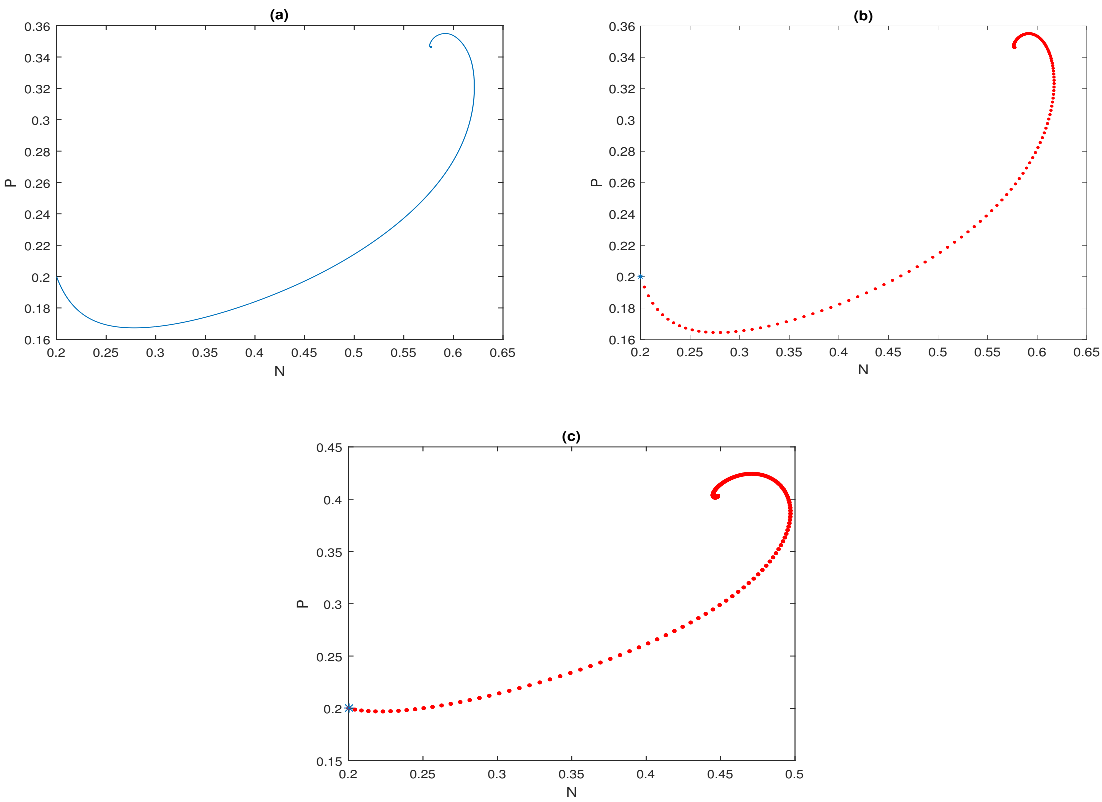

Figure 2.1: Phase diagrams: (**a**) Continuous system (2.2), (**b**) NSFD discrete system (2.7) and (**c**) Euler discrete system (2.14). These figures show that the trajectory in each case converges to the stable coexistence equilibrium E^*. The parameters are $\alpha = 0.7,\ \beta = 0.9,\ \delta = 0.6$ and the initial value is $(0.2, 0.2)$ [52]. Here $G = (1+\alpha\delta)^2(1+\beta\delta) - \delta(2+\alpha\delta) = 1.6533$ and $h = 0.1 < min\{\frac{G}{H}, \frac{2(1+\alpha\delta)^2}{G}\} = \min\{2.6293, 2.4393\}$.

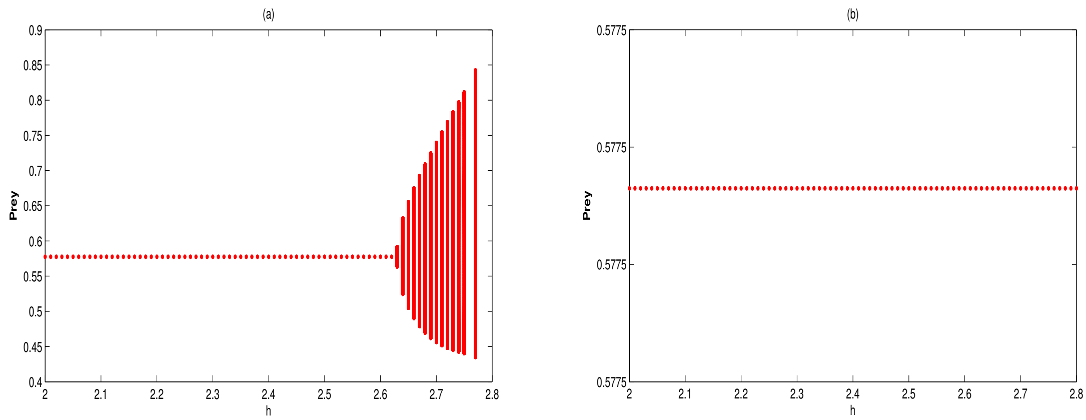

Figure 2.2: Bifurcation diagrams of prey population of Euler forward model (2.14) (Fig. a) and NSFD model (2.7) (Fig. b) with step-size h as the bifurcation parameter. All the parameters and initial value remain the same as in Fig. 2.1. The first figure shows that the prey population is stable for small step-size h and unstable for higher value of h. The second figure shows that the prey population is stable for all step-size.

To compare step-size dependency of the Euler model and NSFD model, we have plotted the bifurcation diagrams of prey population of the systems (2.14) and (2.7) considering step-size h as the bifurcation parameter (Fig. 2.2) for the same parameter values as in Fig. 2.1. Fig. 2.2a shows that behavior of the Euler model depends on the step-size. If step-size is small, system population is stable and the dynamics resembles with the continuous system (2.2). As the step-size is increased, system population becomes unstable and the dynamics is inconsistent with the continuous system. However, the second figure (Fig. 2.2b) shows that the NSFD model (2.7) remains stable for all h, indicating that the dynamics is independent of step-size.

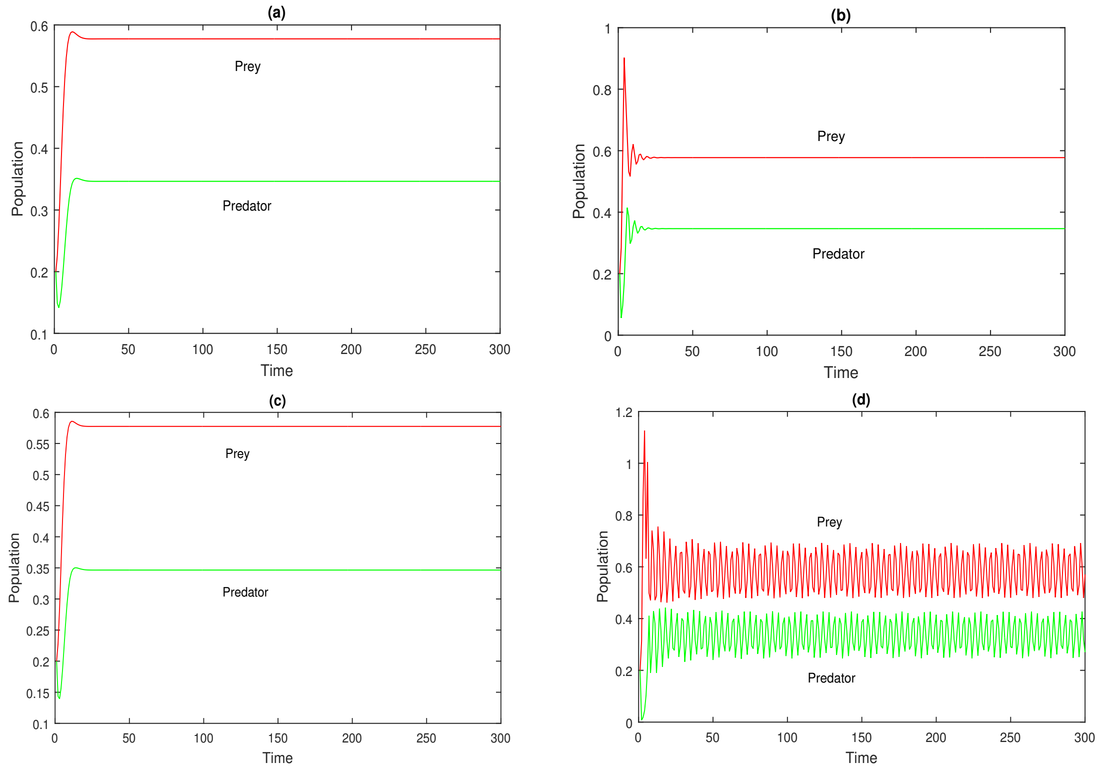

Figure 2.3: Time series solutions of the NSFD system (2.7) and Euler system (2.14) for two particular values of step-size (h). Here $h = 2$ for (**a** and **b**) and $h = 2.67$ for (**c** and **d**). Other parameters are in Fig. 2.2.

In particular, we plot (Fig. 2.3) time series behavior of the NSFD system (2.7) and Euler discrete system (2.14) for $h = 2(< \min\left\{\frac{G}{H}, \frac{2(1+\alpha\delta)^2}{G}\right\} = \min\{2.6293, 2.4393\})$ and for $h = 2.67(> \min\{2.6293, 2.4393\})$. The first two Figs. 2.3a, b show that both populations are stable when the step-size is $h = 2$. Figure 2.3c shows that populations of NSFD system (2.7) remains stable for all step-size, indicating its dynamic consistency with the continuous system, but Fig. 2.3d shows that populations of Euler system (2.14) oscillate for $h = 2.67$, indicating its dynamic inconsistency with its continuous counterpart.

2.6 Summary

Nonstandard finite difference (NSFD) scheme has gained lot of attentions in the last few years mostly for two reasons. First, it generally does not show spurious behavior as compared to other standard finite difference methods and second, dynamics of the NSFD model does not depend on the step-size. NSFD scheme also reduces the computational cost of traditional finite-difference schemes. In this work, we have studied two discrete systems constructed by NSFD scheme and forward Euler scheme of a well studied two-dimensional Holling-Tanner type predator-prey system with ratio-dependent functional response. We have shown that dynamics of the discrete system formulated by NSFD scheme are same as that of the continuous system. It preserves the local stability of the fixed point and the positivity of the solutions of the continuous system for any step-size. Simulation experiments show that NSFD system always converge to the correct steady-state solutions for any arbitrary large value of the step-size (h) in accordance with the theoretical results. However, the discrete model formulated by forward Euler method does not show dynamic consistency with its continuous counterpart. Rather it shows scheme-dependent instability when step-size restriction is violated.

3

Dynamics of vertically and horizontally transmitted parasites: Continuous vs discrete models[1]

3.1 Introduction

Mathematical models play significant role in understanding the dynamics of biological phenomena. System of nonlinear differential equations are frequently used to describe these biological models. Unfortunately, nonlinear differential equations in general can not be solved analytically. For this reason, we go for numerical computations of the model system and discretization of the continuous model is essential in this process. Here we shall explore and compare the dynamics of a continuous-time epidemic model and its subsystems with their corresponding discrete models.

Lipsitch et al. [53] have investigated the dynamics of vertically and horizontally transmitted parasites of the following population model, where the state variables X and Y represent,

[1] *The bulk of this chapter has been published in International Journal of Difference Equations, 13(2), 139-156, 2018.*

respectively, the densities of uninfected and infected hosts at time t:

$$\begin{aligned}\frac{dX}{dt} &= \left\{b_x\left[1-\frac{(X+Y)}{K}\right]-u_x-\beta Y\right\}X+e\left[1-\frac{(X+Y)}{K}\right]Y,\\ \frac{dY}{dt} &= \left\{b_y\left[1-\frac{(X+Y)}{K}\right]-u_y+\beta X\right\}Y.\end{aligned} \tag{3.1}$$

This model demonstrates the density-dependent growth of an asexual host population, where infection spreads through imperfect vertical transmission as well as horizontal transmission. Horizontal transmission of infection follows mass-action law with β as the proportionality constant. Vertical transmission is imperfect because infected hosts not only give birth of infected hosts at a rate b_y but also produce uninfected offspring at a rate e. In case of perfect vertical transmission, however, infected hosts give birth of infected hosts only and in that case $e = 0$. Parasites may affect the fecundity and morbidity rates of its host population [54, 55]. It is assumed here that the death rate of infected hosts is higher than that of susceptible hosts, i.e., $u_y > u_x$ and the birth rate of susceptible hosts is higher than that of infected hosts, i.e., $b_x \geq b_y + e$.

Observe that different sub-models may be constructed from the model (3.1). For example, if $\beta \neq 0$, $e = 0$ then one gets a model with horizontal and perfect vertical transmissions. If $\beta = 0$, $e = 0$ then we get an epidemic model with perfect vertical transmission and no horizontal transmission. Our objectives are to construct a discrete model, following the NSFD scheme, corresponding to each continuous system. We also want to show that dynamic behaviors of the continuous and discrete systems are identical with same parameter restrictions. It is also our intention to prove that the proposed discrete models are positive for all step-size and dynamically consistent.

The chapter is organized as follows. We present the analysis of the continuous-time model and its subsystems in the next section. Section 3.3 contains the corresponding analysis in discrete system constructed by NSFD scheme. In Section 3.4, we present extensive numerical simulations in favour of our theoretical results. Finally, a summary is presented in Section 3.5.

3.2 Analysis of continuous-time models

Lipsitch et al. [53] analyzed the system (3.1) with horizontal transmission and perfect vertical transmissions (the case $e = 0$), and the system with perfect vertical transmission but no horizontal transmission (the case $\beta = 0,\ e = 0$). The general case (when $e \neq 0,\ \beta \neq 0$) was analyzed numerically and its importance in the prevalence of infection was discussed. Here we first give stability analysis of equilibrium points of the general model (3.1) and deduce the results of subcases, whenever applicable.

3.2.1 Model with horizontal and imperfect vertical transmission

The continuous system (3.1) has two boundary equilibrium points $E_0 = (0,0)$, $E_1 = (\bar{X},0)$, where $\bar{X} = K(1-\frac{u_x}{b_x})$ and one interior equilibrium point $E^* = (X^*,Y^*)$, where the equilibrium densities of susceptible and infected hosts are given by

$$X^* = \frac{-B+\sqrt{B^2-4AC}}{2A} \text{ and } Y^* = \frac{(\beta K - b_y)X^*}{b_y} + \frac{K(b_y-u_y)}{b_y},$$

with

$$\begin{cases} A = \frac{\beta K}{b_y^2}[b_y(b_x-b_y-e)+\beta K(b_y+e)], \\ B = -K(b_x-u_x)+K(b_x+\beta K+e)\frac{(b_y-u_y)}{b_y} \\ \quad +2eK\frac{(\beta K-b_y)(b_y-u_y)}{b_y^2} - \frac{eK(\beta K-b_y)}{b_y}, \\ C = -\frac{eK^2(b_y-u_y)u_y}{b_y^2}. \end{cases} \tag{3.2}$$

The trivial equilibrium E_0 exists for all parameter values, but the infection-free equilibrium E_1 exists if $b_x > u_x$. The coexisting equilibrium point E^* exists if $b_x > u_x$, $b_y > u_y$, $b_y > \beta K$ and $\frac{K}{X^*} > \frac{b_y-\beta K}{b_y-u_y}$.

We have the following theorem for the stability of different equilibrium points.

Theorem 3.1. *System (3.1) is locally asymptotically stable around the equilibrium point*

(i) E_0 *if* $b_x < u_x$ *and* $b_y < u_y$.

(ii) E_1 *if* $b_x > u_x$ *and* $R_0 < 1$, *where* $R_0 = V_0 + H_0$ *with* $V_0 = \frac{b_y}{b_x}\frac{u_x}{u_y}$, $H_0 = \frac{\beta}{u_y}K(1-\frac{u_x}{b_x})$ *and it is unstable whenever* $R_0 > 1$.

(iii) E^* *if* $b_x > u_x$, $b_y > u_y$, $b_y > \beta K$ *and* $\frac{K}{X^*} > \frac{b_y-\beta K}{b_y-u_y}$.

Proof. Local stability of the system around an equilibrium point is performed following linearization technique. For it, we compute the variational matrix of system (3.1) at an arbitrary fixed point (X,Y) as

$$V(X,Y) = \begin{pmatrix} a_{11} & a_{12} \\ a_{21} & a_{22} \end{pmatrix}, \tag{3.3}$$

where

$$\begin{cases} a_{11} = b_x\left[1-\frac{(X+Y)}{K}\right] - \frac{b_x X}{K} - u_x - \beta Y - \frac{eY}{K}, \\ a_{12} = -\frac{b_x X}{K} - \beta X + e\left[1-\frac{(X+Y)}{K}\right] - \frac{eY}{K}, \\ a_{21} = -\frac{b_y Y}{K} + \beta Y, \\ a_{22} = b_y\left[1-\frac{(X+Y)}{K}\right] - \frac{b_y Y}{K} - u_y + \beta X. \end{cases} \tag{3.4}$$

At the trivial fixed point E_0, the variational matrix is

$$V(E_0) = \begin{pmatrix} b_x - u_x & e \\ 0 & b_y - u_y \end{pmatrix}.$$

Corresponding eigenvalues are given by $\lambda_1 = b_x - u_x$ and $\lambda_2 = b_y - u_y$. E_0 will be locally asymptotically stable if $\lambda_1 = b_x - u_x < 0$ and $\lambda_2 = b_y - u_y < 0$; i.e., if $b_x < u_x$ and $b_y < u_y$. Thus, if the birth rates of susceptible hosts and infected hosts are less than their respective death rates then both populations goes to extinction and the trivial equilibrium will be stable.
At the axial equilibrium point E_1, the variational matrix is computed as

$$V(E_1) = \begin{pmatrix} -b_x(1-\frac{u_x}{b_x}) & -(b_x+\beta K)(1-\frac{u_x}{b_x}) + \frac{eu_x}{b_x} \\ 0 & \frac{b_y u_x}{b_x} - u_y + \beta K(1-\frac{u_x}{b_x}) \end{pmatrix}.$$

The corresponding eigenvalues are $\lambda_1 = -b_x(1-\frac{u_x}{b_x})$ and $\lambda_2 = \frac{b_y u_x}{b_x} - u_y + \beta K(1-\frac{u_x}{b_x})$. It is to be noted that $\lambda_1 < 0$ whenever E_1 exists. The other eigenvalue can be rearranged as $\lambda_2 = u_y\left\{\frac{b_y}{b_x}\frac{u_x}{u_y} + \frac{\beta}{u_y}K(1-\frac{u_x}{b_x}) - 1\right\}$. Thus $\lambda_2 < 0$ whenever $R_0 < 1$, where $R_0 = V_0 + H_0$. Note that $V_0 = (\frac{b_y}{b_x})(\frac{u_x}{u_y})$ is the basic reproduction number due to vertical transmission and $H_0 = \frac{\beta}{u_y}\bar{X}$ is the basic reproduction number due to horizontal transmission.
At the interior equilibrium point E^*, the variational matrix is

$$V(E^*) = \begin{pmatrix} a_{11}^* & a_{12}^* \\ a_{21}^* & a_{22}^* \end{pmatrix}, \tag{3.5}$$

where

$$\begin{cases} a_{11}^* = -\frac{eY^*}{X^*}\left[1 - \frac{(X^*+Y^*)}{K}\right] - \frac{b_x X^*}{K} - \frac{eY^*}{K}, \\ a_{12}^* = -\frac{b_x X^*}{K} - \beta X^* + e\left[1 - \frac{(X^*+Y^*)}{K}\right] - \frac{eY^*}{K}, \\ a_{21}^* = -\frac{b_y Y^*}{K} + \beta Y^*, \\ a_{22}^* = -\frac{b_y Y^*}{K}. \end{cases} \tag{3.6}$$

E^* will be stable if and only if $Trace(V(E^*)) < 0$ and $Det(V(E^*)) > 0$. From the existence condition of E^*, one can observe that both a_{11}^* and a_{22}^* are negative. Thus, $Trace(V(E^*)) < 0$. After some simple algebraic manipulation, one gets

$$Det(V(E^*)) = \frac{eu_y Y^*}{X^*}\left(1 - \frac{u_y}{b_y}\right) + \frac{\beta X^* Y^*}{K}(b_x - b_y - e) + \beta^2 X^* Y^* + \frac{e\beta^2 X^* Y^*}{b_y}.$$

Thus, whenever E^* exists and $b_x \geq b_y + e$, we have $Det(V(E^*)) > 0$ and E^* becomes locally asymptotically stable. This completes the proof. □

3.2.2 Model with horizontal and perfect vertical transmissions

The vertical transmission is perfect if infected hosts give birth to infected offspring only. In this case $e = 0$ and the system (3.1) becomes

$$\begin{aligned}\frac{dX}{dt} &= b_x X\left[1-\frac{(X+Y)}{K}\right] - u_x X - \beta XY,\\ \frac{dY}{dt} &= b_y Y\left[1-\frac{(X+Y)}{K}\right] - u_y Y + \beta XY.\end{aligned} \tag{3.7}$$

The continuous system (3.7) has four equilibrium points, viz. $E_0^H = (0,0)$, $E_1^H = (\bar{X},0)$, $E_2^H = (0,\bar{Y})$ and an interior equilibrium point $E_H^* = (X_H^*, Y_H^*)$, where

$$\begin{aligned}\bar{X} &= K\left(1-\frac{u_x}{b_x}\right),\ \bar{Y} = K\left(1-\frac{u_y}{b_y}\right) \text{ and}\\ X_H^* &= \frac{b_x u_y - b_y u_x - \beta K(b_y - u_y)}{\beta(\beta K + b_x - b_y)},\ Y_H^* = \frac{b_y u_x - b_x u_y + \beta K(b_x - u_x)}{\beta(\beta K + b_x - b_y)}.\end{aligned}$$

The trivial equilibrium point E_0^H always exists, E_1^H exists if $b_x > u_x$, E_2^H exists if $b_y > u_y$ and the interior fixed point E_H^* exists if $b_x > u_x,\ b_y > u_y,\ \frac{b_x u_y}{b_y} > u_x + \beta K\left(1-\frac{u_y}{b_y}\right)$ and $R_0 > 1$, where $R_0 = V_0 + H_0$ with $V_0 = \frac{b_y}{b_x}\frac{u_x}{u_y}$, $H_0 = \frac{\beta}{u_y}K\left(1-\frac{u_x}{b_x}\right)$. The following results are known [53].

Theorem 3.2. *System (3.7) is locally asymptotically stable around the equilibrium point*

(i) E_0^H *if* $b_x < u_x$ *and* $b_y < u_y$,

(ii) E_1^H *if* $b_x > u_x$ *and* $R_0 < 1$,

(iii) E_2^H *if* $b_y > u_y$ *and* $\frac{b_x u_y}{b_y} < u_x + \beta K\left(1-\frac{u_y}{b_y}\right)$,

(iv) E_H^* *if* $b_x > u_x,\ b_y > u_y,\ \frac{b_x u_y}{b_y} > u_x + \beta K\left(1-\frac{u_y}{b_y}\right)$ *and* $R_0 > 1$.

3.2.3 Model with perfect vertical transmission and no horizontal transmission

In this case, $e = 0,\ \beta = 0$. Then the system (3.1) reduces to

$$\begin{aligned}\frac{dX}{dt} &= b_x X\left[1-\frac{(X+Y)}{K}\right] - u_x X,\\ \frac{dY}{dt} &= b_y Y\left[1-\frac{(X+Y)}{K}\right] - u_y Y.\end{aligned} \tag{3.8}$$

The continuous system (3.8) has three equilibrium points, viz. $E_0^V = (0,0)$, $E_1^V = (\bar{X},0)$ and $E_2^V = (0,\bar{Y})$, where $\bar{X} = K\left(1-\frac{u_x}{b_x}\right)$ and $\bar{Y} = K\left(1-\frac{u_y}{b_y}\right)$. The existence conditions for E_1^V and

E_2^V are $b_x > u_x$ and $b_y > u_y$, respectively. It is to be noted that no interior equilibrium does exist here. The following results are known [53].

Theorem 3.3. *System* (3.8) *is locally asymptotically stable around the equilibrium point*

(i) E_0^V *if* $b_x < u_x$ *and* $b_y < u_y$,

(ii) E_1^V *if* $b_x > u_x$ *and* $\frac{b_y}{u_y} < \frac{b_x}{u_x}$.

(iii) The equilibrium point E_2^V *is always unstable.*

3.3 Discrete Models

In this section, we construct three discrete models corresponding to the continuous models (3.1), (3.7) and (3.8) following nonstandard finite difference method. The objective is to show that all the discrete models have the same dynamic properties corresponding to its continuous counterpart and the dynamics does not depend on the step-size.

3.3.1 Discrete model for horizontal and imperfect vertical transmission

For convenience, we first express the continuous system (3.1) as follows:

$$\begin{aligned} \frac{dX}{dt} &= b_xX - \frac{b_xX^2}{K} - \frac{b_xXY}{K} - u_xX - \beta XY + eY - \frac{eXY}{K} - \frac{eY^2}{K}, \\ \frac{dY}{dt} &= b_yY - \frac{b_yXY}{K} - \frac{b_yY^2}{K} - u_yY + \beta XY. \end{aligned} \tag{3.9}$$

We now employ the following non-local approximations term-wise for the system (3.9):

$$\begin{cases} \frac{dX}{dt} \to \frac{X_{n+1}-X_n}{\phi_1(h)}, & \frac{dY}{dt} \to \frac{Y_{n+1}-Y_n}{\phi_2(h)}, \\ b_xX \to b_xX_n, & b_yY \to b_yY_n, \\ b_xX^2 \to b_xX_nX_{n+1}, & b_yXY \to b_yX_nY_{n+1}, \\ XY \to X_{n+1}Y_n, & b_yY^2 \to b_yY_nY_{n+1}, \\ u_xX \to u_xX_{n+1}, & u_yY \to u_yY_{n+1}, \\ eY \to eY_n, & \beta XY \to \beta X_nY_n, \\ eY^2 \to e\frac{X_{n+1}Y_n^2}{X_n}, & \end{cases} \tag{3.10}$$

where h (> 0) is the step-size and denominator functions are chosen as

$$\phi_1(h) = \frac{b_y\left\{1 - exp\left(-\frac{\beta K u_y}{b_y}h\right)\right\}}{\beta K u_y}, \qquad \phi_2(h) = h. \tag{3.11}$$

Note that $\phi_i(h),\ i=1,2$, are positive for all $h>0$.
By these transformations, the continuous system (3.9) is converted to

$$\begin{aligned}\frac{X_{n+1}-X_n}{\phi_1(h)} &= b_xX_n-\frac{b_x}{K}X_nX_{n+1}-\frac{b_x}{K}X_{n+1}Y_n-u_xX_{n+1}-\beta X_{n+1}Y_n+eY_n\\ &\qquad -\frac{e}{K}X_{n+1}Y_n-\frac{e}{K}\frac{X_{n+1}Y_n^2}{X_n},\\ \frac{Y_{n+1}-Y_n}{\phi_2(h)} &= b_yY_n-\frac{b_y}{K}X_nY_{n+1}-\frac{b_y}{K}Y_nY_{n+1}-u_yY_{n+1}+\beta X_nY_n.\end{aligned} \tag{3.12}$$

System (3.12) can be rearranged to obtain

$$\begin{aligned}X_{n+1} &= \frac{X_n(1+\phi_1(h)b_x)+\phi_1(h)eY_n}{1+\phi_1(h)\left(\frac{b_x}{K}X_n+\frac{b_x}{K}Y_n+u_x+\beta Y_n+\frac{e}{K}Y_n+\frac{e}{K}\frac{Y_n^2}{X_n}\right)},\\ Y_{n+1} &= \frac{Y_n\{1+\phi_2(h)(b_y+\beta X_n)\}}{1+\phi_2(h)\left(\frac{b_y}{K}X_n+\frac{b_y}{K}Y_n+u_y\right)},\end{aligned} \tag{3.13}$$

where $\phi_1(h)$ and $\phi_2(h)$ are given in (3.11).
The model (3.13) is our required discrete model corresponding to the continuous model (3.1). It is to be noted that all terms in the right-hand side of (3.13) are positive, so solutions of the system (3.13) will remain positive if they start with positive initial value. Therefore, the system (3.13) is said to be positive [5].
The fixed points of (3.13) can be calculated by setting $X_{n+1}=X_n=X$ and $Y_{n+1}=Y_n=Y$. One thus get the fixed points as $E_0=(0,0)$, $E_1=(\bar{X},0)$, where $\bar{X}=K\left(1-\frac{u_x}{b_x}\right)$ and $E^*=(X^*,Y^*)$. Note that the equilibrium values and the existence conditions remain same as in the continuous system.
The variational matrix of system (3.13) evaluated at an arbitrary fixed point (X,Y) is given by

$$J(X,Y)=\begin{pmatrix} a_{11} & a_{12}\\ a_{21} & a_{22}\end{pmatrix}, \tag{3.14}$$

where

$$\begin{cases} a_{11} = \dfrac{1+\phi_1(h)b_x}{1+\phi_1(h)\left(\frac{b_x}{K}X+\frac{b_x}{K}Y+u_x+\beta Y+\frac{e}{K}Y+\frac{e}{K}\frac{Y^2}{X}\right)}-\dfrac{\{X(1+\phi_1(h)b_x)+\phi_1(h)eY\}\phi_1(h)\left(\frac{b_x}{K}-\frac{e}{K}\frac{Y^2}{X^2}\right)}{\left\{1+\phi_1(h)\left(\frac{b_x}{K}X+\frac{b_x}{K}Y+u_x+\beta Y+\frac{e}{K}Y+\frac{e}{K}\frac{Y^2}{X}\right)\right\}^2},\\ a_{12} = \dfrac{\phi_1(h)e}{1+\phi_1(h)\left(\frac{b_x}{K}X+\frac{b_x}{K}Y+u_x+\beta Y+\frac{e}{K}Y+\frac{e}{K}\frac{Y^2}{X}\right)}-\dfrac{\{X(1+\phi_1(h)b_x)+\phi_1(h)eY\}\phi_1(h)\left(\frac{b_x}{K}+\beta+\frac{e}{K}+\frac{2e}{K}\frac{Y}{X}\right)}{\left\{1+\phi_1(h)\left(\frac{b_x}{K}X+\frac{b_x}{K}Y+u_x+\beta Y+\frac{e}{K}Y+\frac{e}{K}\frac{Y^2}{X}\right)\right\}^2},\\ a_{21} = \dfrac{\phi_2(h)\beta Y}{1+\phi_2(h)\left(\frac{b_y}{K}X+\frac{b_y}{K}Y+u_y\right)}-\dfrac{Y\{1+\phi_2(h)(b_y+\beta X)\}\phi_2(h)\frac{b_y}{K}}{\left\{1+\phi_2(h)\left(\frac{b_y}{K}X+\frac{b_y}{K}Y+u_y\right)\right\}^2},\\ a_{22} = \dfrac{1+\phi_2(h)(b_y+\beta X)}{1+\phi_2(h)\left(\frac{b_y}{K}X+\frac{b_y}{K}Y+u_y\right)}-\dfrac{Y\{1+\phi_2(h)(b_y+\beta X)\}\phi_2(h)\frac{b_y}{K}}{\left\{1+\phi_2(h)\left(\frac{b_y}{K}X+\frac{b_y}{K}Y+u_y\right)\right\}^2}.\end{cases}$$

One can then prove the following theorem.

Theorem 3.4. *System (3.13) is locally asymptotically stable around the fixed point*

(i) E_0 *if* $b_x < u_x$ *and* $b_y < u_y$.

(ii) E_1 *if* $b_x > u_x$ *and* $R_0 < 1$, *where* $R_0 = V_0 + H_0$ *with* $V_0 = \frac{b_y}{b_x}\frac{u_x}{u_y}$, $H_0 = \frac{\beta}{u_y}K\left(1-\frac{u_x}{b_x}\right)$ *and it is unstable whenever* $R_0 > 1$.

(iii) E^* *if* $b_x > u_x$, $b_y > u_y$, $b_y > \beta K$ *and* $\frac{K}{X^*} > \frac{b_y-\beta K}{b_y-u_y}$.

Proof. At the fixed point E_0, the variational matrix is given by

$$J(E_0) = \begin{pmatrix} \frac{1+\phi_1(h)b_x}{1+\phi_1(h)u_x} & \frac{\phi_1(h)e}{1+\phi_1(h)u_x} \\ \\ 0 & \frac{1+\phi_2(h)b_y}{1+\phi_2(h)u_y} \end{pmatrix}.$$

The corresponding eigenvalues are $\lambda_1 = \frac{1+\phi_1(h)b_x}{1+\phi_1(h)u_x}$ and $\lambda_2 = \frac{1+\phi_2(h)b_y}{1+\phi_2(h)u_y}$. Clearly $|\lambda_1| < 1$ if $b_x < u_x$ and $|\lambda_2| < 1$ if $b_y < u_y$, for $h > 0$. Therefore, E_0 will be stable if $b_x < u_x$ and $b_y < u_y$ hold simultaneously.

One can similarly compute the eigenvalues corresponding to the fixed point E_1 as $\lambda_1 = \frac{1+\phi_1(h)u_x}{1+\phi_1(h)b_x}$ and $\lambda_2 = \frac{1+\phi_2(h)\left\{b_y+\beta K(1-\frac{u_x}{b_x})\right\}}{1+\phi_2(h)\left(b_y-\frac{b_y u_x}{b_x}+u_y\right)}$. Note that $|\lambda_1| < 1$ whenever E_1 exists and $|\lambda_2| < 1$ whenever $R_0 < 1$. Thus, E_1 is stable if $b_x > u_x$ and $R_0 < 1$.

At the interior fixed point E^*, the variational matrix is given by

$$J(E^*) = \begin{pmatrix} a_{11}^* & a_{12}^* \\ a_{21}^* & a_{22}^* \end{pmatrix},$$

where

$$\begin{cases} a_{11}^* &= 1 - \frac{X^*\phi_1(h)}{G}\left[\frac{b_x X^*}{K} + \frac{eY^*}{X^*}\left(1-\frac{X^*+Y^*}{K}\right) + \frac{eY^*}{K}\right], \\ a_{12}^* &= \frac{\phi_1(h)X^*}{G}\left[e\left(1-\frac{X^*+Y^*}{K}\right) - \frac{b_x X^*}{K} - \beta X^* - \frac{eY^*}{K}\right], \\ a_{21}^* &= \frac{\phi_2(h)Y^*\beta K}{KH} - \frac{\phi_2(h)Y^* b_y}{KH}, \\ a_{22}^* &= 1 - \frac{\phi_2(h) b_y Y^*}{KH}, \end{cases}$$

with $G = X^*(1+\phi_1(h)b_x) + \phi_1(h)eY^*$ and $H = 1+\phi_2(h)(b_y+\beta X^*)$.

One can easily verify that $0 < a_{11}^* < 1$ and $0 < a_{22}^* < 1$. On simplifications, one can show

$$1-\det(J(E^*)) = \frac{\phi_1(h)X^*}{KGH}\left\{b_xX^* + \frac{eY^*K}{X^*}\left(1-\frac{X^*+Y^*}{K}\right)+eY^*\right\} + \frac{\phi_1(h)\phi_2(h)X^*Y^*b_y}{KGH}$$
$$\left\{\frac{b_xX^*}{Y^*}+\frac{eK}{X^*}\left(1-\frac{X^*+Y^*}{K}\right)^2+e+\frac{\beta b_xX^{*2}}{b_yY^*}+\frac{2e\beta K}{b_y}\left(1-\frac{X^*+Y^*}{K}\right)\right.$$
$$\left.+\frac{e\beta X^*}{b_y}+b_x\left(1-\frac{\beta X^*}{b_y}\right)+\frac{eY^*}{X^*}\left(1-\frac{\beta X^*}{b_y}\right)+\beta X^*+\beta K\left(1-\frac{X^*+Y^*}{K}\right)\right\}$$
$$+\frac{\phi_2(h)b_yX^*Y^*}{KGH}\left(1-\frac{\phi_1(h)\beta Ku_y}{b_y}\right),$$

$$1-trace(J(E^*))+\det(J(E^*)) = \frac{\phi_1(h)\phi_2(h)X^*Y^*b_y}{KGH}\left\{\frac{eK}{X^*}\left(1-\frac{X^*+Y^*}{K}\right)\left(1-\frac{u_y}{b_y}\right)\right.$$
$$\left.+\frac{\beta^2KX^*}{b_y}+\frac{e\beta Y^*}{b_y}\right\}.$$

From the existence condition, we have $\left(1-\frac{X^*+Y^*}{K}\right) = \frac{u_xX^*+\beta X^*Y^*}{b_xX^*+eY^*} > 0$. Thus, $X^*+Y^* < K$, i.e., $X^* < K$. Also, from $b_y > \beta K$, we have $b_y > \beta X^*$ and $\left(1-\frac{\beta X^*}{b_y}\right) > 0$. It is easy to observe that $\phi_1(h) < \frac{b_y}{\beta K u_y}$. Thus, $1-\det(J(E^*)) > 0$ and $1-trace(J(E^*))+\det(J(E^*)) > 0$. Hence E^* is locally asymptotically stable whenever it exists. This completes the theorem. □

Remark 3.5. *It is interesting to note that the dynamic properties of the discrete system (3.13) are identical with its continuous counterpart (3.1). So the discrete model is dynamically consistent. The stability of the fixed points also does not depend on the step-size. Since all solutions of the discrete model (3.13) remain positive when starts with positive initial value, there is no possibility of numerical instabilities and the model will not show any spurious dynamics.*

3.3.2 Discrete model for horizontal and perfect vertical transmissions

Here we rewrite the continuous model (3.7) as

$$\begin{aligned}\frac{dX}{dt} &= b_xX - \frac{b_xX^2}{K} - \frac{b_xXY}{K} - u_xX - \beta XY,\\ \frac{dY}{dt} &= b_yY - \frac{b_yXY}{K} - \frac{b_yY^2}{K} - u_yY + \beta XY.\end{aligned} \tag{3.15}$$

We employ the same non-local approximations (3.10) with $e=0$ term-wise to have the following system:

$$\begin{aligned}
\frac{X_{n+1}-X_n}{\phi_1(h)} &= b_xX_n - \frac{b_x}{K}X_nX_{n+1} - \frac{b_x}{K}X_{n+1}Y_n - u_xX_{n+1} - \beta X_{n+1}Y_n,\\
\frac{Y_{n+1}-Y_n}{\phi_2(h)} &= b_yY_n - \frac{b_y}{K}X_nY_{n+1} - \frac{b_y}{K}Y_nY_{n+1} - u_yY_{n+1} + \beta X_nY_n.
\end{aligned} \tag{3.16}$$

The required discrete model is obtained after simplification as follows:

$$\begin{aligned}
X_{n+1} &= \frac{X_n(1+\phi_1(h)b_x)}{1+\phi_1(h)\left(\frac{b_x}{K}X_n + \frac{b_x}{K}Y_n + u_x + \beta Y_n\right)},\\
Y_{n+1} &= \frac{Y_n\{1+\phi_2(h)(b_y+\beta X_n)\}}{1+\phi_2(h)\left(\frac{b_y}{K}X_n + \frac{b_y}{K}Y_n + u_y\right)},
\end{aligned} \tag{3.17}$$

where $\phi_1(h)$ and $\phi_2(h)$ have the same expression as in (3.11). It is worth mentioning that the discrete model (3.17) is positive.
One can find the same four fixed points of (3.17) as it were in the continuous case. The stability properties of each fixed point are presented in the following theorem.

Theorem 3.6. *The system (3.17) is stable around the fixed point*

(i) $E_0^H = (0,0)$ *if* $b_x < u_x$ *and* $b_y < u_y$.

(ii) $E_1^H = (\bar{X},0)$ *if* $b_x > u_x$ *and* $R_0 < 1$, *where* $\bar{X} = K\left(1-\frac{u_x}{b_x}\right)$ *and* $R_0 = \frac{b_y}{b_x}\frac{u_x}{u_y} + \frac{\beta}{u_y}\bar{X}$.

(iii) $E_2^H = (0,\bar{Y})$ *if* $b_y > u_y$ *and* $\frac{b_xu_y}{b_y} < u_x + \beta K\left(1-\frac{u_y}{b_y}\right)$, *where* $\bar{Y} = K\left(1-\frac{u_y}{b_y}\right)$.

(iv) E_H^* *if* $b_x > u_x$, $b_y > u_y$, $\frac{b_xu_y}{b_y} > u_x + \beta K\left(1-\frac{u_x}{b_x}\right)$ *and* $R_0 > 1$.

3.3.3 Discrete model for perfect vertical and no horizontal transmission

For convenience, we first express the continuous system (3.8) as

$$\begin{aligned}
\frac{dX}{dt} &= b_xX - \frac{b_xX^2}{K} - \frac{b_xXY}{K} - u_xX,\\
\frac{dY}{dt} &= b_yY - \frac{b_yXY}{K} - \frac{b_yY^2}{K} - u_yY.
\end{aligned} \tag{3.18}$$

In this case, we consider the non-local approximations (3.10) with $e=0$, $\beta=0$. Note that here $\phi_1(h) \to h$ when $\beta \to 0$. Then the system (3.18) reads

$$\begin{aligned}
\frac{X_{n+1}-X_n}{h} &= b_xX_n - \frac{b_x}{K}X_nX_{n+1} - \frac{b_x}{K}X_{n+1}Y_n - u_xX_{n+1},\\
\frac{Y_{n+1}-Y_n}{h} &= b_yY_n - \frac{b_y}{K}X_nY_{n+1} - \frac{b_y}{K}Y_nY_{n+1} - u_yY_{n+1}.
\end{aligned} \tag{3.19}$$

On simplifications, we obtain our desired discrete model as

$$
\begin{aligned}
X_{n+1} &= \frac{X_n(1+hb_x)}{1+h\left(\frac{b_x}{K}X_n+\frac{b_x}{K}Y_n+u_x\right)},\\
Y_{n+1} &= \frac{Y_n(1+hb_y)}{1+h\left(\frac{b_y}{K}X_n+\frac{b_y}{K}Y_n+u_y\right)}.
\end{aligned}
\tag{3.20}
$$

This system also does not contain any negative terms, so solutions remain positive for all step-size as long as initial values are positive.

As in the continuous system (3.8), the discrete system (3.20) has same three fixed points. The stability of each fixed point can be proved similarly and has been summarized in the following theorem.

Theorem 3.7. *The system (3.20) is stable around the fixed point*

(i) $E_0^V = (0,0)$ *if* $b_x < u_x$ *and* $b_y < u_y$.

(ii) $E_1^V = (\bar{X},0)$ *if* $b_x > u_x$ *and* $\frac{b_y}{u_y} < \frac{b_x}{u_x}$.

(iii) The fixed point $E_2^V = (0,\bar{Y})$ *is always unstable.*

3.4 Numerical simulations

In this section, we present some numerical simulations to validate the similar qualitative behavior of our discrete models with its corresponding continuous models. For this, we consider the same parameter set as in Lipsitch et al. [53]: $b_x = 0.6$, $b_y = 0.4$, $u_x = 0.1$, $u_y = 0.2$, $K = 1$, $e = 0.02$. We consider different initial values $I_1 = (0.1,0.1)$, $I_2 = (0.2,0.4)$, $I_3 = (0.7,0.6)$, $I_4 = (1,0.4)$ and $I_5 = (1.2,0.15)$ for both continuous and discrete systems. Step-size $h = 0.1$ is kept fixed in all simulations for the discrete systems. If β takes the value 0.1, the parameter set satisfies conditions of Theorems 3.1(ii) and 3.4(ii). In this case, all trajectories starting from different initial points converge to the infection-free point $E_1 = (0.8333,0)$ in case of both the continuous system (3.1) (Fig. 3.1(a)) and the discrete system (3.13) (Fig. 3.1(b)). For $\beta = 0.3$, conditions of Theorems 3.1(iii) and 3.4(iii) are satisfied and all solution trajectories reach to the coexistence equilibrium point $E^* = (0.1818,0.4545)$ for both the systems as shown in Fig. 3.1(c)-3.1(d). These figures indicate that the behavior of the continuous system (3.1) and the discrete system (3.13) are qualitatively similar.

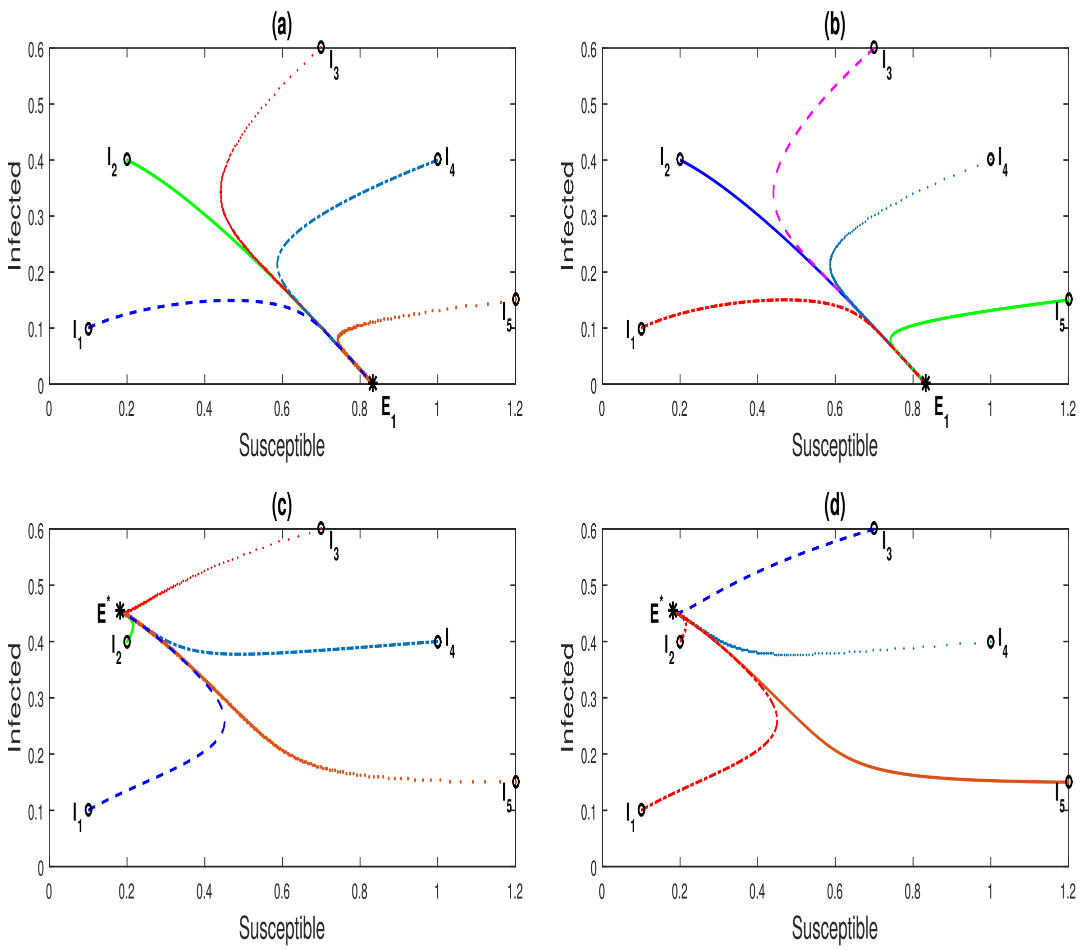

Figure 3.1: Phase portraits of the continuous system (3.1) (left panel) and discrete system (3.13) (right panel). Figs. (**a**) and (**b**) show that all trajectories converge to the disease-free equilibrium point $E_1 = (0.8333, 0)$ for $\beta = 0.1$. Figs. (**c**) and (**d**) depict that all trajectories converge to the endemic equilibrium point $E^* = (0.1818, 0.4545)$ for $\beta = 0.3$. Other parameters are $b_x = 0.6$, $b_y = 0.4$, $u_x = 0.1$, $u_y = 0.2$, $K = 1$, $e = 0.02$ as in [53]. Step-size for the discrete model is considered as $h = 0.1$.

To show dynamic consistency of the continuous system (3.7) and discrete system (3.17), we plotted the phase portraits of both systems in Fig. 3.2. We considered the same initial points, the same set of parameter values as in [53] with $e = 0$ and the same step-size as in Fig. 3.1. The conditions of Theorem 3.2(ii) and Theorem 3.6(ii) are satisfied when $\beta = 0.1$. In this case, all trajectories of both the systems converge to the point $E_1^H = (1, 0)$ (Figs. 3.2(a)-3.2(b)). For $\beta = 0.3$, conditions of Theorem 3.2(iv) and Theorem 3.6(iv) are satisfied. Consequently, all trajectories reach to the interior point $E_H^* = (0.0476, 0.5952)$ (Figs. 3.2(c)-3.2(d)). If we take $\beta = 0.42$ then all conditions of Theorem 3.2(iii) and Theorem 3.6(iii) are satisfied. All trajectories in this case converge to the susceptible-free equilibrium point $E_2^H = (0, 0.6)$ in both cases (Figs. 3.2(e)-3.2(f)).

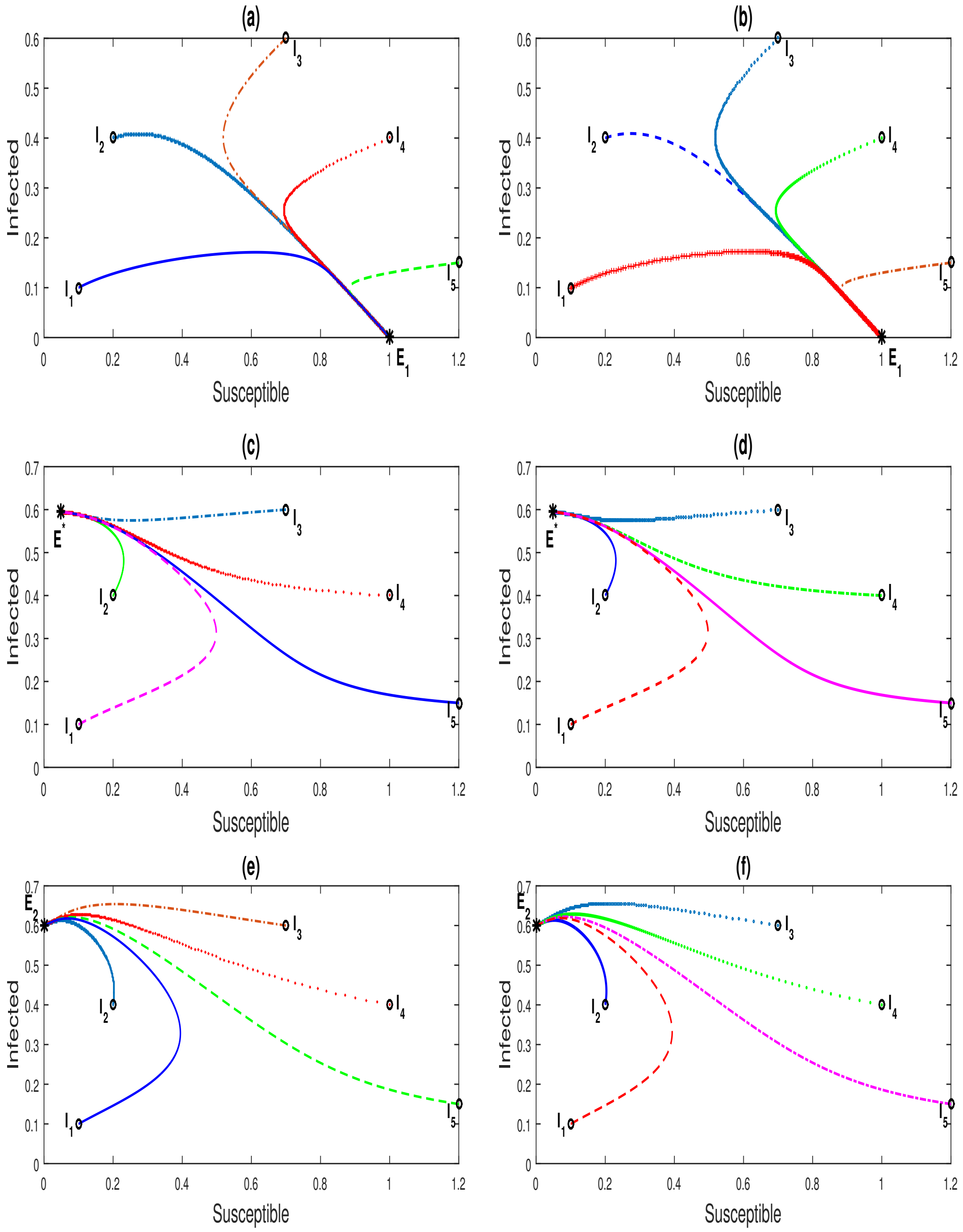

Figure 3.2: Phase portraits of the continuous system (3.7) (left panel) and discrete system (3.17) (right panel). Figs. (**a**) and (**b**) show that all trajectories converge to the disease-free point $E_1^H = (1,0)$ for $\beta = 0.1$. Figs. (**c**) and (**d**) depict that all trajectories converge to the endemic point $E^* = (0.0476, 0.5952)$ for $\beta = 0.3$. Figs. (**e**) and (**f**) show that all trajectories converge to the susceptible-free point $E_2^H = (0, 0.6)$ for $\beta = 0.42$. Other parameters are $b_x = 0.6$, $b_y = 0.4$, $u_x = 0.1$, $u_y = 0.2$, $K = 1.2$ as in [53]. Step-size for the discrete model is considered as $h = 0.1$.

To observe dynamical consistency of the discrete system (3.20) with its corresponding continuous system (3.8), we plotted phase diagrams of both systems in Fig. 3.3. The same parameter set as in [53] with $e = 0$, $\beta = 0$ was considered and the initial points, step-size remained unchanged. Phase portraits of the continuous system (Fig. 3.3(a)) and that of the discrete system (Fig. 3.3(b)) show that all trajectories reach to the infection-free point $E_1^V = (1,0)$, indicating the dynamic consistency of both systems.

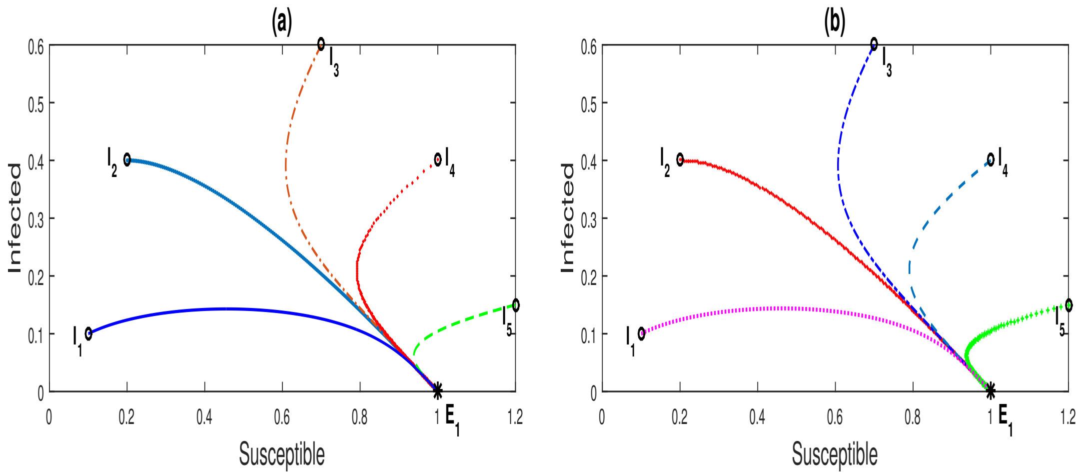

Figure 3.3: Phase portraits of the continuous system (3.8) (Fig. **a**) and that of the discrete system (3.20) (Fig. **b**) indicate that all trajectories converge to the infection-free point $E_1^V = (1,0)$ in each case. The parameters are $b_x = 0.6$, $b_y = 0.4$, $u_x = 0.1$, $u_y = 0.2$ and $K = 1.2$ as in [53]. Step-size for the discrete model is considered as $h = 0.1$.

3.5 Summary

We here considered a continuous-time epidemic model, where infection spreads through imperfect vertical transmission and horizontal transmission in a density-dependent asexual host population. Stability of different equilibrium points are presented with respect to the basic reproduction number and relative birth & death rates of susceptible & infected hosts. A discrete version of the continuous system is constructed following nonlocal approximation technique and its dynamics have been shown to be identical with that of the continuous system. The proposed discrete model is shown to be positive, implying that its solutions remains positive for all future time whenever it starts with positive initial value. The dynamics of the discrete model have been shown to be independent of the step-size. Our simulation results also show dynamic consistency of the discrete models with its corresponding continuous model. Two submodels of the general discrete model have also been shown to have the identical dynamics with their continuous continuous counterparts.

4

Positivity and dynamics preserving discretization schemes for nonlinear evolution equations[1]

4.1 Introduction

In the last few years, nonstandard methods have been successfully applied to various mathematical models in science and engineering [18, 22, 16, 21, 23, 24, 19, 25, 15, 26, 27, 28, 20, 17] mainly because its solution does not depend on the step-size, maintains positivity and converges rapidly. One of the most critical tasks in the NSFD scheme is to discretize the continuous system with nonlocal discrete terms [30, 29, 12]. For example, in a nonstandard finite difference scheme, the first derivative has to be discretized as $\frac{dx}{dt} \approx \frac{x_{k+1}-x_k}{\phi(h)}$, $h = \triangle t$, where $\phi(h)$ is a real, positive and monotonic function of the step-size (h), satisfying the condition $\phi(h) = h + O(h^2)$; and/or both the linear and nonlinear terms have to be represented nonlocally on the discrete computational lattice [30, 5, 12], e.g., $x = 2x - x \approx 2x_k - x_{k+1}$, $x^2 \approx x_k x_{k+1}$, $x^3 \approx 2x_k^3 - x_k^2 x_{k+1}$. Unfortunately, there is no general rule for constructing the denominator function as well as discretizing the nonlinear terms [5, 12]. In fact, one can construct different schemes for a given continuous-time model, but several of them can fail to converge and give desired results [56]. Some techniques for nonlocal discretization are given in [5, 12], and a methodology for calcu-

[1] *The bulk of this chapter has been published in Malaya Journal of Matematik, 12(1), 1-20, 2024.*

lating the form of the denominator function for the positive system is prescribed in [57].

Particular forms of the denominator function have been defined for continuous-time population models, where the total population is either constant (i.e., the system of differential equations can be expressed as $\frac{dL}{dt} = 0$, where L is the total population) or where total population asymptotically reaches to a constant value (i.e., the system can be expressed in the form $\frac{dL}{dt} = b - dL$, where b, d are constants). In the first case, we have to consider any equation of the given continuous system, where the first-order derivative has to be discretized by the Euler-forward method, and appropriate nonlocal approximations have to be given in the right-hand side of the equation so that positivity of the discrete system holds. Then rearrange this discrete equation as $(k+1)$-th time step dependent variable in terms of all k-th time step dependent variables. Thus, if any term of the form $(1+\alpha h)$ occurs in the newly formed discrete equation, where α is composed of one or more system parameters and h is the step-size, then the denominator function will be $\phi(h) = \frac{e^{\alpha h}-1}{\alpha}$. If, however, $\alpha = 0$ then the denominator function can be taken as $\phi(h) = h$ (see pp. 677 in [57]). The denominator function for other equations of the system will be the same. In the second case, the denominator function has to be written as $\phi(h) = \frac{e^{dh}-1}{d}$. The denominator function will also be the same for all equations of this considered system [57, 58].

In other types of system equations, the denominator functions will be different for each equation of the continuous system, and these denominator functions can be obtained by doing the same steps as mentioned in the case of the conservative system [57]. We show that such a predetermined form of denominator function may not work for higher dimensional systems. Instead of considering a predetermined denominator function, it is better to choose a denominator function from the stability condition of the system. The objective of this chapter is to define some uniform rules for the nonlocal discretization of a continuous system to preserve the positivity and dynamic consistency of the discrete system with its continuous mother system. Several highly nonlinear systems from population biology have been considered to demonstrate the application of prescribed rules. In each example, we prove that the proposed NSFD models are positive for all step-size and dynamically consistent.

The rest of this chapter is arranged in the following sequence. The Section 4.2 represents the nonlocal discretization techniques for a system of differential equations. The next Section 4.3 contains the discretization of a two-dimensional epidemic model following the rules developed in the previous section. A three-dimensional epidemic model is discretized in Section 4.4. A three-dimensional ecological model is discretized with the previously described rules in Section 4.5. This chapter ends with a summary in Section 4.6.

4.2 Nonlocal discretization techniques

One of the essential tasks in the NSFD method is the nonlocal representation of linear and nonlinear terms that appear in the differential equation. The primary goal of such discretization is to maintain the positivity of the constructed discrete system and to preserve the dynamics of the continuous system. We will demonstrate the nonlocal discretization technique with a two-dimension system for simplicity. The method, however, can be extended to any higher dimensional system of first-order differential equations.

Consider a two-dimensional continuous system of first-order differential equations:

$$\begin{aligned} \frac{dx}{dt} &= f(x,y), \\ \frac{dy}{dt} &= g(x,y), \end{aligned} \tag{4.1}$$

where f and g are C^1 functions. The following techniques may be adopted for dynamic preserving nonlocal discretization.

(R1) If there is any constant term (say, α) with a negative (or positive) sign in the first equation of (4.1), then it would be discretized as $-\frac{\alpha x_{n+1}}{x_n}$ (or α).

(R2) If there is any linear term with a negative sign in the first equation, e.g., $-ax$, a being a positive constant, then it would be discretized as $-ax_{n+1}$ to keep the positivity for x_{n+1}. However, if the sign is positive, it would be discretized as ax_n.

(R3) For any higher degree term with a negative sign involving the first variable x only, e.g., $-ax^m(m>1)$, the nonlocal approximation would be $-ax_{n+1}x_n^{m-1}$. On the contrary, if the higher degree term appears with a positive sign, it would be expressed as ax_n^m.

(R4) If there is any product term containing first variable x and second variable y of the form $-axy$ (or axy) in the first equation, then it would be discretized by $-ax_{n+1}y_n$ (or ax_ny_n).

(R5) If any function $\phi(y)$ of the second variable appears alone (i.e., without involving the first variable x) in the first equation, then it will be discretized as $\frac{x_{n+1}\phi(y_n)}{x_n}$ (or $\phi(y_n)$) if there is a negative (or positive) sign before $\phi(y)$.

(R6) In the first equation, the second variable y will always be discretized by y_n and can't be y_{n+1} as we have to maintain a sequential form of calculation for using the initial condition. This rule is also valid for all other variables except the first one.

(R7) Similar terms appearing in different equations must be discretized similarly. For example, if the first equation contains the term axy and the second equation also contains axy then it will be replaced by ax_ny_n in both the equations. However, if the first equation contains $-axy$ and the second equation contains axy, then the nonlocal discretization will be

$-ax_{n+1}y_n$ and $ax_{n+1}y_n$, respectively. If the term in the second equation is also negative, i.e., $-axy$, it would be discretized as $-ax_{n+1}y_{n+1}$. Note that y_n has to be changed by y_{n+1} as the term is placed in the second equation, and there is a negative sign before it, following (R2). Also, x_n in this term has to be expressed as x_{n+1} because it was written in the first equation. These rules are also applicable in discretizing other nonlinear terms.

(R8) For any rational function of the form $\frac{F(x,y)}{G(x,y)}$ $(G \neq 0)$, then the denominator function $G(x,y)$ will be replaced by $G(x_n,y_n)$ and the numerator function $F(x,y)$ will be discretized by the techniques prescribed in (R1) to (R7).

These rules are not unique, and one can find different nonlocal discretizations to construct an NSFD model for a given continuous system. What we have tried here is to define some uniform rules that one can follow while using the NSFD scheme of discretization. We here apply these rules to construct various NSFD models from their respective highly nonlinear continuous population models and show that they are dynamically consistent and the dynamics of these discrete systems are independent of the step-size.

4.3 Example 1: Continuous-time epidemic model

O'Keefe [59] has investigated the dynamics of an epidemic model having frequency-dependent disease transmission. The model reads

$$\begin{aligned} \frac{dS}{dt} &= (S+\rho I)(1-S-I) - \frac{\beta SI}{S+I} - \mu S, \\ \frac{dI}{dt} &= \frac{\beta SI}{S+I} - (\alpha+\mu)I, \end{aligned} \tag{4.2}$$

where S and I represent, respectively, the densities of susceptible and infective hosts at time t. Here ρ $(0 \leq \rho \leq 1)$ is the fertility coefficient of infected hosts, and β is the disease transmission rate. μ represents the natural death rate of both hosts, and the additional death of infectives due to disease is represented by α. All parameters are non-negative from a biological point of view. The following stability results are known from [59].

Theorem 4.1. *The disease-free equilibrium point* $E_1^e = (1-\mu, 0)$ *always exists and it is locally asymptotically stable if* $\mu < 1$, $\beta < (\alpha+\mu)$. *The endemic (interior) equilibrium point* $E^{e*} = (S^{e*}, I^{e*})$, *where* $S^{e*} = \frac{A(\alpha+\mu)}{B}$ *and* $I^{e*} = \frac{A(\beta-\alpha-\mu)}{B}$ *with* $A = -\alpha-\mu-\alpha(\alpha+\mu)+\beta(\alpha+\mu)+\rho(\alpha+\mu)-\beta\rho$, $B = \beta\{\rho(\alpha+\mu)-\alpha-\mu-\beta\rho\}$, *exists and is locally asymptotically stable whenever* $\beta > \alpha+\mu$, $A < 0$.

We now construct the NSFD counterpart of the model (4.2) following the rules defined in Section 4.2.

4.3.1 NSFD model and its analysis

For convenience, we rewrite the continuous model (4.2) as

$$\begin{aligned}\frac{dS}{dt} &= S - S^2 - (1+\rho)SI + \rho I - \rho I^2 - \frac{\beta SI}{S+I} - \mu S,\\ \frac{dI}{dt} &= \frac{\beta SI}{S+I} - (\alpha+\mu)I.\end{aligned} \tag{4.3}$$

Using the previous nonlocal discretization techniques (R1)-(R8), the continuous system (4.3) can easily be transformed to the following NSFD system:

$$\begin{aligned}\frac{S_{n+1}-S_n}{\xi_1(h)} &= S_n - S_nS_{n+1} - (1+\rho)S_{n+1}I_n + \rho I_n - \frac{\rho S_{n+1}I_n^2}{S_n} - \frac{\beta S_{n+1}I_n}{S_n+I_n} - \mu S_{n+1},\\ \frac{I_{n+1}-I_n}{\xi_2(h)} &= \frac{\beta S_{n+1}I_n}{S_n+I_n} - (\alpha+\mu)I_{n+1},\end{aligned} \tag{4.4}$$

where the denominator functions $\xi_i(h)$, $i = 1,2$, are such that $\xi_i(h) > 0$, $\forall h > 0$ and $\xi_i(h) = h + O(h^2)$. One should notice that the terms ρI and ρI^2 of the first equation of (4.3) have been discretized following (R5).

Rearranging (4.4), we get

$$\begin{aligned}S_{n+1} &= \frac{S_n\left\{1+\xi_1(h)\left(1+\frac{\rho I_n}{S_n}\right)\right\}}{1+\xi_1(h)\left\{S_n+(1+\rho)I_n+\frac{\rho I_n^2}{S_n}+\frac{\beta I_n}{S_n+I_n}+\mu\right\}},\\ I_{n+1} &= \frac{I_n\left(1+\xi_2(h)\frac{\beta S_{n+1}}{S_n+I_n}\right)}{1+\xi_2(h)(\alpha+\mu)}.\end{aligned} \tag{4.5}$$

As expected, the NSFD system (4.5) is positively invariant. Therefore, all solutions remain positive if they start with a positive initial value. The discrete system (4.5) has the same equilibrium points as the continuous system (4.2). The variational matrix at any arbitrary fixed point (S,I) of (4.5) is given by

$$J(S,I) = \begin{pmatrix} a_{11} & a_{12} \\ a_{21} & a_{22} \end{pmatrix}, \tag{4.6}$$

where

$$a_{11} = \frac{1+\xi_1(h)}{1+\xi_1(h)\left\{S+(1+\rho)I+\frac{\rho I^2}{S}+\frac{\beta I}{S+I}+\mu\right\}} - \frac{\left\{1+\xi_1(h)\left(1+\frac{\rho I}{S}\right)\right\}\xi_1(h)S\left(1-\frac{\rho I^2}{S^2}-\frac{\beta I}{(S+I)^2}\right)}{\left[1+\xi_1(h)\left\{S+(1+\rho)I+\frac{\rho I^2}{S}+\frac{\beta I}{S+I}+\mu\right\}\right]^2},$$

$$a_{12} = \frac{\rho\xi_1(h)}{1+\xi_1(h)\left\{S+(1+\rho)I+\frac{\rho I^2}{S}+\frac{\beta I}{S+I}+\mu\right\}} - \frac{\left\{1+\xi_1(h)\left(1+\frac{\rho I}{S}\right)\right\}\xi_1(h)\left\{(1+\rho)S+2\rho I+\frac{\beta S^2}{(S+I)^2}\right\}}{\left[1+\xi_1(h)\left\{S+(1+\rho)I+\frac{\rho I^2}{S}+\frac{\beta I}{S+I}+\mu\right\}\right]^2},$$
$$a_{21} = \frac{\xi_2(h)\frac{\beta I}{S+I}}{1+\xi_2(h)(\alpha+\mu)}a_{11} - \frac{\xi_2(h)\frac{\beta SI}{(S+I)^2}}{1+\xi_2(h)(\alpha+\mu)},$$
$$a_{22} = \frac{1+\xi_2(h)\frac{\beta S}{S+I}}{1+\phi_2(\alpha+\mu)} + \frac{\xi_2(h)\frac{\beta I}{S+I}}{1+\xi_2(h)(\alpha+\mu)}a_{12} - \frac{\xi_2(h)\frac{\beta SI}{(S+I)^2}}{1+\xi_2(h)(\alpha+\mu)}.$$

The following stability results for the discrete system (4.5) can be proved.

Theorem 4.2. *The disease-free fixed point $E_1^e = (1-\mu, 0)$ is locally asymptotically stable if $\mu < 1$, $\beta < \alpha+\mu$ and the endemic equilibrium point $E^{e*} = (S^{e*}, I^{e*})$ is locally asymptotically stable if $\beta > \alpha+\mu$ and $A < 0$, where $A = -\alpha-\mu-\alpha(\alpha+\mu)+\beta(\alpha+\mu)+\rho(\alpha+\mu)-\beta\rho$, i.e., E^{e*} is stable whenever it exists.*

Proof. It is not a difficult task to check that the eigenvalues evaluated at E_1^e are $\lambda_1 = \frac{1+\xi_1(h)\mu}{1+\xi_1(h)}$ and $\lambda_2 = \frac{1+\xi_2(h)\beta}{1+\xi_2(h)(\alpha+\mu)}$. Note that $0 < \lambda_1 < 1$ as $0 < \mu < 1$, and $\lambda_2 > 0$ for any positive step-size. Thus, for any $h > 0$, $\lambda_2 < 1$ if $\beta < \alpha+\mu$. Therefore, if E_1^e exists then it will be stable if $\beta < \alpha+\mu$. In this case, the interior equilibrium point E^{e*} does not exist.
At the interior equilibrium point $E^{e*} = (S^{e*}, I^{e*})$, the variational matrix is given by

$$J(E^{e*}) = \begin{pmatrix} a_{11}^* & a_{12}^* \\ a_{21}^* & a_{22}^* \end{pmatrix},$$

where

$$\begin{cases} a_{11}^* = 1 - \frac{\xi_1(h)}{G}\left\{\left(S^{e*}+\frac{\rho I^{e*}}{S^{e*}}\right) - \frac{\rho I^{e*2}}{S^{e*}} - \frac{\beta S^{e*}I^{e*}}{(S^{e*}+I^{e*})^2}\right\}, \\ a_{12}^* = \frac{\xi_1(h)}{G}\left\{\rho - S^{e*}(1+\rho) - 2\rho I^{e*} - \frac{\beta S^{e*2}}{(S^{e*}+I^{e*})^2}\right\}, \\ a_{21}^* = \frac{\xi_2(h)}{H}\left\{\frac{\beta I^{e*}}{S^{e*}+I^{e*}}a_{11}^* - \frac{\beta S^{e*}I^{e*}}{(S^{e*}+I^{e*})^2}\right\}, \\ a_{22}^* = 1 - \frac{\xi_2(h)}{H}\left\{\frac{\beta S^{e*}I^{e*}}{(S^{e*}+I^{e*})^2} - \frac{\beta I^{e*}a_{12}^*}{S^{e*}+I^{e*}}\right\}, \\ G = 1+\xi_1(h)\left(1+\frac{\rho I^{e*}}{S^{e*}}\right), \quad H = 1+\xi_2(h)\frac{\beta S^{e*}}{S^{e*}+I^{e*}}. \end{cases}$$

We shall use Lemma 1.14 to prove the local stability of E^{e*}. One can evaluate

$$\begin{aligned} \mathrm{trace}(J(E^{e*})) &= a_{11}^* + a_{22}^* \\ &= \left\{1 - \frac{\xi_1(h)}{G}\left(S^{e*}+\frac{\rho I^{e*}}{S^{e*}}\right)\right\} + \frac{\xi_1(h)}{G}\left(\frac{\rho I^{e*2}}{S^{e*}} + \frac{\beta S^{e*}I^{e*}}{(S^{e*}+I^{e*})^2}\right) + \left\{1 - \left(\frac{I^{e*}}{S^{e*}+I^{e*}}\right)\left(\frac{\beta S^{e*}\xi_2(h)}{(S^{e*}+I^{e*})H}\right)\right\} \\ &\quad + \frac{\beta I^{e*}\xi_1(h)\xi_2(h)}{(S^{e*}+I^{e*})GH}\left\{\rho(1-S^{e*}-I^{e*}) - S^{e*} - \left(\rho I^{e*} + \frac{\beta S^{e*2}}{(S^{e*}+I^{e*})^2}\right)\right\} \\ &= \left\{1 - \frac{\xi_1(h)}{G}\left(S^{e*}+\frac{\rho I^{e*}}{S^{e*}}+\frac{\beta S^{e*}I^{e*}\xi_2(h)}{(S^{e*}+I^{e*})H}\right)\right\} + \left\{1 - \left(\frac{I^{e*}}{S^{e*}+I^{e*}}\right)\left(\frac{\beta S^{e*}\xi_2(h)}{(S^{e*}+I^{e*})H}\right)\right\} \\ &\quad + \frac{\xi_1(h)}{G}\left(\frac{\rho I^{e*2}}{S^{e*}} + \frac{\beta S^{e*}I^{e*}}{(S^{e*}+I^{e*})^2}\right)\left(1 - \frac{\beta S^{e*}\xi_2(h)}{(S^{e*}+I^{e*})H}\right) + \frac{\xi_1(h)\xi_2(h)\beta I^{e*}}{(S^{e*}+I^{e*})GH}\rho(1-S^{e*}-I^{e*}). \end{aligned}$$

Following the existence condition of E^{e*}, we have $S^{e*}+I^{e*} = \frac{\beta A}{B} < 1$ and then $S^{e*} + \frac{\beta S^{e*}I^{e*}\xi_2(h)}{(S^{e*}+I^{e*})H} = \frac{1}{H}(S^{e*}+\xi_2(h)\beta S^{e*}) < 1$ and also $\xi_1(h)\left(S^{e*}+\frac{\rho I^{e*}}{S^{e*}}\right) < G$ and $\frac{\xi_2(h)\beta S^{e*}}{S^{e*}+I^{e*}} < H$.
Thus, $\left\{1 - \frac{\xi_1(h)}{G}\left(S^{e*}+\frac{\rho I^{e*}}{S^{e*}}+\frac{\beta S^{e*}I^{e*}\xi_2(h)}{(S^{e*}+I^{e*})H}\right)\right\} > 0$. Hence we get $\mathrm{trace}(J(E^{e*})) > 0$.

Also,

$$\begin{aligned}\det(J(E^{e*})) &= a_{11}^*a_{22}^* - a_{12}^*a_{21}^*\\ &= a_{11}^*\left[1-\tfrac{\xi_2(h)}{H}\left\{\tfrac{\beta S^{e*}I^{e*}}{(S^{e*}+I^{e*})^2}-\tfrac{\beta I^{e*}}{S^{e*}+I^{e*}}a_{12}^*\right\}\right]-a_{12}^*\tfrac{\xi_2(h)}{H}\left\{\tfrac{\beta I^{e*}}{S^{e*}+I^{e*}}a_{11}^*-\tfrac{\beta S^{e*}I^{e*}}{(S^{e*}+I^{e*})^2}\right\}\\ &= a_{11}^*-\tfrac{\beta S^{e*}I^{e*}\xi_2(h)}{(S^{e*}+I^{e*})^2H}(a_{11}^*-a_{12}^*).\end{aligned}$$

Simple algebraic manipulations show that

$$\begin{aligned}1-\det(J(E^{e*})) &= 1-a_{11}^*+\tfrac{\beta S^{e*}I^{e*}\xi_2(h)}{(S^{e*}+I^{e*})^2H}(a_{11}^*-a_{12}^*)\\ &= \tfrac{\xi_1(h)}{G}\left\{S^{e*}+\tfrac{\rho I^{e*}(1-I^{e*})}{S^{e*}}-\tfrac{\beta S^{e*}I^{e*}}{(S^{e*}+I^{e*})^2}\right\}+\tfrac{\beta S^{e*}I^{e*}\xi_2(h)}{(S^{e*}+I^{e*})^2H}\left(1-\tfrac{\rho\xi_1(h)}{G}+\tfrac{\beta S^{e*}\xi_1(h)}{(S^{e*}+I^{e*})G}\right)\\ &\quad+\tfrac{\beta S^{e*}I^{e*}\xi_1(h)\xi_2(h)}{(S^{e*}+I^{e*})^2GH}\left(\tfrac{\rho I^{e*2}}{S^{e*}}+\rho S^{e*}+\rho I^{e*}\right)\\ &= \tfrac{\xi_1(h)}{G}\left\{S^{e*}+\tfrac{\rho I^{e*}}{S^{e*}}(1-I^{e*})\right\}+\tfrac{\beta S^{e*}I^{e*}}{(S^{e*}+I^{e*})^2}\tfrac{1}{GH}\{-H\xi_1(h)+G\xi_2(h)\\ &\quad+\xi_1(h)\xi_2(h)\left(-\rho+\tfrac{\beta S^{e*}}{S^{e*}+I^{e*}}\right)\Big\}+\tfrac{\beta S^{e*}I^{e*}\xi_1(h)\xi_2(h)}{(S^{e*}+I^{e*})^2GH}\left(\tfrac{\rho I^{e*2}}{S^{e*}}+\rho S^{e*}+\rho I^{e*}\right)\\ &= \tfrac{\xi_1(h)}{G}\left\{S^{e*}+\tfrac{\rho I^{e*}}{S^{e*}}(1-I^{e*})\right\}+\tfrac{\beta S^{e*}I^{e*}}{(S^{e*}+I^{e*})^2}\tfrac{1}{GH}\{\xi_2(h)-\xi_1(h)\}\\ &\quad+\tfrac{\beta S^{e*}I^{e*}\xi_1(h)\xi_2(h)}{(S^{e*}+I^{e*})^2GH}\left\{(1-\rho)+\tfrac{\rho I^{e*}}{S^{e*}}+\tfrac{\rho I^{e*2}}{S^{e*}}+\rho S^{e*}+\rho I^{e*}\right\}.\end{aligned}$$

Again,

$$\begin{aligned}1-\operatorname{trace}(J(E^{e*}))+\det(J(E^{e*})) &= 1-(a_{11}^*+a_{22}^*)+(a_{11}^*a_{22}^*-a_{12}^*a_{21}^*)\\ &= 1-a_{22}^*-\tfrac{\beta S^{e*}I^{e*}\xi_2(h)}{(S^{e*}+I^{e*})^2H}(a_{11}^*-a_{12}^*)\\ &= \tfrac{\beta I^{e*}\xi_2(h)}{(S^{e*}+I^{e*})^2H}\{S^{e*}(1-a_{11}^*)-I^{e*}a_{12}^*\}\\ &= \tfrac{\beta I^{e*}\xi_1(h)\xi_2(h)}{(S^{e*}+I^{e*})^2GH}\left(S^{e*2}+S^{e*}I^{e*}+\rho S^{e*}I^{e*}+\rho I^{e*2}\right)>0.\end{aligned}$$

One can easily check that $1+\operatorname{trace}(J(E^{e*}))+\det(J(E^{e*}))>0$, as $\operatorname{trace}(J(E^{e*}))>0$ and also $1-\operatorname{trace}(J(E^{e*}))+\det(J(E^{e*}))>0$. If we choose the denominator functions $\xi_1(h)$ and $\xi_2(h)$ such that $\xi_2(h)\geq\xi_1(h)$, $\forall h>0$, then $1-\det(J(E^{e*}))$ is also positive. An obvious choice is $\xi_i(h)=h$, $i=1,2$, $\forall h>0$. Thus, the interior equilibrium point E^{e*} is stable whenever it exists. Hence the theorem is proven. □

Remark 4.3. *The system* (4.2) *does not satisfy the conservation law. In such a case, following Mickens [57] rules, the denominator functions for the first and second equations will be* $\xi_1(h)=\frac{e^{\mu h}-1}{\mu}$ *and* $\xi_2(h)=\frac{e^{(\alpha+\mu)h}-1}{\alpha+\mu}$, *respectively. To hold the condition* $1-\det(J(E^{e*}))>0$, *the denominator functions* $\xi_i(h)$, $i=1,2$, *have to satisfy* $\xi_2(h)\geq\xi_1(h)$. *However, as mentioned above, the denominator functions* $\xi_1(h)$ *and* $\xi_2(h)$ *do not satisfy this restriction for the non-zero value of* α.

4.3.2 Numerical experiments

Again, we construct the following Euler discrete system for the continuous-time system (4.2)

$$\begin{aligned}S_{n+1} &= S_n+h\left\{(S_n+\rho I_n)(1-S_n-I_n)-\frac{\beta S_nI_n}{S_n+I_n}-\mu S_n\right\},\\ I_{n+1} &= I_n+h\left\{\frac{\beta S_nI_n}{S_n+I_n}-(\alpha+\mu)I_n\right\},\end{aligned}\tag{4.7}$$

and compare its dynamics with the NSFD discrete system (4.5). We have plotted bifurcation diagrams for both the systems taking h as the bifurcation parameter (Figure 4.1). It shows that the dynamics of NSFD system (4.5) is independent of the step-size (Figure 4.1a), but the Euler discrete system (4.7) shows step-size dependent dynamics (Figure 4.1b) and produces spurious behaviour for higher step-size. Therefore, the Euler-discrete model is dynamically inconsistent, but the NSFD model is dynamically consistent.

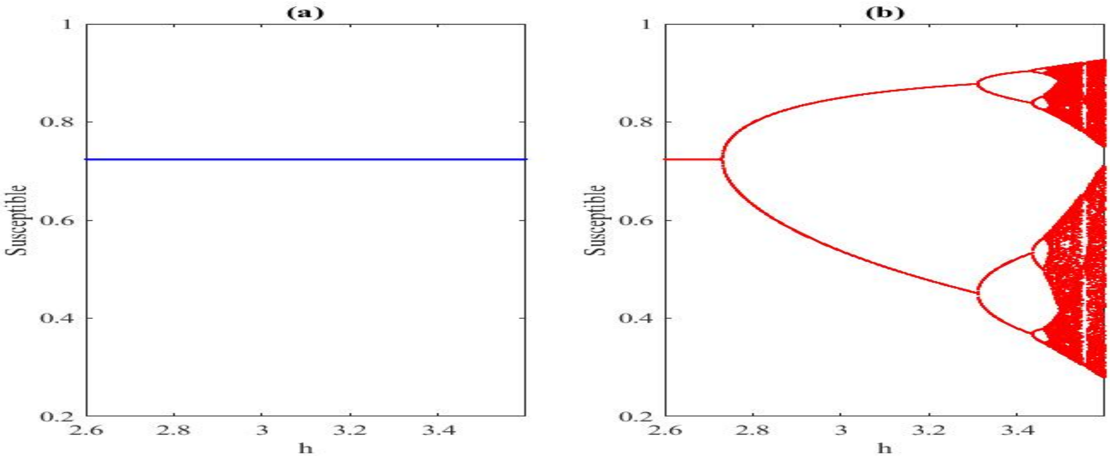

Figure 4.1: (**a**) Bifurcation diagram of the susceptible population with respect to step-size (h) for NSFD system (4.5). It shows that the population is stable for any positive value of the step-size. (**b**) Bifurcation diagram of the susceptible population with respect to step-size (h) for Euler discrete system (4.7). It shows that the population becomes unstable as step-size h exceeds 2.73. Parameters are $\rho = 0.65$, $\beta = 0.45$, $\mu = 0.23$, $\alpha = 0.2$.

4.4 Example 2: Continuous-time epidemic model

Fayeldi et al. [60] have studied the following SIR (susceptible-infective-recovered) epidemic model with constant birth and nonmonotonic incidence rate:

$$\begin{aligned} \frac{dS}{dt} &= b - dS - \frac{kSI}{1+\alpha I^2}, \\ \frac{dI}{dt} &= \frac{kSI}{1+\alpha I^2} - (d+\mu)I, \\ \frac{dR}{dt} &= \mu I - dR, \end{aligned} \tag{4.8}$$

where S, I and R denote the numbers of susceptible, infective and recovered individuals at time t. The parameters b and d represent, respectively, the recruitment and natural death rates of the host population; μ is the natural recovery rate of the infected individuals. The term $\frac{kSI}{1+\alpha I^2}$ is the nonmonotone incidence rate, where k is the disease transmission coefficient and α measures the inhibitory effect. Further description of the model can be seen in [60, 61].

4.4.1 Stability results of the continuous-time epidemic model

The model (4.8) has been analyzed in [60]. It has two equilibrium points, viz., the disease-free equilibrium point $E_1 = \left(\frac{b}{d}, 0, 0\right)$ and the interior fixed point $E^* = (S^*, I^*, R^*)$, where $S^* = \frac{1}{d}\{b-(d+\mu)I^*\}$, $I^* = \frac{-k+\sqrt{k^2-4d^2\alpha(1-R_0)}}{2\alpha d}$ and $R^* = \frac{\mu I^*}{d}$, with $R_0 = \frac{bk}{d(d+\mu)}$. Stability results of the equilibrium points are stated in the following theorems.

Theorem 4.4. *[60] The continuous system* (4.8) *is locally asymptotically stable around the fixed point E_1 if $R_0 < 1$, and it is stable around the fixed point E^* if $R_0 > 1$.*

We now use the nonlocal discretization techniques (R1) to (R8) for the construction of the NSFD model corresponding to the continuous-time model (4.8).

4.4.2 Construction of NSFD model and its analysis

The first-order derivative $\frac{dS}{dt}$ will be replaced by $\frac{S_{n+1}-S_n}{\phi_1(h)}$, where $\phi_1(h) > 0$ and can be expressed as $\phi_1(h) = h + O(h^2)$. The constant term on the right-hand side will be left unaltered following (R1) because its sign is positive. Observe that S appears in the first equation of system (4.8) with a negative sign, indicating that it has to be replaced by S_{n+1}, following (R2). The nonlinear term $\frac{SI}{1+\alpha I^2}$ is present in both the first and second equations of system (4.8) with opposite signs. The negative sign of this term in the first equation indicates that we have to replace it by $\frac{S_{n+1}I_n}{1+\alpha I_n^2}$, following (R7) & (R8). Note that we can not replace I_n by I_{n+1} in the first equation because the sequential order will be lost. Similarly, the linear term I, which appears in the second and third equations of system (4.8) with opposite signs, has to be replaced by I_{n+1}, following (R2) and (R7). Also, to hold the positivity condition, the negative term $-dR$ in the third equation of system (4.8) has to be replaced by $-dR_{n+1}$, following (R2). Based on these nonlocal discretizations, we obtain the following discrete system corresponding to continuous system (4.8):

$$\begin{aligned}
\frac{S_{n+1}-S_n}{\phi_1(h)} &= b - dS_{n+1} - \frac{kS_{n+1}I_n}{1+\alpha I_n^2}, \\
\frac{I_{n+1}-I_n}{\phi_2(h)} &= \frac{kS_{n+1}I_n}{1+\alpha I_n^2} - (d+\mu)I_{n+1}, \\
\frac{R_{n+1}-R_n}{\phi_3(h)} &= \mu I_{n+1} - dR_{n+1},
\end{aligned} \tag{4.9}$$

where $\phi_i(h)$, $i = 1, 2, 3$, are denominator functions such that $\phi_i(h) > 0$ and $\phi_i(h) = h + O(h^2)$. After rearranging, one have

$$\begin{aligned} S_{n+1} &= \frac{S_n + b\phi_1(h)}{1 + \phi_1(h)\left(d + \frac{kI_n}{1+\alpha I_n^2}\right)}, \\ I_{n+1} &= \frac{I_n\left(1 + \frac{\phi_2(h)kS_{n+1}}{1+\alpha I_n^2}\right)}{1 + \phi_2(h)(d+\mu)}, \\ R_{n+1} &= \frac{R_n + \phi_3(h)\mu I_{n+1}}{1 + \phi_3(h)d}. \end{aligned} \tag{4.10}$$

It is to be noted that all terms in the right-hand side of (4.10) are positive and therefore $S_n > 0$, $I_n > 0$, $R_n > 0$, for all n and any value of the step-size h when initial values are positive.

Next, we show that the fixed points of the discrete system (4.10) are the same as in the continuous system (4.8) and their linear stability properties are also the same. Equilibrium points or fixed points of (4.10) are determined by substituting $S_{n+1} = S_n$, $I_{n+1} = I_n$, $R_{n+1} = R_n$ in (4.10) and then solving the following simultaneous equations for S_n, I_n, R_n:

$$\begin{aligned} S_n &= \frac{S_n + b\phi_1(h)}{1 + \phi_1(h)\left(d + \frac{kI_n}{1+\alpha I_n^2}\right)}, \\ I_n &= \frac{I_n\left(1 + \frac{\phi_2(h)kS_n}{1+\alpha I_n^2}\right)}{1 + \phi_2(h)(d+\mu)}, \\ R_n &= \frac{R_n + \phi_3(h)\mu I_n}{1 + \phi_3(h)d}. \end{aligned}$$

On simplifications, one can obtain the same equilibrium points E_1 and E^* as in the continuous case. The variational matrix at any arbitrary fixed point (S, I, R) of (4.10) is given by

$$J(S,I,R) = \begin{pmatrix} a_{11} & a_{12} & 0 \\ a_{21} & a_{22} & 0 \\ a_{31} & a_{32} & a_{33} \end{pmatrix}, \tag{4.11}$$

where

$$\begin{cases} a_{11} = \frac{1}{1+\phi_1(h)\left(d+\frac{kI}{1+\alpha I^2}\right)}, \quad a_{12} = -\frac{\phi_1(h)k(S+b\phi_1(h))(1-\alpha I^2)}{\left\{1+\phi_1(h)\left(d+\frac{kI}{1+\alpha I^2}\right)\right\}^2(1+\alpha I^2)^2}, \\ a_{21} = \frac{\phi_2(h)kI}{\{1+\phi_2(h)(d+\mu)\}(1+\alpha I^2)} a_{11}, \\ a_{22} = \frac{1}{1+\phi_2(h)(d+\mu)}\left[1 + \frac{\phi_2(h)kI}{(1+\alpha I^2)} a_{12} + \frac{\phi_2(h)kS(1-\alpha I^2)}{(1+\alpha I^2)^2}\right], \\ a_{31} = \frac{\phi_3(h)\mu}{1+\phi_3(h)d} a_{21}, \quad a_{32} = \frac{\phi_3(h)\mu}{1+\phi_3(h)d} a_{22}, \quad a_{33} = \frac{1}{1+\phi_3(h)d}. \end{cases}$$

We have the following theorem about the stability of fixed points of (4.10).

Theorem 4.5. *The disease-free fixed point* $E_1 = \left(\frac{b}{d}, 0, 0\right)$ *is locally asymptotically stable if* $R_0 < 1$ *and the endemic fixed point* E^* *is stable if* $R_0 > 1$*, where* $R_0 = \frac{bk}{d(d+\mu)}$.

Proof. It is easy to check that the eigenvalues at E_1 are $\lambda_1 = \frac{1}{1+\phi_1(h)d}$, $\lambda_2 = \frac{1+\frac{bk\phi_2(h)}{d}}{1+\phi_2(h)(b+\mu)}$ and $\lambda_3 = \frac{1}{1+d\phi_3(h)}$. Here, $0 < |\lambda_{1,3}| < 1$ and $\lambda_2 > 0$ for any step-size $h > 0$. Thus, for any $h > 0$, $\lambda_2 < 1$ if $\frac{bk}{d} < d + \mu$, i.e., if $R_0 < 1$. Therefore, E_1 is stable if $R_0 < 1$.

At the endemic fixed point $E^* = (S^*, I^*, R^*)$, the variational matrix is given by

$$J(E^*) = \begin{pmatrix} a_{11}^* & a_{12}^* & 0 \\ a_{21}^* & a_{22}^* & 0 \\ a_{31}^* & a_{32}^* & a_{33}^* \end{pmatrix},$$

where

$$\begin{cases} a_{11}^* = \frac{1}{G}, \ a_{12}^* = -\frac{\phi_1(h)kS^*(1-\alpha I^{*2})}{(1+\alpha I^{*2})^2 G}, \ a_{21}^* = \frac{\phi_2(h)kI^*}{(1+\alpha I^{*2})H} a_{11}^*, \\ a_{22}^* = 1 + \frac{\phi_2(h)kI^*}{(1+\alpha I^{*2})H} a_{12}^* - \frac{2\phi_2(h)kS^*\alpha I^{*2}}{(1+\alpha I^{*2})^2 H}, \ a_{31}^* = \frac{\phi_3(h)\mu}{F} a_{21}^*, \ a_{32}^* = \frac{\phi_3(h)\mu}{F} a_{22}^*, \\ a_{33}^* = \frac{1}{F}, \ G = 1 + \frac{b\phi_1(h)}{S^*}, \ H = 1 + \frac{\phi_2(h)kS^*}{1+\alpha I^{*2}}, \ F = 1 + \frac{\phi_3(h)\mu I^*}{R^*}. \end{cases}$$

Note that $0 < a_{11}^* < 1$ and $0 < a_{22}^* < 1$ for any $h > 0$.
Here, one eigenvalue of the variational matrix $J(E^*)$ is $\lambda_3 = a_{33}^*$, which is always positive and less than unity for any $h > 0$. Other two eigenvalues $\lambda_i, \ i = 1, 2$, of $J(E^*)$ can be obtained by finding the eigenvalues of the matrix

$$J_1(E^*) = \begin{pmatrix} a_{11}^* & a_{12}^* \\ a_{21}^* & a_{22}^* \end{pmatrix}.$$

Here $\text{trace}(J_1(E^*)) = a_{11}^* + a_{22}^*$ and

$$\begin{aligned} \det(J_1(E^*)) &= a_{11}^* a_{22}^* - a_{12}^* a_{21}^* \\ &= a_{11}^* \left\{1 + \frac{\phi_2(h)kI^*}{(1+\alpha I^{*2})H} a_{12}^* - \frac{2\phi_2(h)kS^*\alpha I^{*2}}{(1+\alpha I^{*2})^2 H}\right\} - \frac{\phi_2(h)kI^*}{(1+\alpha I^{*2})H} a_{11}^* a_{12}^* \\ &= a_{11}^* \left(1 - \frac{2\phi_2(h)k\alpha S^* I^{*2}}{(1+\alpha I^{*2})^2 H}\right). \end{aligned}$$

Since $0 < a_{11}^* < 1$ for any $h > 0$, so $\det(J_1(E^*)) < 1$ and the condition $1 - \det(J_1(E^*)) > 0$ always holds. Simple algebraic manipulations show that

$$\begin{aligned} 1 - \text{trace}(J_1(E^*)) + \det(J_1(E^*)) &= 1 - (a_{11}^* + a_{22}^*) + a_{11}^* \left\{1 - \frac{2\phi_2(h)k\alpha S^* I^{*2}}{(1+\alpha I^{*2})^2 H}\right\} \\ &= -\frac{\phi_2(h)kI^*}{(1+\alpha I^{*2})H} \left\{-\frac{\phi_1(h)kS^*}{(1+\alpha I^{*2})G} + \frac{2\phi_1(h)k\alpha S^* I^{*2}}{(1+\alpha I^{*2})^2 G}\right\} + \frac{2\phi_2(h)k\alpha S^* I^{*2}}{(1+\alpha I^{*2})^2 H} \frac{b\phi_1(h)}{S^* G} \\ &= \frac{\phi_1(h)\phi_2(h)kI^*}{(1+\alpha I^{*2})^2 GH} \left[kS^* + 2\alpha I^* \left\{b - \frac{kS^* I^*}{(1+\alpha I^{*2})}\right\}\right] \\ &= \frac{\phi_1(h)\phi_2(h)kS^* I^*}{(1+\alpha I^{*2})^2 GH} (k + 2\alpha d I^*) > 0, \end{aligned}$$

and

$$
\begin{aligned}
1+\operatorname{trace}(J_1(E^*))+\det(J_1(E^*)) &= 1+(a_{11}^*+a_{22}^*)+a_{11}^*\left\{1-\frac{2\phi_2(h)k\alpha S^* I^{*2}}{(1+\alpha I^{*2})^2 H}\right\}\\
&= 1+a_{11}^*+\left\{1-\frac{2\phi_2(h)k\alpha S^* I^{*2}}{(1+\alpha I^{*2})^2 H}\right\}(1+a_{11}^*)-\frac{\phi_2(h)kI^*}{(1+\alpha I^{*2})H}\frac{\phi_1(h)kS^*(1-\alpha I^{*2})}{(1+\alpha I^{*2})^2 G}\\
&= 1+a_{11}^*+\left\{1-\frac{2\phi_2(h)k\alpha S^* I^{*2}}{(1+\alpha I^{*2})^2 H}\right\}(1+a_{11}^*)\\
&\qquad -\frac{\phi_2(h)kS^*}{(1+\alpha I^{*2})H}\frac{\phi_1(h)kI^*}{(1+\alpha I^{*2})G}\left\{1-\frac{2\alpha I^{*2}}{(1+\alpha I^{*2})}\right\}\\
&= a_{11}^*+\left[1-\frac{2\phi_2(h)kS^*}{(1+\alpha I^{*2})H}\frac{\alpha I^{*2}}{(1+\alpha I^{*2})}\right](1+a_{11}^*)+\frac{2\phi_1(h)\phi_2(h)k^2\alpha S^* I^{*3}}{(1+\alpha I^{*2})^3 GH}\\
&\qquad +\left\{1-\frac{\phi_1(h)\left(\frac{b}{S^*}-d\right)}{G}\frac{\phi_2(h)\frac{kS^*}{(1+\alpha I^{*2})}}{H}\right\}.
\end{aligned}
\tag{4.12}
$$

Now, we show the positivity of each term on the right hand side of (4.12). Note that $a_{11}^*=\frac{1}{G}$, so $0<a_{11}^*<1$. Using the values of G and H, one can check that $0<\frac{\phi_1(h)\left(\frac{b}{S^*}-d\right)}{G}<1$ and $0<\frac{\phi_2(h)\frac{kS^*}{(1+\alpha I^{*2})}}{H}<1$. It is then easy to see that the expression in curly bracket is positive. The third term is always positive as $\phi_1(h)$, $\phi_2(h)$, G and H are all positive. To prove that the expression in the third bracket is also positive, we note that $\frac{\alpha I^{*2}}{1+\alpha I^{*2}}<1$. Thus, if $\frac{2\phi_2(h)kS^*}{(1+\alpha I^{*2})H}<1$, then $\left\{1-\frac{2\phi_2(h)kS^*}{(1+\alpha I^{*2})H}\frac{\alpha I^{*2}}{(1+\alpha I^{*2})}\right\}>0$. The first term gives $\frac{2\phi_2(h)kS^*}{(1+\alpha I^{*2})}<H=1+\frac{\phi_2(h)kS^*}{(1+\alpha I^{*2})}\Rightarrow\frac{\phi_2(h)kS^*}{(1+\alpha I^{*2})}<1\Rightarrow$ $\phi_2(h)<\frac{(1+\alpha I^{*2})}{kS^*}=\frac{1}{(d+\mu)}$. Therefore $1+\operatorname{trace}(J_1(E^*))+\det(J_1(E^*))>0$ if $\phi_2(h)<\frac{1}{(d+\mu)}$. One can then choose the denominator function as $\phi_2(h)=\frac{1-e^{-(d+\mu)h}}{(d+\mu)}$, so that $\phi_2(h)<\frac{1}{(d+\mu)}$ holds. Also, the denominator function is in the form $\phi_2(h)=h+O(h^2)$. It is to be noted that no restriction is required on $\phi_1(h)$ and $\phi_3(h)$ to hold the stability conditions of E^*, and therefore simplest form can be considered for $\phi_1(h)$ and $\phi_3(h)$ such that $\phi_1(h)=h=\phi_3(h)$. Therefore, following Lemma 1.14, $|\lambda_i|<1$, $i=1,2$. By Theorem 1.12, the endemic fixed point E^* is stable whenever it exists, i.e., if $R_0>1$. This completes the theorem. □

Remark 4.6. *The system* (4.8) *can be written as*

$$\frac{dN}{dt}=b-dN, \tag{4.13}$$

where $N(t)=S(t)+I(t)+R(t)$ is the total population at time t. Following Mickens rule as described in [57], all the denominator functions $\phi_i(h)$, $i=1,2,3$, will be the same and it is $\phi_i(h)=\frac{e^{dh}-1}{d}$. It is to be noted that the stability condition $1+\operatorname{trace}(J(E^*))+\det(J(E^*))>0$ does not hold for this choice of denominator function. However, one can easily determine the *denominator function $\phi_2(h)$ as shown above such that the stability condition holds.*

4.4.3 Euler discrete-time epidemic model

Discretization of the continuous model (4.8) by Euler forward technique gives the following system:

$$\begin{aligned} S_{n+1} &= S_n + bh - hS_n\left(d + \frac{kI_n}{1+\alpha I_n^2}\right), \\ I_{n+1} &= I_n + hI_n\left\{\frac{kS_n}{1+\alpha I_n^2} - (d+\mu)\right\}, \\ R_{n+1} &= \mu h I_n + R_n(1-dh), \end{aligned} \tag{4.14}$$

where $h(>0)$ is the step-size. Due to the presence of negative terms on the right-hand side, the solutions are not unconditionally positive as in the case of NSFD model (4.10). Such systems are prone to exhibit spurious dynamics. The following results are known for the Euler discrete system (4.14).

Theorem 4.7. *[60] The discrete system* (4.14) *is stable around the fixed point E_1 if $R_0 < 1$, $h < \min\left\{\frac{2}{d}, \frac{2}{(1-R_0)(d+\mu)}, \frac{2}{\mu}\right\}$ and it is locally asymptotically stable around the fixed point E^* if one of the following condition holds: (a) $R_0 > R_1 > 1$ and $h < \min\left\{h^*, \frac{2}{\mu}\right\}$, or (b) $1 < R_0 < R_1$ and $h < \min\left\{h_1, h^*, \frac{2}{\mu}\right\}$, where $R_1 = \frac{kI^*}{\phi_e^*}\left\{1 + \frac{k(d+\phi_e^*+p)^2}{4d(d+\mu)(2d\alpha I^{*2}+k)}\right\}$, $h^* = \frac{d+\phi_e^*+p}{dp+\phi_e^*(d+\mu)}$, $h_1 = h^* - \frac{\sqrt{4(d+\phi_e^*+p)^2 - 16\phi_e^*(d+\mu)\left(\frac{2d\alpha I^*}{k}+1\right)}}{2\phi_e^*(d+\mu)\left(\frac{2d\alpha I^*}{k}+1\right)}$, $\phi_e^* = \frac{kI^*}{1+\alpha I^{*2}}$, $p = \frac{2\alpha(d+\mu)I^*\phi_e^*}{k}$.*

4.4.4 Numerical experiments

We perform numerical experiments to compare the dynamics and step-size dependency of the NSFD model (4.10) and Euler model (4.14). We have plotted bifurcation diagrams for both the systems (Figure 4.2) with respect to h. Population density of system (4.10) remains at its steady-state value for all h (Fig. 4.2a), indicating consistent dynamics with its continuous counterpart. It shows that the dynamic behaviour of NSFD system (4.10) is independent of the step-size. However, the dynamic behaviour of the Euler system (4.14) depends on the step-size (Figure 4.2b). Here population density remains stable for $h < 3.4647$ and becomes unstable for $h > 3.4647$. In fact, it exhibits spurious dynamics as the step-size is larger ($h > 3.4647$).

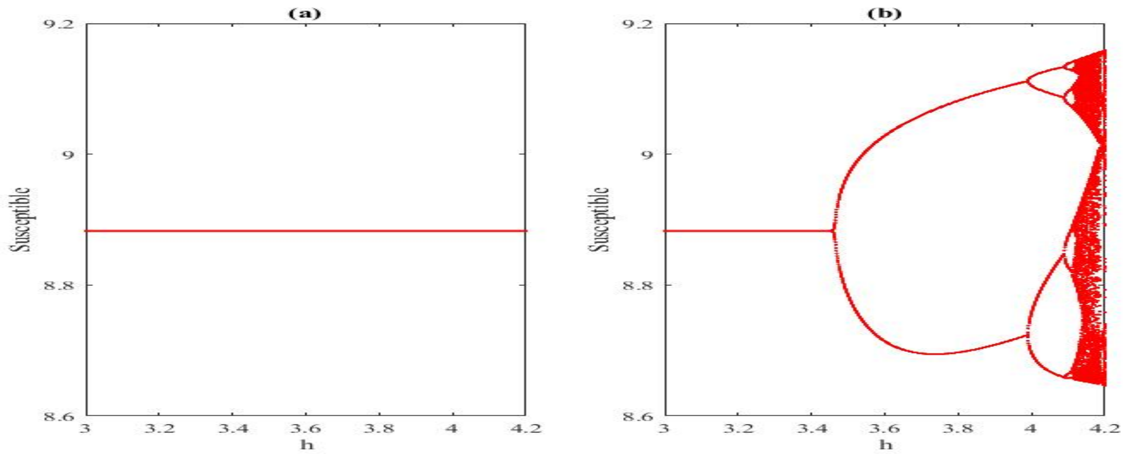

Figure 4.2: (**a**) Bifurcation diagram of the susceptible population of the NSFD system (4.10) with respect to the step-size h. It shows no instability, and population density is always maintained at its stable value for all step-size. (**b**) A similar bifurcation diagram of Euler system (4.14) shows that population density remains stable for $h < 3.4647$ and becomes unstable for $h > 3.4647$. It shows chaotic dynamics as h is further increased. Parameters are [60]: $b = 2,\ k = 0.2,\ d = 0.2,\ \mu = 0.15,\ \alpha = 10$.

4.5 Example 3: Continuous-time ecological model

Here we consider another population model in continuous time and construct the corresponding NSFD model using our nonlocal discretization technique. Chattopadhyay et al. [62] investigated the dynamics of following continuous-time plant-herbivore-parasite ecological model:

$$\begin{aligned} \frac{dx}{dt} &= rx\left(1 - \frac{x}{K}\right) - \alpha xy, \\ \frac{dy}{dt} &= -sy + \beta xy - \gamma yz, \\ \frac{dz}{dt} &= \delta yz - \mu z, \end{aligned} \tag{4.15}$$

where x, y and z represent, respectively, the densities of plant biomass, herbivore and parasite populations at time t. This model says that the plant population grows logistically to the environmental carrying capacity K with an intrinsic growth rate r when there is no herbivore. Herbivore eats plant population following mass action law with α as the rate constant. The parasite attacks herbivores, and the attack rate is proportional to the product of herbivore and parasite densities with γ as the proportionality constant. Natural death rates of herbivores and parasites are s and μ, respectively. The parameters β and δ represent the growth rates of herbivores and parasites. All parameters are positive. The following results [62] are known for the system (4.15).

Theorem 4.8. *The system* (4.15) *has four equilibrium points. (i) The equilibrium point* $E_0^P = (0,0,0)$ *is always unstable. (ii) The axial equilibrium point* $E_1^P = (K,0,0)$ *is stable if* $\beta K < s$.

(iii) The planar equilibrium point $E_2^P = (\bar{x}, \bar{y}, 0)$*, where* $\bar{x} = \frac{s}{\beta}$*,* $\bar{y} = \frac{r}{\alpha}\left(1 - \frac{s}{\beta K}\right)$*, exists and is locally asymptotically stable if* $\beta K > s$ *and* $\delta < \frac{\beta K \alpha \mu}{r(\beta K - s)}$*. (iv) The interior equilibrium point* $E_P^* = (x_P^*, y_P^*, z_P^*)$*, where* $x_P^* = K\left(1 - \frac{\alpha\mu}{r\delta}\right)$*,* $y_P^* = \frac{\mu}{\delta}$*,* $z_P^* = \frac{1}{\gamma}\left\{-s + \beta K\left(1 - \frac{\alpha\mu}{r\delta}\right)\right\}$*, exists and is locally asymptotically stable if* $\beta K > s$ *and* $\delta > \frac{\beta K \alpha \mu}{r(\beta K - s)}$*.*

4.5.1 NSFD model and its analysis

For convenience, we rewrite the continuous model (4.15) as

$$\begin{aligned} \frac{dx}{dt} &= rx - \frac{r}{K}x^2 - \alpha xy, \\ \frac{dy}{dt} &= -sy + \beta xy - \gamma yz, \\ \frac{dz}{dt} &= \delta yz - \mu z. \end{aligned} \tag{4.16}$$

The continuous system (4.16) is transformed to the following NSFD system using the previous nonlocal discretization techniques (R1) to (R7):

$$\begin{aligned} \frac{x_{n+1} - x_n}{\psi_1(h)} &= rx_n - \frac{rx_{n+1}x_n}{K} - \alpha x_{n+1}y_n, \\ \frac{y_{n+1} - y_n}{\psi_2(h)} &= -sy_{n+1} + \beta x_{n+1}y_n - \gamma y_{n+1}z_n, \\ \frac{z_{n+1} - z_n}{\psi_3(h)} &= \delta y_{n+1}z_n - \mu z_{n+1}, \end{aligned} \tag{4.17}$$

where $\psi_i(h)$, $i = 1, 2, 3$, are such that $\psi_i(h) > 0$ and $\psi_i(h) = h + O(h^2)$. Note that the similar term xy in the first & second equations and yz in the second & third equations have been discretized following the rule (R7).

Rearranging (4.17), we get

$$\begin{aligned} x_{n+1} &= \frac{x_n(1 + r\psi_1(h))}{1 + \psi_1(h)\left(\frac{rx_n}{K} + \alpha y_n\right)}, \\ y_{n+1} &= \frac{y_n(1 + \beta\psi_2(h)x_{n+1})}{1 + \psi_2(h)(s + \gamma z_n)}, \\ z_{n+1} &= \frac{z_n(1 + \delta\psi_3(h)y_{n+1})}{1 + \psi_3(h)\mu}. \end{aligned} \tag{4.18}$$

Thus, the solutions of the discrete system (4.18) remain positive for all step-size h whenever the initial values are positive.

As before, one can observe that the NSFD system (4.18) has the same four fixed points with the same existence conditions as it were in the continuous system (4.15). The variational matrix corresponding to the system (4.18) at any arbitrary fixed point (x,y,z) is given by

$$J(x,y,z)=\begin{pmatrix} a_{11} & a_{12} & 0 \\ a_{21} & a_{22} & a_{23} \\ a_{31} & a_{32} & a_{33} \end{pmatrix}, \tag{4.19}$$

where

$$\begin{cases} a_{11}=\frac{1+r\psi_1(h)}{1+\psi_1(h)\left(\frac{rx}{K}+\alpha y\right)}-\frac{x(1+r\psi_1(h))}{\left\{1+\psi_1(h)\left(\frac{rx}{K}+\alpha y\right)\right\}^2}\left(\frac{r\psi_1(h)}{K}\right), \; a_{12}=-\frac{x(1+r\psi_1(h))}{\left\{1+\psi_1(h)\left(\frac{rx}{K}+\alpha y\right)\right\}^2}\alpha\psi_1(h), \\ a_{21}=\frac{\beta\psi_2(h)y}{1+\psi_2(h)(s+\gamma z)}a_{11}, \; a_{22}=\frac{1+\beta\psi_2(h)x}{1+\psi_2(h)(s+\gamma z)}+\frac{\beta\psi_2(h)y}{1+\psi_2(h)(s+\gamma z)}a_{12}, \; a_{23}=-\frac{y(1+\beta\psi_2(h)x)\gamma\psi_2(h)}{\{1+\psi_2(h)(s+\gamma z)\}^2}, \\ a_{31}=\frac{\delta\psi_3(h)z}{1+\psi_3(h)\mu}a_{21}, \; a_{32}=\frac{\delta\psi_3(h)z}{1+\psi_3(h)\mu}a_{22}, \; a_{33}=\frac{1+\delta\psi_3(h)y}{1+\psi_3(h)\mu}+\frac{\delta\psi_3(h)z}{1+\psi_3(h)\mu}a_{23}. \end{cases}$$

Then the following results are true for the system (4.18).

Theorem 4.9. *(i) E_0^P is always an unstable fixed point. (ii) E_1^P is locally asymptotically stable if $\beta K < s$. (iii) E_2^P is stable if $\beta K > s$ and $\delta < \frac{\beta K\alpha\mu}{r(\beta K-s)}$. (iv) The interior fixed point E_P^* is always stable if $\beta K > s$ and $\delta > \frac{\beta K\alpha\mu}{r(\beta K-s)}$.*

Proof. At the trivial fixed point E_0^P, the eigenvalues are $\lambda_1 = 1+r\psi_1(h)$, $\lambda_2=\frac{1}{1+s\psi_2(h)}$ and $\lambda_3=\frac{1}{1+\psi_3(h)\mu}$. As $\lambda_1>1$, E_0^P is always unstable $\forall\, h>0$.

At E_1^P, the eigenvalues are given by $\lambda_1=\frac{1}{1+r\psi_1(h)}$, $\lambda_2=\frac{1+\beta K\psi_2(h)}{1+s\psi_2(h)}$ and $\lambda_3=\frac{1}{1+\psi_3(h)\mu}$. Here λ_1 and λ_3 both are positive and less than unity. λ_2 will be positive and less than unity for all $h>0$ if $\beta K<s$. Therefore, E_1^P is stable if $\beta K<s$.

At the boundary fixed point $E_2^P(\bar{x},\bar{y},0)$, the variational matrix is given by

$$J(E_2^P)=\begin{pmatrix} \bar{a}_{11} & \bar{a}_{12} & 0 \\ \bar{a}_{21} & \bar{a}_{22} & \bar{a}_{23} \\ 0 & 0 & \bar{a}_{33} \end{pmatrix}, \tag{4.20}$$

where

$$\begin{cases} \bar{a}_{11}=1-\left(\frac{\bar{x}}{K}\right)\left(\frac{r\psi_1(h)}{1+r\psi_1(h)}\right), \; \bar{a}_{12}=-\frac{\bar{x}}{1+r\psi_1(h)}\alpha\psi_1(h), \; \bar{a}_{21}=\frac{\beta\psi_2(h)\bar{y}}{1+\beta\psi_2(h)\bar{x}}\bar{a}_{11}, \\ \bar{a}_{22}=1+\frac{\beta\psi_2(h)\bar{y}}{1+\beta\psi_2(h)\bar{x}}\bar{a}_{12}, \; \bar{a}_{23}=-\frac{\bar{y}}{1+\beta\psi_2(h)\bar{x}}\gamma\psi_2(h), \; \bar{a}_{33}=\frac{1+\delta\psi_3(h)\bar{y}}{1+\psi_3(h)\mu}. \end{cases}$$

One eigenvalue of the above variational matrix $J(E_2^P)$ is $\bar{a}_{33}=\frac{1+\delta\psi_3(h)\bar{y}}{1+\psi_3(h)\mu}$, which is always positive and less than unity if $\delta<\frac{\mu}{\bar{y}}=\frac{\beta K\alpha\mu}{r(\beta K-s)}$. Other two eigenvalues of the matrix $J(E_2^P)$ will be the characteristics roots of the matrix

$$J_1=\begin{pmatrix} \bar{a}_{11} & \bar{a}_{12} \\ \bar{a}_{21} & \bar{a}_{22} \end{pmatrix}.$$

From the existence condition of E_2^P, it is easy to see that $0<\bar{a}_{11}<1$. After some algebraic manipulations, one have

$$\bar{a}_{22} = 1 - \frac{\beta\psi_2(h)\bar{y}}{\{1+\beta\psi_2(h)\bar{x}\}}\frac{\alpha\psi_1(h)\bar{x}}{\{1+r\psi_1(h)\}} = 1 - \left(\frac{\beta\psi_2(h)\bar{x}}{1+\beta\psi_2(h)\bar{x}}\right)\left\{\frac{r\left(1-\frac{s}{\beta K}\right)\psi_1(h)}{1+r\psi_1(h)}\right\},$$

implying that $0 < \bar{a}_{22} < 1$. On substitution the values of $\bar{a}_{22}$, $\bar{a}_{21}$ and noting that $\bar{x} < K$, one can obtain

$$\begin{aligned} 1-\det(J_1) &= 1-\bar{a}_{11}\,\bar{a}_{22}+\bar{a}_{12}\,\bar{a}_{21} \\ &= 1-\bar{a}_{11}-\tfrac{\beta\psi_2(h)\bar{y}}{1+\beta\psi_2(h)\bar{x}}\bar{a}_{11}\bar{a}_{12}+\tfrac{\beta\psi_2(h)\bar{y}}{1+\beta\psi_2(h)\bar{x}}\bar{a}_{11}\bar{a}_{12} \\ &= 1-\bar{a}_{11} > 0, \end{aligned}$$

$$\begin{aligned} 1-\mathrm{trace}(J_1)+\det(J_1) &= 1-(\bar{a}_{11}+\bar{a}_{22})+\bar{a}_{11} \\ &= 1-\bar{a}_{22} > 0 \end{aligned}$$

and $1+\mathrm{trace}(J_1)+\det(J_1) = 1+2\bar{a}_{11}+\bar{a}_{22} > 0$.

Thus, whenever it exists, E_2^P is locally asymptotically stable if $\delta < \frac{\beta K\alpha\mu}{r(\beta K-s)}$.

At the interior fixed point E_P^*, the variational matrix is given by

$$J(E_P^*) = \begin{pmatrix} a_{11}^* & a_{12}^* & 0 \\ a_{21}^* & a_{22}^* & a_{23}^* \\ a_{31}^* & a_{32}^* & a_{33}^* \end{pmatrix}, \tag{4.21}$$

where

$$\begin{cases} a_{11}^* = 1-\left(\frac{x_P^*}{K}\right)\left(\frac{r\psi_1(h)}{G}\right) > 0,\ a_{12}^* = -\frac{x_P^*\alpha\psi_1(h)}{G} < 0,\ a_{21}^* = \frac{\beta\psi_2(h)y_P^*}{H}a_{11}^* > 0, \\ a_{22}^* = 1+\frac{\beta\psi_2(h)y_P^*}{H}a_{12}^* = 1-\frac{\beta\psi_2(h)x_P^*}{H} * \frac{\alpha\psi_1(h)y_P^*}{G} > 0,\ a_{23}^* = -\frac{y_P^*\gamma\psi_2(h)}{H} < 0, \\ a_{31}^* = \frac{\delta\psi_3(h)z_P^*}{E}a_{21}^* > 0,\ a_{32}^* = \frac{\delta\psi_3(h)z_P^*}{E}a_{22}^* > 0, \\ a_{33}^* = 1+\frac{\delta\psi_3(h)z_P^*}{E}a_{23}^* = 1-\left(\frac{\delta\psi_3(h)y_P^*}{E}\right)\left(\frac{z_P^*\gamma\psi_2(h)}{H}\right) > 0, \\ G = 1+r\psi_1(h),\ H = 1+\beta\psi_2(h)x_P^*,\ E = 1+\delta\psi_3(h)y_P^*. \end{cases}$$

Following the existence conditions of the interior fixed point E_P^*, $0 < a_{ii}^* < 1$, $i = 1,2,3$. The characteristic equation corresponding to the matrix $J(E_P^*)$ has the form

$$p_1(\lambda) = \lambda^3 + A_1\lambda^2 + A_2\lambda + A_3 = 0, \tag{4.22}$$

where the coefficients are

$A_1 = -\mathrm{trace}(J(E_P^*)) = -a_{11}^* - a_{22}^* - a_{33}^*$,

$A_2 =$ sum of principle minors of $J(E_P^*)$

$\quad = (a_{11}^*a_{22}^* - a_{12}^*a_{21}^*) + (a_{22}^*a_{33}^* - a_{23}^*a_{32}^*) + a_{11}^*a_{33}^*$,

$A_3 = -\det(J(E_P^*)) = -a_{11}^*(a_{22}^*a_{33}^* - a_{23}^*a_{32}^*) + a_{12}^*(a_{21}^*a_{33}^* - a_{23}^*a_{31}^*) < 0$.

Simple manipulations give

$a_{11}^*a_{22}^* - a_{12}^*a_{21}^* = a_{11}^* + \frac{\beta\phi_2(h)y^*}{H}a_{11}^*a_{12}^* - \frac{\beta\phi_2(h)y^*}{H}a_{11}^*a_{12}^* = a_{11}^*$,

$a_{22}^*a_{33}^* - a_{23}^*a_{32}^* = a_{22}^*$ and $a_{21}^*a_{33}^* - a_{31}^*a_{23}^* = a_{21}^*$.
Thus, the coefficients simplify to
$A_1 = -a_{11}^* - a_{22}^* - a_{33}^*\ (<0)$, $A_2 = a_{11}^* + a_{22}^* + a_{11}^*a_{33}^*\ (>0)$, $A_3 = -a_{11}^*\ (<0)$.
Now our objective is to show that all the conditions of Lemma 1.16 are satisfied for the characteristic equation (4.22). One can compute
$p_1(1) = 1 + A_1 + A_2 + A_3 = 1 - a_{33}^* - a_{11}^* + a_{11}^*a_{33}^* = (1-a_{11}^*)(1-a_{33}^*)$,
$(-1)^3 p_1(-1) = 1 - A_1 + A_2 - A_3$.
Noting the signs of a_{ij}^*, A_i and $a_{ii}^* < 1$, $i,j = 1,2,3$, one can easily observe that $p_1(1)$ and $(-1)^3 p_1(-1)$ both are positive. Thus, first two conditions of Lemma 1.16 are satisfied. For the third condition, we first note that $|A_2 - A_3A_1| < 1 - A_3^2$ gives $A_2 - A_3A_1 - A_3^2 + 1 > 0$ and $A_2 - A_3A_1 + A_3^2 - 1 < 0$.
Here,

$$\begin{aligned}
A_2 - A_3A_1 - A_3^2 + 1 &= (a_{11}^* + a_{22}^* + a_{11}^*a_{33}^*) - a_{11}^*(a_{11}^* + a_{22}^* + a_{33}^*) - {a_{11}^*}^2 + 1 \\
&= (a_{11}^* + a_{22}^*)(1 - a_{11}^*) + (1 - {a_{11}^*}^2) = (1 - a_{11}^*)(1 + 2a_{11}^* + a_{22}^*), \\
A_2 - A_3A_1 + A_3^2 - 1 &= (a_{11}^* + a_{22}^* + a_{11}^*a_{33}^*) - a_{11}^*(a_{11}^* + a_{22}^* + a_{33}^*) + {a_{11}^*}^2 - 1 \\
&= a_{11}^* + a_{22}^*(1 - a_{11}^*) - 1 = (1 - a_{11}^*)(a_{22}^* - 1).
\end{aligned}$$

Observing the signs as before, one can then easily have

$$A_2 - A_3A_1 - A_3^2 + 1 > 0 \ \text{ and } \ A_2 - A_3A_1 + A_3^2 - 1 < 0.$$

Combining these two inequalities, we have $|A_2 - A_3A_1| < 1 - A_3^2$. Thus, all three conditions of Lemma 1.16 hold and therefore, the interior fixed point E_P^* is locally asymptotically stable whenever it exists, i.e., $\beta K > s$ and $\delta > \frac{\beta K \alpha \mu}{r(\beta K - s)}$. Hence the theorem. □

Remark 4.10. *It is to be noted that we do not need any restriction on $\psi_i(h)$, $i = 1,2,3$, to prove the positivity and dynamic consistency of the discrete system* (4.18). *Therefore, $\psi_i(h)$ can take any form that satisfies $\psi_i(h) > 0$ and $\psi_i(h) = h + O(h^2)$, $i = 1,2,3$. In the simulations, we consider the simplest form of $\psi_i(h) = h$.*

Remark 4.11. *It is to be noted that the system* (4.15) *does not satisfy the conservation law. For this type of system, Mickens [57] defined a rule for choosing the denominator functions $\psi_i(h)$, $i = 1,2,3$. Following that rule, one has to use the Euler forward scheme for the first derivative and nonlocal approximations for other terms in all three equations of system* (4.15). *After doing this for the first equation of system* (4.15) *and then solving for x_{n+1}, one has*

$$x_{n+1} = \frac{x_n(1+rh)}{1 + h\left(\frac{rx_n}{K} + \alpha y_n\right)}.$$

Since $(1+rh)$ occurs [57], it implies that the denominator function will be $\psi_1(h) = \frac{e^{rh}-1}{r}$.

Similarly, from the other two equations of system (4.15)*, one can find the other two denominator functions as* $\psi_2(h) = \frac{e^{sh}-1}{s}$ *and* $\psi_3(h) = \frac{e^{\mu h}-1}{\mu}$*. Thus, all three denominator functions have to be determined separately using the Euler forward scheme and nonlocal approximations if the continuous system is not conservative and the transformed nonlocal system contains terms like* $(1+rh)$*. But such a choice of separate denominator function for each equation of a higher-order equation will multiply the complexity for analytical computation of stability conditions.*

4.5.2 Numerical experiments

For numerical comparison, we first write the Euler-forward discrete version of the continuous model (4.15):

$$\begin{aligned} x_{n+1} &= x_n + h\left\{rx_n\left(1-\frac{x_n}{K}\right) - \alpha x_n y_n\right\}, \\ y_{n+1} &= y_n + h(-sy_n + \beta x_n y_n - \gamma y_n z_n), \\ z_{n+1} &= z_n + h(\delta y_n z_n - \mu z_n). \end{aligned} \tag{4.23}$$

To compare the step-size independency and dynamic consistency of the NSFD model (4.18) with that of the Euler model (4.23), we have plotted two bifurcation diagrams (Figure 4.3) of plant biomass with respect to the step-size h. As there is no restriction on $\psi_i(h)$, we consider $\psi_i(h) = h$ for all i in (4.18). Figure 4.3a shows that the dynamic behaviour of the NSFD system (4.18) is independent of the step-size, and Figure 4.3b depicts step-size dependent numerical instabilities in Euler system (4.23). In the last case, plant biomass population density remains stable for $h < 1.1113$ and shows instability for $h > 1.1113$.

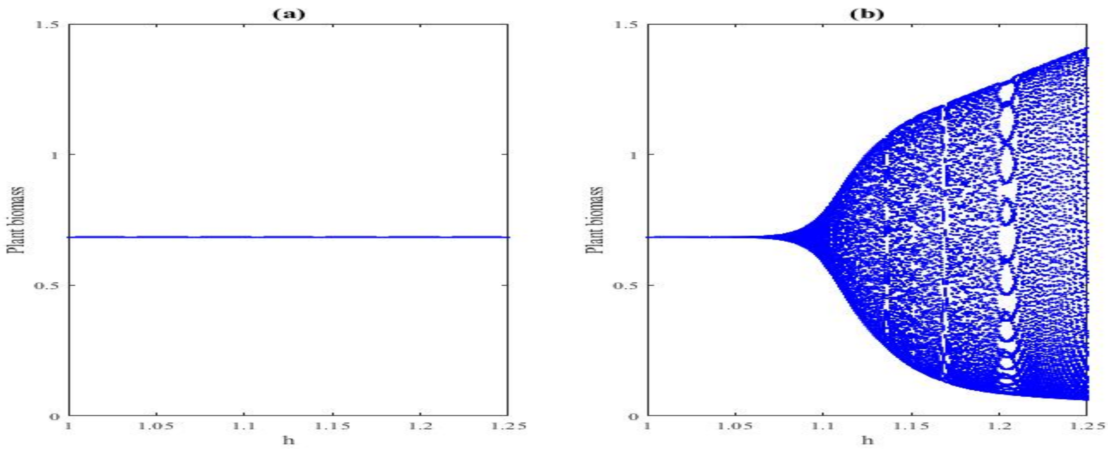

Figure 4.3: Bifurcation diagram of plant biomass (Fig. **a**) of the NSFD system (4.18) with varying step-size (h). This figure shows no instability in system (4.18) when step-size is varied. Similar bifurcation diagram (Fig. **b**) of Euler system (4.23) shows that the solution remains stable for $h < 1.1113$ and loses its stability for $h > 1.1113$. Parameters are $r = 0.95$, $K = 2.2$, $\alpha = 0.8$, $s = 0.25$, $\beta = 0.55$, $\gamma = 0.23$, $\mu = 0.09$, $\delta = 0.11$.

4.6 Summary

In the last two-three decades, nonstandard finite difference scheme has received significant interest in the discretization of the continuous system due to its superiority over other discretization techniques for various reasons. First, the transformed discrete system can be made positively invariant using proper nonlocal discretization techniques, though the standard discretization techniques often fail. Secondly, the NSFD model can be shown to be dynamically consistent with its continuous counterpart, which means the stability property of each equilibrium point of the continuous system remains the same for the NSFD model. However, in many cases, the discrete model formulated by the standard discretization technique shows (spurious) dynamics that are not at all the dynamics of the original continuous system. Another great advantage of the NSFD technique is that the dynamics, in this case, can be shown to be independent of the step-size, which can reduce the computational cost.

There are two main steps in the construction of an NSFD system from a given continuous system of first-order differential equations. The first one is discretization of the first-order derivative of the continuous system, where one has to choose a denominator function. The second one is the discretization of the interaction terms, where one has to use nonlocal discretization for both the linear and nonlinear terms of the differential equation. Unfortunately, there is no general rule for both of these steps [5, 12]. Some techniques have been defined [5, 12, 57] and successfully preserved both the positivity and dynamic properties of specific (relatively simple) continuous systems. However, previous techniques of choosing the denominator function may fail in many cases to preserve the dynamic properties of the continuous system. This study extends other studies mainly in two ways. First, we have defined some uniform rules for nonlocal discretization that one can follow while using the NSFD scheme. Secondly, the selection of the denominator function plays a crucial role in proving the dynamic consistency of the discrete model with its continuous systems. Mickens and others have defined some denominator functions for conservative and nonconservative systems. Such a predetermined form of the denominator function may not work well, and the dynamics of the discrete system constructed after nonlocal discretization may depend on the step-size [63]. So we proposed an alternative way so that the dynamics of the nonlocal discretized system do not depend on the step-size. For this, we initially consider $\phi(h)$ as the general form of the denominator function for the NSFD discrete system. Subsequently, we determine the appropriate expression for $\phi(h)$ from the system's local stability conditions so that the NSFD discrete system remains dynamically consistent. Choosing the denominator functions from the converted discrete system's stability criteria is more beneficial instead of considering a predetermined denominator function. Using our uniform rules for the nonlocal discretization of a continuous positive system, we have shown that highly complex population models not only preserve the positivity and dynamic consistency of the continuous system, but the dynamics also become independent of step-size, which has significant computational facility, especially for coupled nonlinear systems.

5

Nonstandard finite difference scheme for diffusion-induced ratio-dependent predator-prey model

5.1 Introduction

Mathematical models have become pretty important for scientists as it plays an enormous role in describing various biological, physical and chemical systems [53, 64, 60, 24, 65, 27, 28, 20, 17, 66, 67]. In contemporary biological, physical, and chemical systems, species dispersal is a noteworthy topic [68, 69, 70, 71, 72, 73, 74, 75, 76]. In an ecological system, dispersion of prey and predators are highly natural. Numerous factors impact these diffusions of predator and prey. As a basic illustration, it is evident that predator densities will be higher in areas where prey is easily accessible for consumption and also a location with easy access to resources will have a higher prey density.

Chakraborty et al. [72] have investigated the dynamics of diffusion-induced predator-prey model with a type II ratio-dependent functional response, prey refuge and fear factor. If $U(x,t)$ and $V(x,t)$ are, respectively, the number of prey and predator individuals at position $x \in \Omega$ and at time t, then the reaction-diffusion system may be expressed as [72]

$$\begin{aligned}\frac{\partial U}{\partial t} &= \frac{U}{1+KV}(a-bU) - \frac{c(1-m)UV}{(1-m)U+dV} + D_1\frac{\partial^2 U}{\partial x^2},\\ \frac{\partial V}{\partial t} &= -eV + \frac{f(1-m)UV}{(1-m)U+dV} + D_2\frac{\partial^2 V}{\partial x^2}.\end{aligned} \tag{5.1}$$

Here, a represents the prey's intrinsic growth rate and b represents the intra-species competition coefficient. Predational fear can decrease the prey population's reproduction rate as well as its level of activity, and it increases with the predator density. Thus, there is a negative feedback term in the prey growth function, where K represents the degree of fear a predator has caused. The predator's maximal rate of prey capture is denoted by c, while the predator's interference is measured by d. Due to refuge, a portion of the prey, $m \in (0,1)$, escapes predation. The per capita mortality rate of predators in the absence of prey is e, and the predator conversion efficiency is f. The parameters D_1 and D_2 represent the diffusivity of prey and predator species. All parameters are positive. For further descriptions of the system, one may consult [72]. The initial conditions are $U(x_0,0) > 0$, $V(x_0,0) > 0$, $x_0 \in \Omega$ and the boundary conditions (Neumann) are $\frac{\partial U}{\partial \nu} = \frac{\partial V}{\partial \nu} = 0$ on $\partial\Omega$ for all $t > 0$, where Ω is the domain bounded by $\partial\Omega$ and ν is the outward unit normal vector on the boundary.

Numerical solutions of both ordinary and partial differential equations are commonly achieved by using standard finite difference techniques, such as the Runge-Kutta method and the Euler method. However, standard finite discretization causes certain additional parameters to emerge, which causes numerical instability [1, 2, 3]. This further leads to a change in the alignment between the dynamics of the actual continuous system and its corresponding discretized system. In this background, nonstandard finite difference scheme proposed by Mickens [4, 10, 5] during 1989 – 1991 can be a commendable candidate in the way forward towards solving these differential equations. As opined by several researchers in the past, this technique is well-established for ordinary differential equations [77, 78, 79] but for partial differential equations, it is still in the infantry stage. Nevertheless, a number of research papers have previously studied NSFD schemes for partial differential equations [24, 64, 80, 81]. However, the NSFD schemes for PDE systems are either unable to ensure the positivity of their corresponding discrete systems without step-size restrictions, or they are unable to give consistency of solutions or first-order accuracy in time.

This chapter's major goal is to offer an NSFD scheme that will be accurate in both time and space. Further, it will preserve solution's consistency and will be Von Neumann stable. Simultaneously, neither step-size nor other parameter will affect the positivity of the discrete system.

The subsequent study is arranged in the following sequence. Some standard results of the continuous system are given in the next Section 5.2. The schemes for the NSFD model is given in Section 5.3. This section also contains the accuracy, consistency of the scheme. Positivity of the solutions and system's stability are also provided here. Numerical results are presented in Section 5.4. The chapter ends with a summary in Section 5.5.

5.2 Properties of the predator-prey continuous system

The continuous system (5.1) was rigorously analyzed in [72]. Here we rewrite some required results. The system (5.1) has one axial equilibrium point $E_1 = (\frac{a}{b}, 0)$ and one coexisting equilibrium point $E^* = (U^*, V^*)$, where $U^* = \frac{ad^2ef - cde(1-m)(f-e)}{bd^2ef + cK(1-m)^2(f-e)^2}$ and $V^* = \frac{(1-m)(f-e)U^*}{de}$. The coexisting equilibrium point $E^* = (U^*, V^*)$ exists if $m > m^*$ and $a < \frac{c(f-e)}{df}$ with $f > e$, where $m^* = 1 - \frac{adf}{c(f-e)}$.

Theorem 5.1. *[72] If the interior equilibrium point $E^* = (U^*, V^*)$ of the continuous system (5.1) in absence of diffusion exists, then it will be locally asymptotically stable if $K < K^*$ and $\max(m^*, m_1) < m < m_2$, where*
$K^* = \frac{abd^2f^2 - bcdf(1-m)(f-e) - bde(f-e)\{c(1-m)-df\}}{a(1-m)(f-e)^2\{c(1-m)-df\}}$ *and* $m_1 = 1 - \frac{df(af+ef-e^2)}{c(f^2-e^2)}$, $m_2 = 1 - \frac{df}{c}$.

5.3 NSFD model construction

We provide the discretization techniques so that the solutions of the NSFD system remain positive without any restriction, and renders accuracy and consistency with respect to both time and space.

We discretize the partial first-order time derivatives of (5.1) as

$$\frac{\partial U}{\partial t} \rightarrow \frac{U_m^{n+1} - U_m^n}{\phi_1(\Delta t)} \quad \text{and} \quad \frac{\partial V}{\partial t} \rightarrow \frac{V_m^{n+1} - V_m^n}{\phi_2(\Delta t)},$$

where the denominator functions $\phi_i(\Delta t)$, $i = 1, 2$, satisfy the condition $\phi_i(\Delta t) = \Delta t + O(\Delta t)^2$. The partial second-order space derivative terms with their corresponding diffusion coefficient are discretized as

$$D_1 \frac{\partial^2 U}{\partial x^2} \rightarrow D_1 \frac{U_{m+1}^{n+1} - 2U_m^{n+1} + U_{m-1}^{n+1}}{(\Delta x)^2} \quad \text{and} \quad D_2 \frac{\partial^2 V}{\partial x^2} \rightarrow D_2 \frac{V_{m+1}^{n+1} - 2V_m^{n+1} + V_{m-1}^{n+1}}{(\Delta x)^2},$$

where the other nonlinear terms of (5.1) are discretized as follows:

$$\begin{cases} \frac{aU}{1+KV} \rightarrow \frac{aU_m^n}{1+KV_m^n}, & eV \rightarrow eV_m^{n+1}, \\ \frac{bU^2}{1+KV} \rightarrow \frac{bU_m^{n+1}U_m^n}{1+KV_m^n}, & \frac{f(1-m)UV}{(1-m)U+dV} \rightarrow \frac{f(1-m)U_m^nV_m^n}{(1-m)U_m^n+dV_m^n}, \\ \frac{c(1-m)UV}{(1-m)U+dV} \rightarrow \frac{c(1-m)U_m^{n+1}V_m^n}{(1-m)U_m^n+dV_m^n}, & \end{cases} \tag{5.2}$$

with Δt and Δx as the step-sizes for time and space. Here U_m^n, V_m^n denote $U(m\Delta x, n\Delta t)$ and $V(m\Delta x, n\Delta t)$, respectively.
These nonlocal discretizations enable us to construct the following discrete system corresponding to the continuous system (5.1):

$$
\begin{aligned}
U_m^{n+1} &= U_m^n + \phi_1(\Delta t)\left\{\frac{aU_m^n}{1+KV_m^n} - \frac{bU_m^{n+1}U_m^n}{1+KV_m^n} - \frac{c(1-m)U_m^{n+1}V_m^n}{(1-m)U_m^n + dV_m^n} + D_1\frac{U_{m+1}^{n+1} - 2U_m^{n+1} + U_{m-1}^{n+1}}{(\Delta x)^2}\right\}, \\
V_m^{n+1} &= V_m^n + \phi_2(\Delta t)\left\{-eV_m^{n+1} + \frac{f(1-m)U_m^n V_m^n}{(1-m)U_m^n + dV_m^n} + D_2\frac{V_{m+1}^{n+1} - 2V_m^{n+1} + V_{m-1}^{n+1}}{(\Delta x)^2}\right\}.
\end{aligned} \tag{5.3}
$$

In the following, we investigate the NSFD scheme's temporal accuracy and consistency.

5.3.1 Accuracy

In case of discretization, it is required that the approximate solution and the exact solution of a system to be close to each other. How closely an approximated numerical solution coincides with the exact solution is known as accuracy. For this, we adopt the technique of [81].
Expanding U_m^{n+1} with the Taylor series, $U_m^{n+1} = U_m^n + \Delta t \frac{\partial U}{\partial t}\Big|_m^n + O(\Delta t)^2$ and also using Taylor series expansion, we get $U_{m+1}^{n+1} + U_{m-1}^{n+1} = U_{m+1}^n + U_{m-1}^n + 2\Delta t \frac{\partial U}{\partial t}\Big|_m^n + O\left((\Delta t)^2, (\Delta x)^2\right)$. Now, substituting these in the first equation of (5.3) and then after doing some algebraic manipulations, we get

$$
\begin{aligned}
U_m^n &+ \Delta t \frac{\partial U}{\partial t}\bigg|_m^n + O(\Delta t)^2 \\
&= U_m^n + \phi_1(\Delta t)\left\{\frac{aU_m^n}{1+KV_m^n} - \frac{bU_m^n}{1+KV_m^n}\left(U_m^n + \Delta t\frac{\partial U}{\partial t}\bigg|_m^n\right) - \frac{c(1-m)V_m^n}{(1-m)U_m^n + dV_m^n}\left(U_m^n + \Delta t\frac{\partial U}{\partial t}\bigg|_m^n\right)\right. \\
&\qquad \left. + \frac{D_1}{(\Delta x)^2}\left(U_{m+1}^n - 2U_m^n + U_{m-1}^n\right) + O\left((\Delta t)^2, (\Delta x)^2\right)\right\}.
\end{aligned}
$$

More compactly, we can write

$$
\begin{aligned}
U_m^n &+ \Delta t \frac{\partial U}{\partial t}\bigg|_m^n + O(\Delta t)^2 \\
&= U_m^n + \phi_1(\Delta t)\frac{\partial U}{\partial t}\bigg|_m^n \left\{1 - \Delta t\left(\frac{bU_m^n}{1+KV_m^n} + \frac{c(1-m)V_m^n}{(1-m)U_m^n + dV_m^n}\right)\right\} + O\left((\Delta t)^2, (\Delta x)^2\right).
\end{aligned} \tag{5.4}
$$

Comparing the coefficients of $\frac{\partial U}{\partial t}\Big|_m^n$ on the both sides of (5.4), we get

$$\Delta t = \phi_1(\Delta t)\left\{1-\Delta t\left(\frac{bU_m^n}{1+KV_m^n}+\frac{c(1-m)V_m^n}{(1-m)U_m^n+dV_m^n}\right)\right\}.$$

To hold the equality, we have to choose

$$\phi_1(\Delta t) = \Delta t\left\{1-\Delta t\left(\frac{bU_m^n}{1+KV_m^n}+\frac{c(1-m)V_m^n}{(1-m)U_m^n+dV_m^n}\right)\right\}^{-1}. \tag{5.5}$$

Also, using the similar process for the second equation of (5.3), we get

$$\phi_2(\Delta t) = \Delta t\,(1-e\Delta t)^{-1}. \tag{5.6}$$

Therefore, the NSFD system (5.3) will be first-order accurate in time by selecting these denominator functions $\phi_i(\Delta t)$, $i=1,2$ and, by construction, second-order accurate in space.

5.3.2 Consistency

If a numerical scheme leads to a discretized system that converges to its equivalent continuous system, then the scheme is considered consistent (see Definition 1.8).
After substituting the expressions of $\phi_i(\Delta t)$, $i=1,2$, the NSFD system (5.3) converted to

$$\begin{aligned} U_m^{n+1} &= U_m^n\left\{1-\Delta t\left(\frac{bU_m^n}{1+KV_m^n}+\frac{c(1-m)V_m^n}{(1-m)U_m^n+dV_m^n}\right)\right\}+\Delta t\frac{aU_m^n}{1+KV_m^n} \\ &\quad +\frac{D_1\Delta t}{(\Delta x)^2}\left(U_{m+1}^{n+1}-2U_m^{n+1}+U_{m-1}^{n+1}\right), \\ V_m^{n+1} &= V_m^n(1-e\Delta t)+\Delta t\frac{f(1-m)U_m^nV_m^n}{(1-m)U_m^n+dV_m^n}+\frac{D_2\Delta t}{(\Delta x)^2}\left(V_{m+1}^{n+1}-2V_m^{n+1}+V_{m-1}^{n+1}\right). \end{aligned} \tag{5.7}$$

Using Taylor series expansion,

$$U_{m+1}^{n+1}+U_{m-1}^{n+1} = 2U_m^n+2\Delta t\frac{\partial u}{\partial t}\Big|_m^n+(\Delta x)^2\frac{\partial^2 U}{\partial x^2}\Big|_m^n+O\left((\Delta t)^2,(\Delta x)^4\right)$$

along with the Taylor series expansion of U_m^{n+1} and substituting these in the first equation of (5.7), we get

$$\begin{aligned} U_m^n+\Delta t\frac{\partial U}{\partial t}\Big|_m^n+O(\Delta t)^2 &= U_m^n\left\{1-\Delta t\left(\frac{bU_m^n}{1+KV_m^n}+\frac{c(1-m)V_m^n}{(1-m)U_m^n+dV_m^n}\right)\right\} \\ &\quad +\Delta t\frac{aU_m^n}{1+KV_m^n}+\frac{D_1\Delta t}{(\Delta x)^2}\left\{(\Delta x)^2\frac{\partial^2 U}{\partial x^2}\Big|_m^n+O\left((\Delta t)^2,(\Delta x)^4\right)\right\}, \end{aligned}$$

giving

$$\Delta t \frac{\partial U}{\partial t}\bigg|_m^n + O(\Delta t)^2 = \Delta t \left\{ \frac{aU_m^n}{1+KV_m^n} - \frac{bU_m^{n2}}{1+KV_m^n} - \frac{c(1-m)U_m^nV_m^n}{(1-m)U_m^n+dV_m^n} + D_1 \frac{\partial^2 U}{\partial x^2}\bigg|_m^n \right\} + O\left((\Delta t)^2, (\Delta x)^4\right). \tag{5.8}$$

Following the same process, the second equation of (5.7) gives

$$\Delta t \frac{\partial V}{\partial t}\bigg|_m^n + O(\Delta t)^2 = \Delta t \left\{ -eV_m^n + \frac{f(1-m)U_m^nV_m^n}{(1-m)U_m^n+dV_m^n} + D_2 \frac{\partial^2 V}{\partial x^2}\bigg|_m^n + O\left((\Delta t)^2, (\Delta x)^4\right) \right\}. \tag{5.9}$$

Now dividing both sides of (5.8) and (5.9) by Δt and then taking $\lim \Delta t \to 0$ and $\lim \Delta x \to 0$, then (5.8) and (5.9) will obtain the form of the system (5.1) at $(x,t) \equiv (x_m, t_n)$. As a result, the suggested NSFD scheme (5.7) is consistent at both spatial and temporal levels.

5.3.3 Positivity

The NSFD system (5.7) can be expressed as

$$\begin{aligned} B_1U^{n+1} &= U^n \left\{ 1 - \Delta t \left(\frac{bU^n}{1+KV^n} + \frac{c(1-m)V^n}{(1-m)U^n+dV^n} \right) \right\} + \Delta t \frac{aU^n}{1+KV^n}, \\ B_2V^{n+1} &= V^n(1-e\Delta t) + \Delta t \frac{f(1-m)U^nV^n}{(1-m)U^n+dV^n}, \end{aligned} \tag{5.10}$$

where

$$B_i = \begin{bmatrix} b_{i1} & -b_{i2} & 0 & \cdots & 0 & 0 & 0 \\ -b_{i2} & b_{i3} & -b_{i2} & \cdots & 0 & 0 & 0 \\ 0 & -b_{i2} & b_{i3} & \cdots & 0 & 0 & 0 \\ \vdots & \vdots & \vdots & \ddots & \vdots & \vdots & \vdots \\ 0 & 0 & 0 & \cdots & b_{i3} & -b_{i2} & 0 \\ 0 & 0 & 0 & \cdots & -b_{i2} & b_{i3} & -b_{i2} \\ 0 & 0 & 0 & \cdots & 0 & -b_{i2} & b_{i1} \end{bmatrix}$$

with the coefficients $b_{i1} = 1 + \frac{D_i\Delta t}{(\Delta x)^2}$, $b_{i2} = \frac{D_i\Delta t}{(\Delta x)^2}$ and $b_{i3} = 1 + \frac{2D_i\Delta t}{(\Delta x)^2}$ for $i = 1,2$.
Here B_i, $i = 1,2$, are square matrices of order $M \times M$, where M is the total number of mesh points along the space (x). These matrices B_i, $i = 1,2$, both are M-matrices (by Definition 1.11). So, these matrices are inverse-positive, i.e., the inverse matrices can't have any non-negative element. Thus, it is easy to check that the NSFD system (5.10) will be positive for all positive initial values if $\Delta t < \min\left\{ \left(\frac{bU_m^n}{1+KV_m^n} + \frac{c(1-m)V_m^n}{(1-m)U_m^n+dV_m^n} \right)^{-1}, \frac{1}{e} \right\}$. One can choose

$$\Delta t = \frac{1-e^{-\lambda \Delta x}}{\lambda}, \tag{5.11}$$

where $\lambda = \max\left\{\frac{bU_m^n}{1+KV_m^n} + \frac{c(1-m)V_m^n}{(1-m)U_m^n+dV_m^n}, e\right\}$ so that $\Delta t < \min\left\{\left(\frac{bU_m^n}{1+KV_m^n} + \frac{c(1-m)V_m^n}{(1-m)U_m^n+dV_m^n}\right)^{-1}, \frac{1}{e}\right\}$ holds. Then, the denominator functions are also in the form $\phi_i(\Delta t) = \Delta t + O(\Delta t)^2$, $i = 1,2$. Thus, one have the following theorem.

Theorem 5.2. *The NSFD system (5.10) is*

(i) second-order spatially accurate and first-order in time.

(ii) consistent for both time step-length and space step-length.

(iii) positive for all positive initial values.

5.3.4 Stability of the proposed NSFD scheme

We know that the round-off error grows at every stage of the process for estimating the solution to the system of nonlinear partial differential equations [37]. Because of this, even a slight alteration in the system's initial values might result in a significant discrepancy between the approximate and exact solutions. The behaviour of the numerical scheme can be considered stable if this change does not occur. To ascertain the stability of the suggested NSFD scheme, we employ Von Neumann stability analysis or Fourier stability analysis (see Section 1.5 of Chapter 1).

We consider the Fourier components

$$U_m^n = a_1^n e^{im\theta},\ U_m^{n+1} = a_1^{n+1} e^{im\theta},\ U_{m+1}^{n+1} = a_1^{n+1} e^{i(m+1)\theta},\ U_{m-1}^{n+1} = a_1^{n+1} e^{i(m-1)\theta}$$

and similarly

$$V_m^n = a_2^n e^{im\theta},\ V_m^{n+1} = a_2^{n+1} e^{im\theta},\ V_{m+1}^{n+1} = a_2^{n+1} e^{i(m+1)\theta},\ V_{m-1}^{n+1} = a_2^{n+1} e^{i(m-1)\theta},$$

where a_1, a_2 are the amplitude and $\theta = 2\pi/\lambda$, where λ is the wavelength.

Now, from the first equation of (5.7), performing the linearization process, we get

$$a_1^{n+1} e^{im\theta} = a_1^n e^{im\theta} + \frac{D_1 \Delta t}{(\Delta x)^2} a_1^{n+1} \left(e^{i(m+1)\theta} - 2e^{im\theta} + e^{i(m-1)\theta}\right)$$
$$a_1^{n+1}\left[1 + \frac{D_1 \Delta t}{(\Delta x)^2}\left\{2 - \left(e^{i\theta} + e^{-i\theta}\right)\right\}\right] = a_1^n$$
$$\left|\frac{a_1^{n+1}}{a_1^n}\right| = \left|\frac{1}{1 + \frac{2D_1\Delta t}{(\Delta x)^2}(1-\cos\theta)}\right| \leq 1.$$

Performing the same method for the second equation of system (5.7), we get

$$\left|\frac{a_2^{n+1}}{a_2^n}\right| = \left|\frac{1 - e\Delta t}{1 + \frac{2D_2\Delta t}{(\Delta x)^2}(1-\cos\theta)}\right| \leq 1.$$

It shows that the proposed NSFD scheme is Von Neumann stable.

Remark 5.3. *The stability conditions of the equilibrium points in the proposed discrete system (5.10) are identical to those of the analogous continuous system (5.1), and so are their existence conditions.*

5.4 Numerical analysis

This section contains a few numerical simulations that we have used to confirm that the qualitative behaviour of our suggested discrete system and its corresponding continuous system are identical. We take the identical set of parameters as in [72]: $a = 1.3,\ b = 1.2,\ c = 2,\ d = 0.5,\ e = 0.4,\ f = 1.4,\ m = 0.6,\ K = 0.5,\ D_1 = 0.1,\ D_2 = 0.5$ and the initial value $(0.2, 0.3)$.

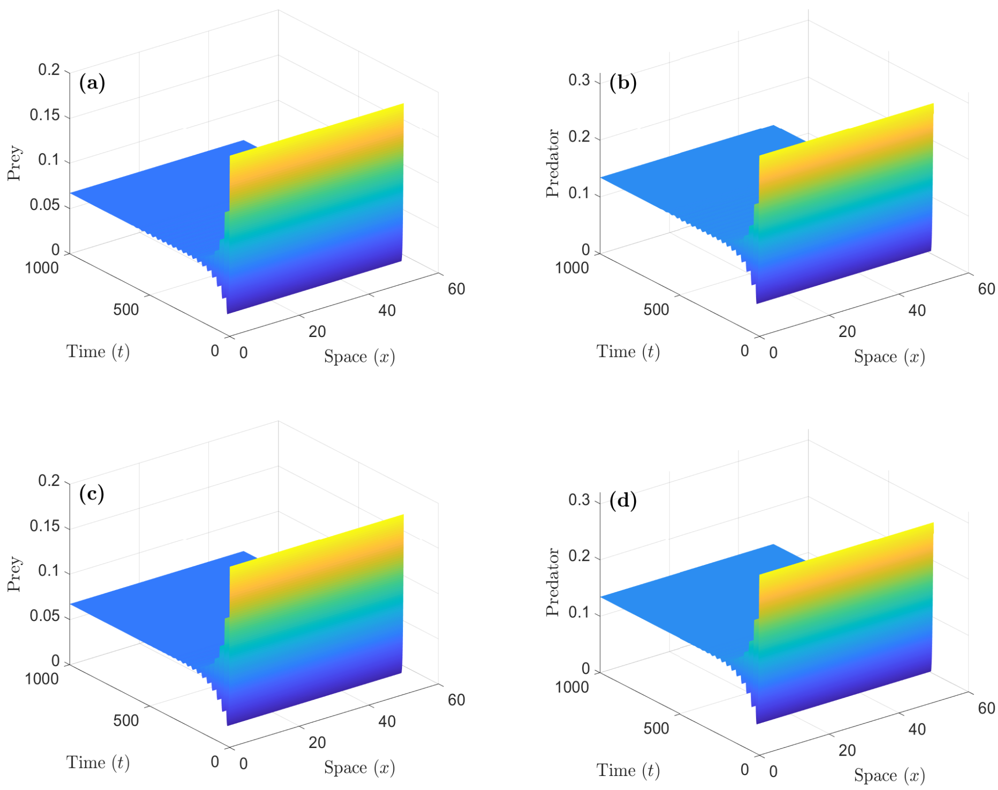

Figure 5.1: Surface plots of prey and predator populations of the continuous system (5.1) (first row) and the proposed discrete system (5.10) (second row). The steady state $E^* = (0.0671, 0.1341)$ is stable for the continuous system (5.1), as shown in the surface plots Figs. (**a**), (**b**), and the discrete system (5.10), shown in the surface plots Figs. (**c**), (**d**). Space step-size for the discrete system is $\Delta x = 0.1$ and its corresponding time step-size (see Equation (5.11)) is $\Delta t = 0.0934$. Parameters are considered from [72] $a = 1.3,\ b = 1.2,\ c = 2,\ d = 0.5,\ e = 0.4,\ f = 1.4,\ m = 0.6,\ K = 0.5,\ D_1 = 0.1,\ D_2 = 0.5$ with the initial value $(0.2, 0.3)$.

We consider the space step-size $\Delta x = 0.1$ for the entire simulation study. Both the existence and stability conditions given in Theorem 5.1 of the coexisting equilibrium point are satisfied by this parameter set. In this instance, $E^* = (0.0671, 0.1341)$ is the coexisting equilibrium point to which all solutions converge in case of the continuous system (5.1) (Fig.5.1a-5.1b) and the discrete system (5.10) (Fig. 5.1c-5.1d).

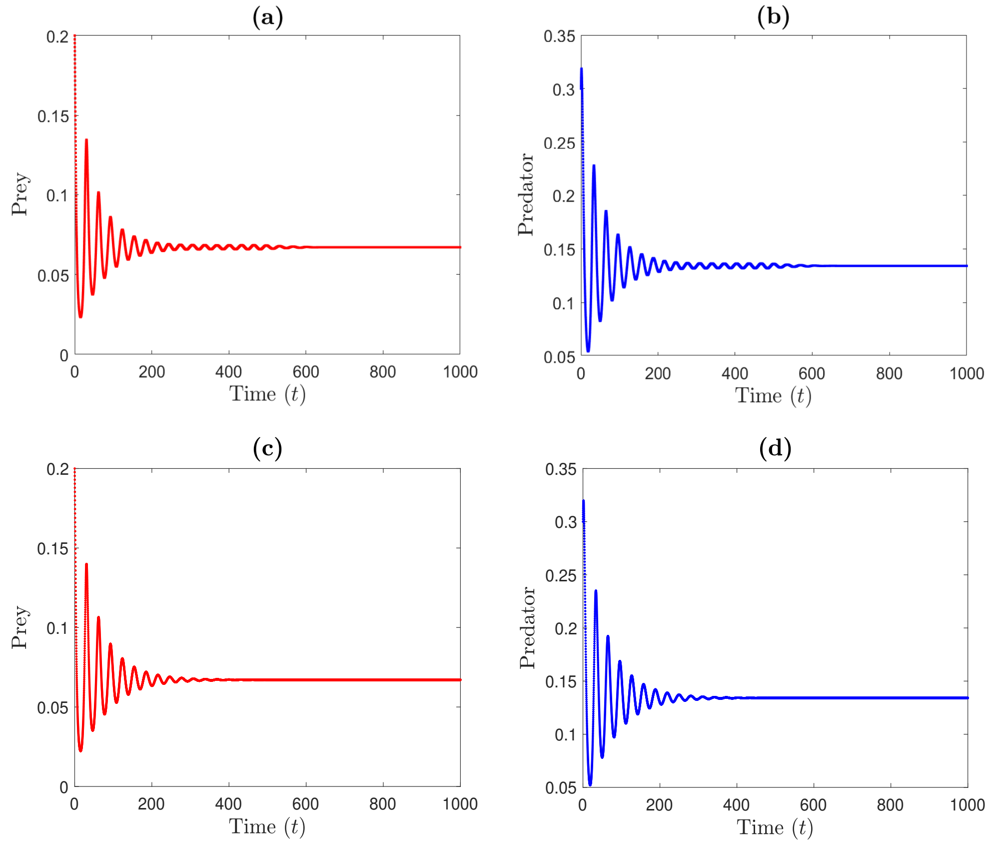

Figure 5.2: Time series of prey and predator populations of the continuous system (5.1) (first row) and the proposed discrete system (5.10) (second row). Here Figs. (**a**) and (**c**) are for prey population, and Figs. (**b**) and (**d**) are for predator population. The other parameters remain the same as in Fig. 5.1 with $\Delta t = 0.0934$ and $\Delta x = 0.1$.

We present a comparison study with the Crank-Nicolson scheme to serve as a benchmark in order to illustrate the performance of the proposed discrete system (5.10) and the discrete system (5.3) with $\phi_i(\Delta t) = \Delta t$, $i = 1, 2$.

The equivalent Crank-Nicolson discretization of the continuous system (5.1) reads

$$\begin{aligned} U_m^{n+1} &= U_m^n + \Delta t \left[\frac{aU_m^n}{1+KV_m^n} - \frac{bU_m^n(U_m^{n+1}+U_m^n)}{2(1+KV_m^n)} - \frac{c(1-m)V_m^n(U_m^{n+1}+U_m^n)}{2[(1-m)U_m^n+dV_m^n]} \right. \\ &\qquad \left. + \frac{D_1}{2(\Delta x)^2} \left\{ (U_{m+1}^{n+1} - 2U_m^{n+1} + U_{m-1}^{n+1}) + (U_{m+1}^n - 2U_m^n + U_{m-1}^n) \right\} \right], \\ V_m^{n+1} &= V_m^n + \Delta t \left[-\frac{e(V_m^{n+1}+V_m^n)}{2} + \frac{f(1-m)U_n^n V_m^n}{(1-m)U_m^n + dV_m^n} \right. \\ &\qquad \left. + \frac{D_2}{2(\Delta x)^2} \left\{ (V_{m+1}^{n+1} - 2V_m^{n+1} + V_{m-1}^{n+1}) + (V_{m+1}^n - 2V_m^n + V_{m-1}^n) \right\} \right]. \end{aligned} \tag{5.12}$$

In order to demonstrate the superior accuracy of the proposed scheme over the other scheme, we generated heat maps of absolute error of the numerical solution obtained from the proposed NSFD discrete system (5.10) (first row), from the discrete system (5.3) with $\phi_i(\Delta t) = \Delta t$, $i = 1,2$, (second row) and from the Crank-Nicolson discrete system (5.12) (third row) in Fig.

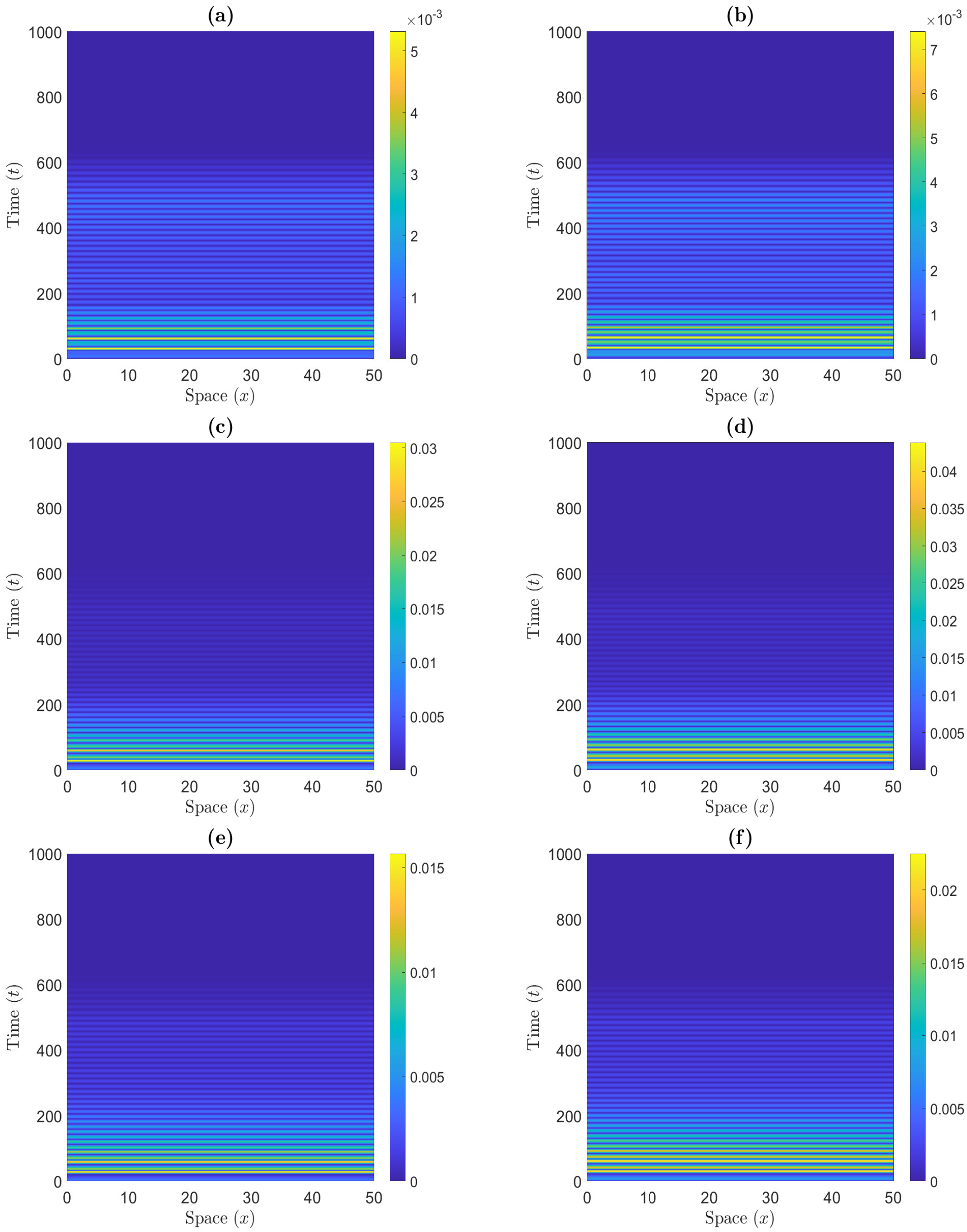

Figure 5.3: Heat maps of the absolute error using proposed NSFD scheme (5.10) (first row), discrete scheme (5.3) with $\phi_i(\Delta t) = \Delta t$ for $i = 1,2$ (second row), and Crank-Nicolson scheme (5.12) (third row). Here Figs. (**a**), (**c**) and (**e**) are for prey population and Figs. (**b**), (**d**) and (**f**) are for predator population. Parameters are [72]: $a = 1.3,\ b = 1.2,\ c = 2,\ d = 0.5,\ e = 0.4,\ f = 1.4,\ m = 0.6,\ K = 0.5,\ D_1 = 0.1,\ D_2 = 0.5$ and the initial value in $(0.2, 0.3)$.

5.3. The first column in Fig. 5.3 displays the error in the prey population estimates, whereas the second column displays the error in the predator population estimations. For all three discrete systems the error peaks around $t = 25$ and $t = 60$. The absolute error is constant for space but fluctuates with time for all systems. From the colour bars of Fig. 5.3, it can be seen that for prey solution, the maximum absolute value of errors for the proposed NSFD system (5.10) is 0.0053 and for the discrete system (5.3) with $\phi_i(\Delta t) = \Delta t$, $i = 1,2$ is 0.0305, and for the Crank-Nicolson discrete system (5.12) is 0.0157, and for predator solution, the maximum absolute value of errors for the proposed NSFD system (5.10) is 0.0074 and for the discrete system (5.3) with $\phi_i(\Delta t) = \Delta t$, $i = 1,2$ is 0.0438, and for the Crank-Nicolson discrete system (5.12) is 0.0225, which confirms that the error from the suggested NSFD discrete system (5.10) is pretty much smaller than the error obtained from other two discrete systems.

5.5 Summary

Nonstandard finite difference schemes have gained a lot of attraction recently in the discretization of continuous systems in both systems of ODEs and systems of PDEs. Its reduced computational cost compared to other conventional finite difference methods and its dynamically consistent property, which allows the dynamics to be independent of step-size, are some of the key factors contributing to its popularity. For ordinary differential equation systems, the NSFD scheme has advanced significantly both analytically and numerically, while for partial differential equation systems, it has not advanced as much.

To discretize the system of PDE using the NSFD scheme the major obstacles are how to discretize the second-order derivative terms and how to give the nonlocal transformations to both linear and nonlinear terms so that the positivity of the NSFD discrete system does not depend on the step-sizes and also the proposed NSFD scheme should guarantee accuracy and consistency concerning both time and space step-sizes, maintaining stability. However, some studies have been done on the NSFD scheme for PDE systems. Although the proposed NSFD schemes guaranteed accuracy and consistency in both time and space step-sizes and also Von Neumann stable, unfortunately, the positivity of the NSFD discrete systems discretized by the previously defined NSFD schemes is not independent of step-sizes.

In this study, we consider a two-dimensional diffusion-induced continuous-time ratio-dependent predator-prey system and proposed an NSFD dicretization scheme to discretize this continuous system which ensures first-order precision in time and second-order accuracy in space for the discretized system. Also, the positivity of the proposed NSFD scheme is proven to be preserved irrespective of step-size and other parameter constraints, and its consistency is also shown. A convergence analysis is shown based on Von-Neumann stability analysis or Fourier stability analysis. A few numerical simulations are presented to corroborate our approach, where the dynamical behavior of the suggested discrete system is identical to that of its corresponding continuous system. Furthermore, these simulations confirm that absolute value of errors of the solutions for the proposed NSFD system is minimum comparing with two other systems.

6

Positivity preserving nonstandard finite difference scheme for an in-host HIV reaction-diffusion model

6.1 Introduction

Mathematical models are becoming increasingly significant for scientists in the twenty-first century as they are helpful in demonstrating different phenomena in ecology, epidemiology, physics, chemistry and many other fields [17, 20, 24, 27, 28, 53, 64, 60, 65, 66, 67]. These mathematical models involve various types of differential equations, namely, ordinary differential equations, partial differential equations, fractional-order differential equations, etc. However, there exists a major bottleneck, that makes the trouble to find the exact solution of these differential equations except in some special cases. In this scenario, the equation discretization technique was observed to be worthy. Nevertheless, standard finite discretization leads to the rise of some extra parameters that are responsible for numerical instability [1, 2, 3]. The dynamics of the continuous system and the corresponding built discretized system become less aligned as a result of this. The nonstandard finite difference approach put forward by Mickens [4, 10, 5] in 1989–1991 can be a worthy contender in the quest to solve these differential equations given the existing circumstances. Many researchers have previously said that while this method is well-established for ordinary differential equations [77, 78, 79], it is still in its infancy when it comes to partial differential equations.

In the specified case of disease dynamics, diffusion takes an important place and it depends on a lot of factors. To determine the dynamics of these reaction-diffusion systems we need system of partial differential equations [72, 73, 74, 75, 76]. To solve the system of partial differential equations numerically with minimum error by discretization, the nonstandard finite difference (NSFD) scheme may play a crucial role.

We consider the following in-host HIV infection model with diffusion:

$$\begin{aligned}
\frac{\partial u}{\partial t} &= r - du - \beta uv + D_1 \frac{\partial^2 u}{\partial x^2}, \\
\frac{\partial w}{\partial t} &= \beta uv - aw + D_2 \frac{\partial^2 w}{\partial x^2}, \\
\frac{\partial v}{\partial t} &= \gamma w - \rho v + D_3 \frac{\partial^2 v}{\partial x^2}
\end{aligned} \tag{6.1}$$

with initial conditions $u(x_0,0) > 0$, $w(x_0,0) > 0$ and $v(x_0,0) > 0$, $x_0 \in \Omega$, along with homogeneous Neumann boundary conditions $\frac{\partial u}{\partial \nu} = \frac{\partial w}{\partial \nu} = \frac{\partial v}{\partial \nu} = 0$ on $\partial\Omega$ for all $t > 0$, where Ω is domain bounded by $\partial\Omega$ and ν is the outward unit normal vector on the boundary. Here $u(x,t)$, $w(x,t)$ and $v(x,t)$ are, respectively, the numbers of healthy $CD4^{+}T$ cells, infected $CD4^{+}T$ cells and free virus particles at position $x \in \Omega$ and at time t. The parameters r and d represent the intrinsic growth rate and natural death rate of healthy $CD4^{+}T$ cell, respectively. β denotes the disease transmission coefficient and a denotes the death rate of the infected $CD4^{+}T$ cell. γ is the production rate of free virus from infected $CD4^{+}T$ cell as because of cell-lysis and ρ is the death rate of free virus particles. The parameters D_1, D_2 and D_3 represent the diffusivity of healthy $CD4^{+}T$ cells, infected $CD4^{+}T$ cells and free viruses, respectively. All parameters are positive. The model in the absence of diffusion, where $D_1 = D_2 = D_3 = 0$, was studied by Nowak and Bangham [82].

On the NSFD scheme for systems of partial differential equations, some studies have already been done. A diffusion-driven HBV model [24] is numerically solved using the NSFD scheme. The study is done on the global stability features of the discrete system and the positivity of the system retained. A computer virus system with an advection-reaction-diffusion model is approximately solved using the NSFD scheme in [64], and some structural properties, such as consistency and stability, are verified further. An epidemic model involving reaction and diffusion in [80] is numerically solved using an NSFD scheme, and the dynamics of that NSFD discrete system are compared with a few other well-known numerical techniques. However, the NSFD scheme doesn't provide consistency of solution or first-order precision in time. Recently, the reaction-diffusion SIR epidemic model has been numerically solved in [81] using the NSFD technique. While the NSFD scheme ensures consistency and accuracy in time and space, the suggested discrete system's positivity is dependent on the time step-size.

The main objective of this study is to provide an NSFD scheme, with the requirement that the proposed discrete system is positive and dynamically consistent with the continuous system. To be dynamically consistent, the proposed discrete system must be accurate in both time and space, as well as consistent in both time step-size and space step-size, and also the discrete system should be Von Neumann stable. Furthermore, we also give simulated examples to illustrate the efficacy of the proposed NSFD scheme in contrast with various existing NSFD methods.

The following is the order in which the chapter is structured. Some standard results of the three-dimensional in-host HIV continuous system are provided in the following Section 6.2. Section 6.3 provides a description of the suggested NSFD scheme. This section also covers the system's accuracy and consistency, as well as its positivity and stability. Section 6.4 presents a few numerical simulations. Section 6.5 contains a summary that brings the chapter to a close.

6.2 Properties of the continuous system

The continuous system (6.1) has one axial equilibrium point $\bar{E} = (\frac{r}{d}, 0, 0)$ and one endemic equilibrium point $E^* = (u^*, w^*, v^*)$, where $u^* = \frac{a\rho}{\beta\gamma}$, $w^* = \frac{r\beta\gamma - da\rho}{\beta a\gamma}$ and $v^* = \frac{r\beta\gamma - da\rho}{\beta a\rho}$. The endemic equilibrium point exists if $\frac{r\beta\gamma}{da\rho} > 1$.

Theorem 6.1. *[82] In absence of diffusion the following properties hold for the continuous system (6.1):*

(i) the disease-free equilibrium point $\bar{E} = (\frac{r}{d}, 0, 0)$ is locally asymptotically stable if $\frac{r\beta\gamma}{da\rho} < 1$.

(ii) the endemic equilibrium point $E^* = (u^*, w^*, v^*)$ is locally asymptotically stable whenever it exists, i.e., if $\frac{r\beta\gamma}{da\rho} > 1$ holds.

6.3 NSFD model construction

Our main motive is to define a discretization techniques so that the NSFD discrete system guarantee accuracy with respect to time and space, consistency of all solutions and the discrete system remain positive without any condition.

We discretize the partial first-order time derivatives of (6.1) as

$$\frac{\partial u}{\partial t} \to \frac{u_m^{n+1} - u_m^n}{\psi_1(\Delta t)}, \quad \frac{\partial w}{\partial t} \to \frac{w_m^{n+1} - w_m^n}{\psi_2(\Delta t)}, \quad \text{and} \quad \frac{\partial v}{\partial t} \to \frac{v_m^{n+1} - v_m^n}{\psi_3(\Delta t)}$$

and the partial second-order space derivative terms with their corresponding diffusion coefficients as

$$\begin{aligned}
D_1\frac{\partial^2 u}{\partial x^2} &\to D_1\frac{u_{m+1}^{n+1}-2u_m^{n+1}+u_{m-1}^{n+1}}{(\Delta x)^2},\\
D_2\frac{\partial^2 w}{\partial x^2} &\to D_2\frac{w_{m+1}^{n+1}-2w_m^{n+1}+w_{m-1}^{n+1}}{(\Delta x)^2},\\
D_3\frac{\partial^2 v}{\partial x^2} &\to D_3\frac{v_{m+1}^{n+1}-2v_m^{n+1}+v_{m-1}^{n+1}}{(\Delta x)^2}.
\end{aligned}$$

The other terms of (6.1) are discretized as

$$\begin{cases}
-du \to -du_m^{n+1}, & \beta uv \to \beta u_m^n v_m^n, \qquad \gamma w \to \gamma w_m^n,\\
-\beta uv \to -\beta u_m^{n+1} v_m^n, & -aw \to -aw_m^{n+1}, \qquad -\rho v \to -\rho v_m^{n+1},
\end{cases}$$

where Δt and Δx represent time step-size and space step-size, respectively, and the denominator functions $\psi_i(\Delta t)$, $i=1,2,3$, satisfies the condition $\psi_i(\Delta t)=\Delta t+O(\Delta t)^2$. Here u_m^n, w_m^n and v_m^n denote $u(m\Delta x, n\Delta t)$, $w(m\Delta x, n\Delta t)$ and $v(m\Delta x, n\Delta t)$, respectively.

With the use of these nonlocal discretizations, we are able to generate the following NSFD discrete system corresponding to the continuous system (6.1):

$$\begin{aligned}
u_m^{n+1} &= u_m^n+\psi_1(\Delta t)\left[r-du_m^{n+1}-\beta u_m^{n+1}v_m^n+D_1\frac{u_{m+1}^{n+1}-2u_m^{n+1}+u_{m-1}^{n+1}}{(\Delta x)^2}\right],\\
w_m^{n+1} &= w_m^n+\psi_2(\Delta t)\left[\beta u_m^n v_m^n-aw_m^{n+1}+D_2\frac{w_{m+1}^{n+1}-2w_m^{n+1}+w_{m-1}^{n+1}}{(\Delta x)^2}\right],\\
v_m^{n+1} &= v_m^n+\psi_3(\Delta t)\left[\gamma w_m^n-\rho v_m^{n+1}+D_3\frac{v_{m+1}^{n+1}-2v_m^{n+1}+v_{m-1}^{n+1}}{(\Delta x)^2}\right].
\end{aligned} \tag{6.2}$$

Now we investigate the NSFD scheme's accuracy and consistency with respect to both time and space.

6.3.1 Accuracy

Accuracy is the degree to which an approximate numerical solution coincides with the exact solution. In the case of discretization, it is necessary that the approximate solution and the exact solution be close to each other. In the first equation of (6.2), using Taylor series expansion, we get

$$u_m^{n+1}=u_m^n+\Delta t\left.\frac{\partial u}{\partial t}\right|_m^n+O(\Delta t)^2 \text{ and}$$

$$u_{m+1}^{n+1}+u_{m-1}^{n+1}=u_{m+1}^n+u_{m-1}^n+2\Delta t\left.\frac{\partial u}{\partial t}\right|_m^n+O\left((\Delta t)^2,(\Delta x)^2\right).$$

Substituting these in the first equation of (6.2) and then doing some algebraic calculations, we get

$$u_m^n + \Delta t \frac{\partial u}{\partial t}\bigg|_m^n + O(\Delta t)^2 = u_m^n + \psi_1(\Delta t)\left\{ r - d\left(u_m^n + \Delta t \frac{\partial u}{\partial t}\bigg|_m^n \right) - \beta v_m^n \left(u_m^n + \Delta t \frac{\partial u}{\partial t}\bigg|_m^n \right) \right.$$
$$\left. + \frac{D_1}{(\Delta x)^2}\left(u_{m+1}^n - 2u_m^n + u_{m-1}^n\right) + O\left((\Delta t)^2, (\Delta x)^2\right) \right\},$$

We can write more compactly

$$u_m^n + \Delta t \frac{\partial u}{\partial t}\bigg|_m^n + O(\Delta t)^2 = u_m^n + \psi_1(\Delta t) \frac{\partial u}{\partial t}\bigg|_m^n \{1 - \Delta t(d + \beta v_m^n)\} + O\left((\Delta t)^2, (\Delta x)^2\right). \quad (6.3)$$

Comparing the coefficients of $\frac{\partial u}{\partial t}\Big|_m^n$ from the both sides of (6.3), we get

$$\Delta t = \psi_1(\Delta t)\{1 - \Delta t(d + \beta v_m^n)\}.$$

To hold the equality, we have to consider

$$\psi_1(\Delta t) = \Delta t\{1 - \Delta t(d + \beta v_m^n)\}^{-1}. \quad (6.4)$$

Also, using the similar process for the second and third equations of (6.2), we get

$$\psi_2(\Delta t) = \Delta t(1 - a\Delta t)^{-1} \quad (6.5)$$

and

$$\psi_3(\Delta t) = \Delta t(1 - \rho\Delta t)^{-1}. \quad (6.6)$$

Thus, by selecting these previously stated denominator functions $\psi_i(\Delta t)$, $i = 1, 2, 3$, the NSFD discretized system (6.2) will be first-order accurate in time, and by construction, the discrete system is second-order accurate in space.

6.3.2 Consistency

A numerical method is deemed consistent if it results in a discretized system that converges to its corresponding continuous system (see Definition 1.8).

Substituting the expressions of $\psi_i(\Delta t)$, $i = 1,2,3$, the NSFD system (6.2) is converted to

$$\begin{aligned} u_m^{n+1} &= u_m^n \left\{1 - \Delta t(d + \beta v_m^n)\right\} + r\Delta t + \frac{D_1 \Delta t}{(\Delta x)^2}\left(u_{m+1}^{n+1} - 2u_m^{n+1} + u_{m-1}^{n+1}\right), \\ w_m^{n+1} &= w_m^n (1 - a\Delta t) + \beta u_m^n v_m^n \Delta t + \frac{D_2 \Delta t}{(\Delta x)^2}\left(w_{m+1}^{n+1} - 2w_m^{n+1} + w_{m-1}^{n+1}\right), \\ v_m^{n+1} &= v_m^n (1 - \rho\Delta t) + \gamma w_m^n \Delta t + \frac{D_3 \Delta t}{(\Delta x)^2}\left(v_{m+1}^{n+1} - 2v_m^{n+1} + v_{m-1}^{n+1}\right). \end{aligned} \tag{6.7}$$

Using Taylor series expansion of $u_m^{n+1} = u_m^n + \Delta t \frac{\partial u}{\partial t}\Big|_m^n + O(\Delta t)^2$ and

$$u_{m+1}^{n+1} + u_{m-1}^{n+1} = 2\left\{u_m^n + \Delta t \frac{\partial u}{\partial t}\Big|_m^n + (\Delta x)^2 \frac{\partial^2 u}{\partial x^2}\Big|_m^n\right\} + O\left((\Delta t)^2, (\Delta x)^4\right),$$

and then substituting these two in the first equation of (6.7), we get

$$\begin{aligned} u_m^n + \Delta t \frac{\partial u}{\partial t}\Big|_m^n + O(\Delta t)^2 &= u_m^n \left\{1 - \Delta t \ (d + \beta v_m^n)\right\} + r\Delta t \\ &\quad + \frac{D_1 \Delta t}{(\Delta x)^2}\left\{(\Delta x)^2 \frac{\partial^2 u}{\partial x^2}\Big|_m^n + O\left((\Delta t)^2, (\Delta x)^4\right)\right\}, \end{aligned}$$

which gives

$$\Delta t \frac{\partial u}{\partial t}\Big|_m^n + O(\Delta t)^2 = \Delta t \left\{r - d u_m^n - \beta u_m^n v_m^n + D_1 \frac{\partial^2 u}{\partial x^2}\Big|_m^n + O\left((\Delta t)^2, (\Delta x)^4\right)\right\}. \tag{6.8}$$

Repeating the same process for the second and third equation of (6.7), we get

$$\Delta t \frac{\partial w}{\partial t}\Big|_m^n + O(\Delta t)^2 = \Delta t \left\{\beta u_m^n v_m^n - a w_m^n + D_2 \frac{\partial^2 w}{\partial x^2}\Big|_m^n + O\left((\Delta t)^2, (\Delta x)^4\right)\right\} \tag{6.9}$$

and

$$\Delta t \frac{\partial v}{\partial t}\Big|_m^n + O(\Delta t)^2 = \Delta t \left\{\gamma w_m^n - \rho v_m^n + D_3 \frac{\partial^2 v}{\partial x^2}\Big|_m^n + O\left((\Delta t)^2, (\Delta x)^4\right)\right\}. \tag{6.10}$$

Dividing both sides by Δt and taking $\lim \Delta t \to 0$ and $\lim \Delta x \to 0$ in (6.8), (6.9) and (6.10), then (6.8), (6.9) and (6.10) will obtain the form of system (6.1) at $(x,t) \equiv (x_m, t_n)$. As a result, the suggested NSFD scheme (6.7) is consistent at both space and time levels.

6.3.3 Positivity

The NSFD discrete system (6.7) can be expressed as:

$$\begin{aligned} A_1 u^{n+1} &= u^n \{1-\Delta t(d+\beta v^n)\} + r\Delta t, \\ A_2 w^{n+1} &= w^n \{1-a\Delta t\} + \beta u^n v^n \Delta t, \\ A_3 v^{n+1} &= v^n \{1-\rho\Delta t\} + \gamma w^n \Delta t, \end{aligned} \tag{6.11}$$

where

$$A_i = \begin{bmatrix} a_{i1} & -a_{i2} & 0 & \cdots & 0 & 0 & 0 \\ -a_{i2} & a_{i3} & -a_{i2} & \cdots & 0 & 0 & 0 \\ 0 & -a_{i2} & a_{i3} & \cdots & 0 & 0 & 0 \\ \vdots & \vdots & \vdots & \ddots & \vdots & \vdots & \vdots \\ 0 & 0 & 0 & \cdots & -a_{i2} & a_{i3} & -a_{i2} \\ 0 & 0 & 0 & \cdots & 0 & -a_{i2} & a_{i1} \end{bmatrix}, \; i = 1,2,3,$$

with the coefficients $a_{i1} = 1 + \frac{D_i\Delta t}{(\Delta x)^2}$, $a_{i2} = \frac{D_i\Delta t}{(\Delta x)^2}$ and $a_{i3} = 1 + \frac{2D_i\Delta t}{(\Delta x)^2}$.
Here A_i, $i = 1,2,3$, are square matrices of order $N \times N$, where N is the total number of mesh points along the space (x). These matrices A_i, $i = 1,2,3$, all are M-matrices (by Definition 1.11). Thus, these matrices are inverse-positive, and these matrices are incapable of having any non-negative element. Thus, it becomes easy to check that the NSFD discrete system (6.11) will be positive for all positive initial values if $\Delta t < \min\left\{\frac{1}{(d+\beta v_m^n)}, \frac{1}{a}, \frac{1}{\rho}\right\}$. One can choose

$$\Delta t = \frac{1-e^{-\lambda\Delta x}}{\lambda},$$

where $\lambda = \max\{(d+\beta v_m^n), a, \rho\}$, so that $\Delta t < \min\left\{\frac{1}{(d+\beta v_m^n)}, \frac{1}{a}, \frac{1}{\rho}\right\}$ holds. Then, the denominator functions are also in the form $\psi_i(\Delta t) = \Delta t + O(\Delta t)^2$, $i = 1,2,3$. One can then state the following theorem.

Theorem 6.2. *The NSFD system (6.11) is*

(i) first-order accurate with time and second-order in space.

(ii) consistent for both time and space step-size.

(iii) positive for all positive initial values without any restrictions.

6.3.4 Stability of the suggested NSFD scheme

As we estimate the solution to the system of nonlinear partial differential equations, we found that at each step the round-off error increases [37]. This is why there might be a large difference between the approximate and exact solutions for even a little change in the initial conditions

of the system. If there is no change in the numerical scheme's behavior, it can be considered stable. We use Fourier or Von Neumann stability analysis to determine if the proposed NSFD system is stable (see Section 1.5 of Chapter 1).
We take the Fourier components

$$u_m^n = k_1^n e^{im\theta},\ u_m^{n+1} = k_1^{n+1} e^{im\theta},\ u_{m+1}^{n+1} = k_1^{n+1} e^{i(m+1)\theta},\ u_{m-1}^{n+1} = k_1^{n+1} e^{i(m-1)\theta},$$

and similarly

$$w_m^n = k_2^n e^{im\theta},\ w_m^{n+1} = k_2^{n+1} e^{im\theta},\ w_{m+1}^{n+1} = k_2^{n+1} e^{i(m+1)\theta},\ w_{m-1}^{n+1} = k_2^{n+1} e^{i(m-1)\theta},$$

$$v_m^n = k_3^n e^{im\theta},\ v_m^{n+1} = k_3^{n+1} e^{im\theta},\ v_{m+1}^{n+1} = k_3^{n+1} e^{i(m+1)\theta},\ v_{m-1}^{n+1} = k_3^{n+1} e^{i(m-1)\theta},$$

where k_1, k_2 and k_3 are the amplitude and $\theta = 2\pi/\phi$, where ϕ is the wavelength.
Now from the first equation of (6.7), performing the process of linearization, we get

$$\begin{aligned}
&k_1^{n+1} e^{im\theta} = k_1^n e^{im\theta}(1 - d\Delta t) + \frac{D_1 \Delta t}{(\Delta x)^2} k_1^{n+1}\left(e^{i(m+1)\theta} - 2e^{im\theta} + e^{i(m-1)\theta}\right)\\
&k_1^{n+1}\left[1 + \left\{2 - \left(e^{i\theta} + e^{-i\theta}\right)\right\}\right] = k_1^n(1 - d\Delta t)\\
&\left|\frac{k_1^{n+1}}{k_1^n}\right| = \left|\frac{1 - d\Delta t}{1 + \frac{2D_1\Delta t}{(\Delta x)^2}(1 - \cos\theta)}\right| \le \left|1 - d\Delta t\right| < 1.
\end{aligned}$$

After processing the same method from the second and third equation of the system (6.7), we get

$$\left|\frac{k_2^{n+1}}{k_2^n}\right| \le \left|1 - a\Delta t\right| < 1 \quad \text{and} \quad \left|\frac{k_3^{n+1}}{k_3^n}\right| \le \left|1 - \rho\Delta t\right| < 1.$$

Thus, we can conclude that the proposed NSFD scheme is Von Neumann stable.

Remark 6.3. *The existence criteria and stability conditions of the equilibrium points in the proposed discrete system (6.11) are the same as those in the corresponding continuous system (6.1).*

6.4 Numerical analysis

A few numerical simulations that we ran to verify that our proposed discrete system and the matching continuous system behave exactly the same way qualitatively are included in this section. We consider the following set of parameters (see Table 6.1) [83, 84, 85, 86, 87] with $D_1 = 0.015$, $D_2 = 0.015$, $D_3 = 0.015$ and the starting value $(15, 0.1, 0.2)$. We consider a spatial step-size of $\Delta x = 0.1$, which is kept same in each simulation. This parameter configuration satisfies the coexisting equilibrium point's existence and stability requirements. The coexisting equilibrium point in this case, for both the continuous system (6.1) (Fig.6.1a-6.1c) and the

NSFD discrete system (6.11) (Fig. 6.1d-6.1f), is $E^* = (5.9524, 2.2470, 37.75)$.

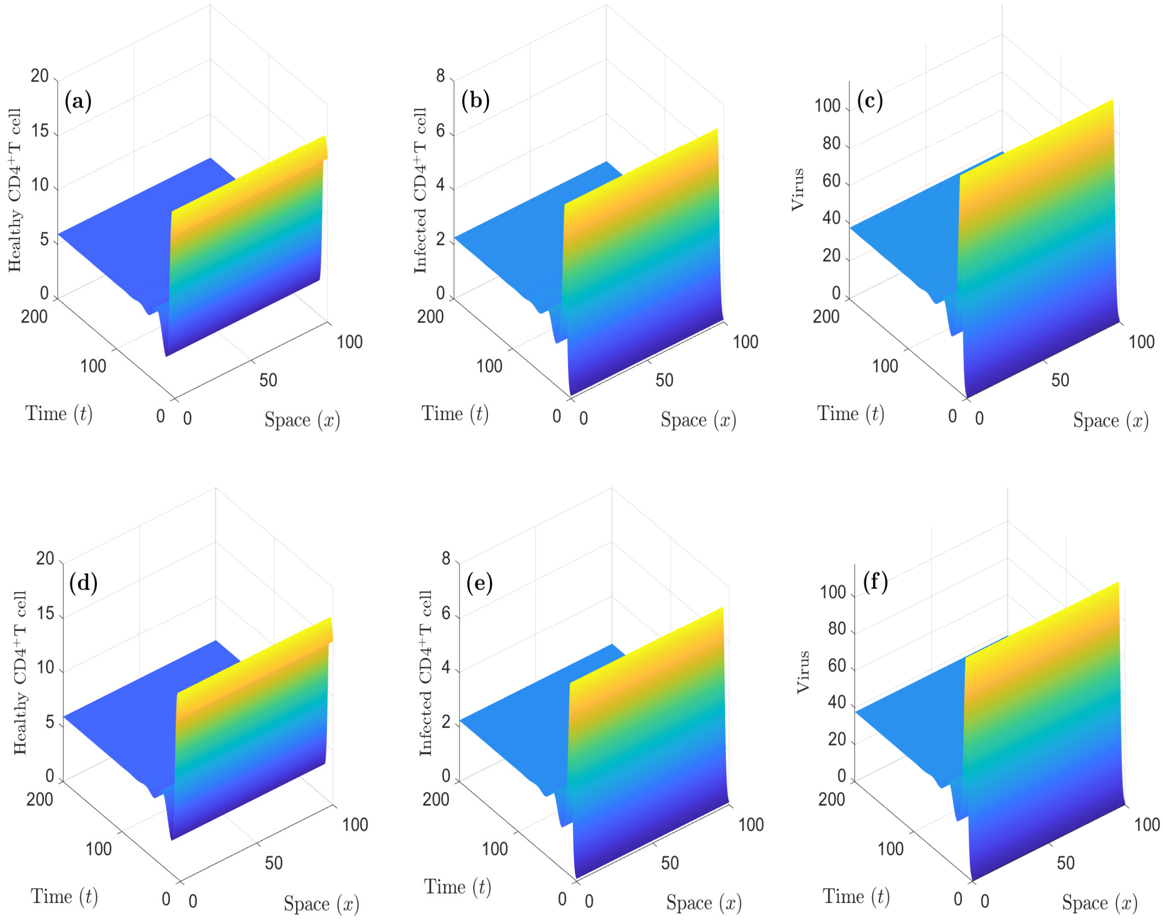

Figure 6.1: surface plots for healthy CD4$^+$T cell, infected CD4$^+$T cell and virus populations of the continuous system (6.1) (first row) and of the proposed NSFD discrete system (6.11) (second row). The endemic equilibrium point $E^* = (5.9524, 2.2470, 37.75)$ is stable for the continuous system (6.1) as shown in the surface plot Fig. (**a**), (**b**) and (**c**), and also stable for the NSFD discrete system (6.11) which is shown in the surface plot Fig. (**d**), (**e**) and (**f**). Time step-size for the discrete system is $\Delta t = 0.0885$ and its corresponding space step-size is $\Delta x = 0.1$. Parameters are $r = 1.0$, $d = 0.017$, $\beta = 0.004$, $a = 0.4$, $\gamma = 42$, $\rho = 2.5$, $D_1 = 0.015$, $D_2 = 0.015$, $D_3 = 0.015$ with the initial value $(15, 0.1, 0.2)$.

Table 6.1: Parameter values for numerical simulations

Parameter	Description	Reported range	Default value
r	Intrinsic growth rate of healthy $CD4^{+}T$ cells	$0-10$ cells/mm^3	1.0 cells/mm^3
d	Natural death rate of healthy $CD4^{+}T$ cells	$0.0014-0.03$	0.017
β	Disease transmission coefficient	$0.00027-0.0007$ cells/virion	0.004 cells/virion
a	Total death rate of infected $CD4^{+}T$ cells	$0.3-0.49$	0.4
γ	Virus production rate due to cell lysis	$42-88$	42
ρ	Death rate of virus	$2-3$	2.5

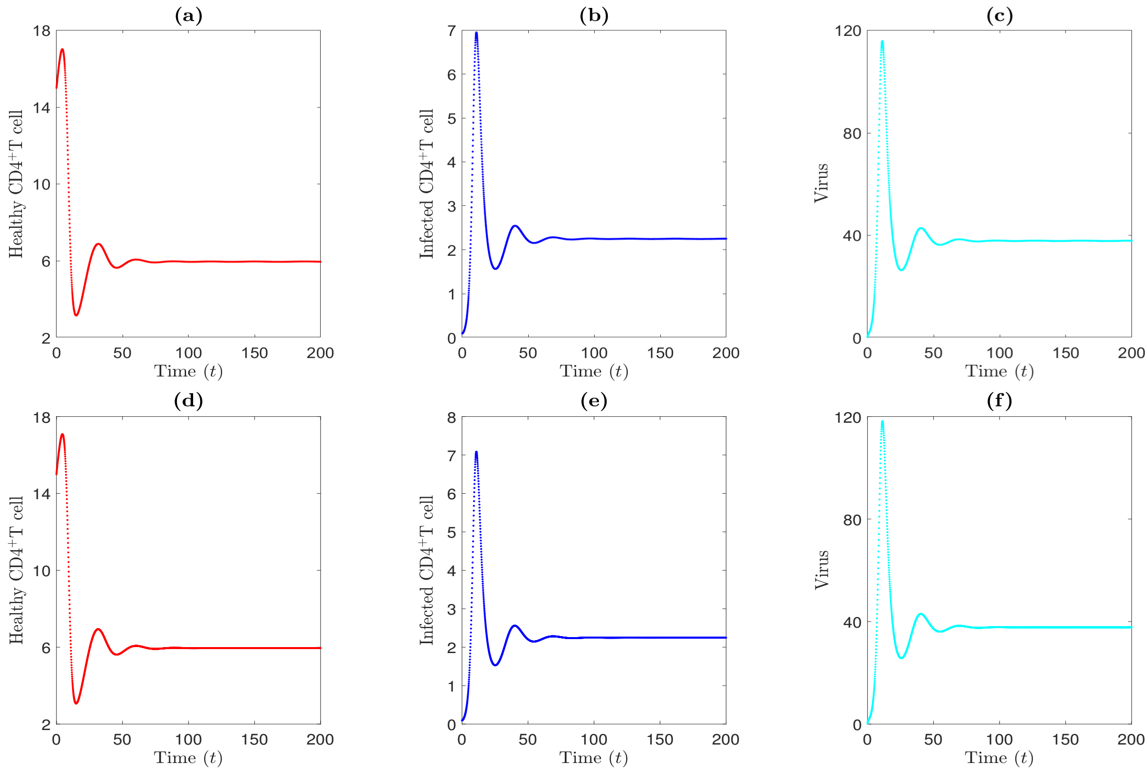

Figure 6.2: Time series of healthy $CD4^{+}T$ cell, infected $CD4^{+}T$ cell and virus populations of the continuous system (6.1) (first row) and the proposed discrete system (6.11) (second row). Here Figs. (**a**) and (**d**) are for healthy $CD4^{+}T$ cell population, Figs. (**b**) and (**e**) are for infected $CD4^{+}T$ cell population, and Figs. (**c**) and (**f**) are for virus population. Here $\Delta t = 0.0885$, $\Delta x = 0.1$ and the other parameters are remained the same as in Fig. 6.1.

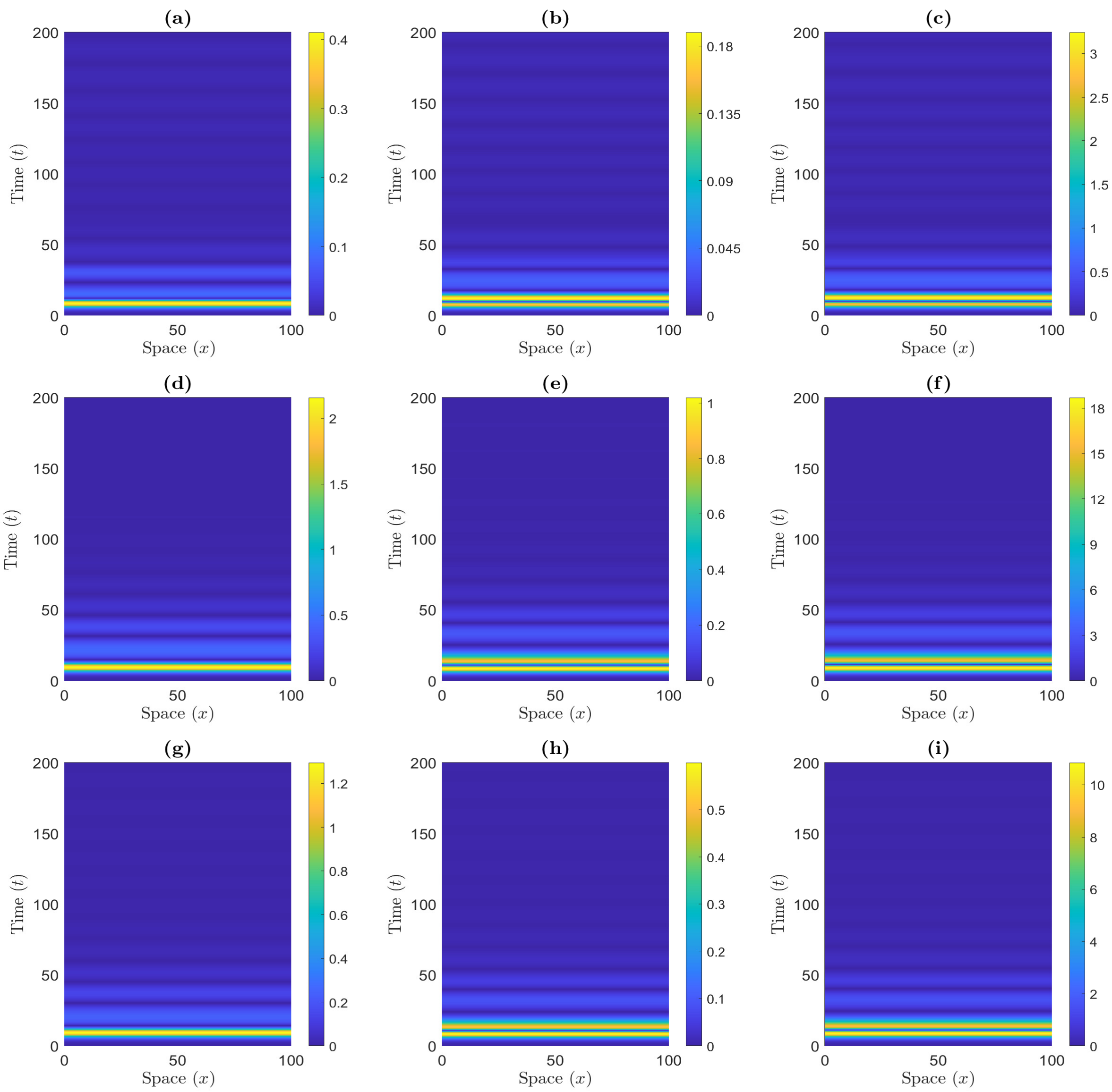

Figure 6.3: Heat maps of absolute error of the solutions obtained from the proposed NSFD discrete system (6.11) (first row), from the discrete system (6.2) with $\phi_i(\Delta t) = \Delta t$ for $i = 1,2$ (second row) and from the Crank-Nicolson discrete system (6.12) (third row). Here Figs. (**a**), (**d**) and (**g**) are for healthy CD4$^+$T cell solutions; Figs. (**b**), (**e**) and (**h**) are for infected CD4$^+$T cell solutions, and Figs. (**c**), (**f**) and (**i**) are for virus solutions. Parameters are $r = 1.0$, $d = 0.017$, $\beta = 0.004$, $a = 0.4$, $\gamma = 42$, $\rho = 2.5$, $D_1 = 0.015$, $D_2 = 0.015$, $D_3 = 0.015$ with the starting value $(15, 0.1, 0.2)$.

The performance of the suggested discrete system (6.11) and the discrete system (6.2) with $\psi_i(\Delta t) = \Delta t$, $i = 1,2,3$, are compared using the Crank-Nicolson scheme as a benchmark.

The corresponding Crank-Nicolson discretization of the continuous-time system (6.1) gives

$$\begin{aligned}
u_m^{n+1} &= u_m^n + \Delta t \Bigg[r - \frac{d}{2}(u_m^{n+1}+u_m^n) - \frac{\beta v_m^n}{2}(u_m^{n+1}+u_m^n) \\
&\quad + \frac{D_1}{2(\Delta x)^2}\left\{(u_{m+1}^{n+1}-2u_m^{n+1}+u_{m-1}^{n+1})+(u_{m+1}^n-2u_m^n+u_{m-1}^n)\right\}\Bigg], \\
w_m^{n+1} &= w_m^n + \Delta t \Bigg[\beta u_m^n v_m^n - \frac{a}{2}(w_m^{n+1}+w_m^n) \\
&\quad + \frac{D_2}{2(\Delta x)^2}\left\{(w_{m+1}^{n+1}-2w_m^{n+1}+w_{m-1}^{n+1})+(w_{m+1}^n-2w_m^n+w_{m-1}^n)\right\}\Bigg], \\
v_m^{n+1} &= v_m^n + \Delta t \Bigg[\gamma w_m^n - \frac{\rho}{2}(v_m^{n+1}+v_m^n) \\
&\quad + \frac{D_3}{2(\Delta x)^2}\left\{(v_{m+1}^{n+1}-2v_m^{n+1}+v_{m-1}^{n+1})+(v_{m+1}^n-2v_m^n+v_{m-1}^n)\right\}\Bigg].
\end{aligned} \tag{6.12}$$

In Fig. 6.3, we created heat maps of the absolute error of the numerical solutions obtained from the proposed NSFD discrete system (6.11) (first row), from the discrete system (6.2) with $\psi_i(\Delta t) = \Delta t,\ i = 1,2,3$, (second row), and from the Crank-Nicolson discrete system (6.12) (third row). This was done to show the excellent precision of the proposed NSFD scheme over the other schemes. The error in the estimates of the healthy $CD4^+T$ cell population is shown in the first column in Fig. 6.3 whereas the error in the estimates of the infected $CD4^+T$ cell population is shown in the second column, and the error in the estimates of the virus population is shown in the third column. The error peaks around $t = 9$ for all three discrete systems. For space, the absolute inaccuracy is constant, but for all the discrete systems, it varies with time. The colour bars of Fig. 6.3, show that the maximum absolute value of errors for healthy $CD4^+T$ cell solutions, infected $CD4^+T$ cell solutions, and virus solutions are 0.4102, 0.1891 and 3.2417, respectively, for the proposed NSFD system (6.11). It is also found that the same for the discrete system (6.2) with $\psi_i(\Delta t) = \Delta t,\ i = 1,2,3$, are 2.1573, 1.0193 and 18.6945, respectively. Also, the same for the Crank-Nicolson discrete system (6.12) are 1.2938, 0.5988 and 10.8339, respectively. Thus it becomes easy to observe that the error obtained from the recommended NSFD discrete system (6.11) is, nonetheless, substantially less than the error obtained from the other two discrete systems, as shown in Fig. 6.3.

6.5 Summary

In both population and disease dynamics, diffusion plays a very important role, which gives systems of partial differential equations. However, it is too tough to solve all these systems of PDEs analytically. That's why the discretization of continuous systems also became crucial to know the dynamics of those continuous systems. Unfortunately, the dynamics of the standard finite discrete systems are not the same as the dynamics of their corresponding continuous systems. The major reason for this drawback is the dependency of the discrete system's positivity and other dynamic properties on step-sizes. At this crossroad situation, the nonstandard finite discretization scheme becomes more essential. Unfortunately, till now this technique is not so much developed for the systems of partial differential equations. Although some researchers already have done some work to propose the NSFD discretization technique for systems of PDEs, some of them failed to show the discrete system positivity without any limitations on step-sizes or how to choose the denominator functions.

This study elaborated on the applicability of the nonstandard finite difference (NSFD) scheme in solving three-dimensional system of partial differential equations. In this work, we proposed an NSFD scheme, which is used to discretize a three-dimensional in-host HIV reaction-diffusion model, which is first-order accurate in time and second-order accurate in space; and also consistent. Especially it is also clearly shown how to choose the denominator functions for the NSFD discrete system so that its positivity is always maintained regardless of step-size or any other parameter restrictions. Premised on Fourier stability analysis or Von Neumann stability analysis a convergence analysis is presented. Also, the proposed NSFD system produces a lower absolute value of errors than the absolute value of errors obtained from the other two discrete systems, which is justified by the provided numerical simulations.

7

Discussions and future work

In the preceding chapters of this thesis for the system of ordinary differential equations (ODE), the standard finite difference schemes, like the Euler forward method, that we have proposed, exhibit dynamic behaviours that are not observed in the corresponding continuous system and demonstrate dynamic inconsistency. Specifically, the step-size affects the discrete systems' dynamics that are discretized using a conventional finite difference scheme. The discrete system's dynamics resemble those of its continuous counterpart when the step-size is tiny. But as the step-size rose, the discrete system displayed complicated dynamics like chaos that are not seen in its parent system. By building several discrete systems in accordance with the Non-Standard Finite Difference (NSFD) scheme, we have demonstrated the dynamic consistency of the discrete systems with their corresponding continuous systems. In contrast to other discrete systems discretized by standard finite difference schemes, it is also demonstrated that all solutions of the discrete system discretized by NSFD scheme stay positive for all possible initial values. We also provide some consistent rules to discretize the nonlinear terms in the case of the ODE system for the NSFD scheme. Additionally, we define the technique for constructing the denominator functions of the discrete system discretized by the NSFD scheme.

When dealing with a system of partial differential equations (PDE), we define a Non-Standard Finite Difference (NSFD) scheme that is accurate in both space and time, consistent for all step-sizes in both time and space, and positive for all positive initial values and positive step-sizes of the discretized system that the NSFD scheme discretizes. The proposed NSFD scheme exhibits Von Neumann stability. Furthermore, it is demonstrated that the discrete system solutions obtained through the suggested NSFD scheme exhibit a higher degree of accuracy to the continuous system solutions compared to the solutions obtained using the Euler discretization scheme and the Crank-Nicolson method. Although the NSFD scheme for the PDE system is positive, stable, accurate, and consistent with its corresponding continuous system, but the analytical part has not yet been fully developed because of the presence of the state variables at consecutive three space grid points on the right-hand side of the linearized discrete system. Our upcoming research will concentrate on the following subjects, among others:

- To propose a general rule for choosing non local approximation to get proper NSFD discrete system and develop the scheme analytically for reaction diffusion model.
- In almost every biological process, time delay occurs, this is why for mathematicians, it is more interesting to work on delayed biological systems. Also, in our upcoming work, we will try to discretize higher dimensional continuous systems in the presence of time delay.
- Recently, systems of fractional order differential equations have grabbed a lot of attention because they provide greater degrees of freedom than systems with integer orders. We intend to investigate the dynamic consistency of the NSFD discrete system of biological systems based on fractional order differential equations.

Bibliography

[1] X.-W. Jiang, X.-S. Zhan, Z.-H. Guan, X.-H. Zhang, L. Yu, Neimark–Sacker bifurcation analysis on a numerical discretization of Gause-type predator–prey model with delay, Journal of the Franklin Institute 352 (2015) 1–15.

[2] M. Peng, Bifurcation and chaotic behavior in the Euler method for a Kaplan–Yorke prototype delay model, Chaos, Solitons & Fractals 20 (2004) 489–496.

[3] J. Printems, On the discretization in time of parabolic stochastic partial differential equations, ESAIM: Mathematical Modelling and Numerical Analysis 35 (2001) 1055–1078.

[4] R. E. Mickens, Difference equation models of differential equations, Mathematical and Computer Modelling 11 (1988) 528–530.

[5] R. E. Mickens, Nonstandard finite difference models of differential equations, World Scientific, 1994.

[6] K. Hasan, M. Hama, Complex dynamics behaviors of a discrete prey–predator model with Beddington–DeAngelis functional response, International Journal of Contemporary Mathematical Sciences 7 (2012) 2179–2195.

[7] D. Wu, H. Zhang, Bifurcation analysis of a two-species competitive discrete model of plankton allelopathy, Advances in Difference Equations 2014 (2014) 1–10.

[8] M. Pal, Numerical analysis for scientists and engineers: theory and C programs, Alpha Science International, Limited, 2007.

[9] R. E. Mickens, Difference equation models of differential equations having zero local truncation errors, in: North-Holland Mathematics Studies, volume 92, Elsevier, 1984, pp. 445–449.

[10] R. E. Mickens, Exact solutions to a finite-difference model of a nonlinear reaction-advection equation: Implications for numerical analysis, Numerical Methods for Partial Differential Equations 5 (1989) 313–325.

[11] R. Anguelov, J. M.-S. Lubuma, Contributions to the mathematics of the nonstandard finite difference method and applications, Numerical Methods for Partial Differential Equations: An International Journal 17 (2001) 518–543.

[12] R. E. Mickens, Dynamic consistency: a fundamental principle for constructing nonstandard finite difference schemes for differential equations, Journal of Difference Equations and Applications 11 (2005) 645–653.

[13] Y. Li, Bifurcation analysis of a non-standard finite difference scheme for a time-delayed model of asset prices, Journal of Difference Equations and Applications 19 (2013) 507–519.

[14] R. J. Spiteri, M. C. MacLachlan, An efficient non-standard finite difference scheme for an ionic model of cardiac action potentials, Journal of Difference Equations and Applications 9 (2003) 1069–1081.

[15] S. Moghadas, M. Alexander, B. Corbett, A. Gumel, A positivity-preserving Mickens-type discretization of an epidemic model, Journal of Difference Equations and Applications 9 (2003) 1037–1051.

[16] M. Biswas, N. Bairagi, Discretization of an eco-epidemiological model and its dynamic consistency, Journal of Difference Equations and Applications 23 (2017) 860–877.

[17] M. Sekiguchi, E. Ishiwata, Global dynamics of a discretized SIRS epidemic model with time delay, Journal of Mathematical Analysis and Applications 371 (2010) 195–202.

[18] N. Bairagi, M. Biswas, Dynamic consistency in a predator–prey model with habitat complexity: Nonstandard versus standard finite difference methods, International Journal of Difference Equations 11 (2016) 139–162.

[19] M. Biswas, N. Bairagi, On the dynamic consistency of a two-species competitive discrete system with toxicity: Local and global analysis, Journal of Computational and Applied Mathematics 363 (2020) 145–155.

[20] L.-I. W. Roeger, G. Lahodny Jr, Dynamically consistent discrete Lotka–Volterra competition systems, Journal of Difference Equations and Applications 19 (2013) 191–200.

[21] G. Gabbriellini, Nonstandard finite difference scheme for mutualistic interaction description, International Journal of Difference Equations 9 (2014) 147–161.

[22] N. Bairagi, M. Biswas, A predator-prey model with Beddington-DeAngelis functional response: a non-standard finite-difference method, Journal of Difference Equations and Applications 22 (2016) 581–593.

[23] I. Darti, A. Suryanto, Stability preserving non-standard finite difference scheme for a harvesting Leslie–Gower predator–prey model, Journal of Difference Equations and Applications 21 (2015) 528–534.

[24] K. Manna, S. P. Chakrabarty, Global stability and a non-standard finite difference scheme for a diffusion driven HBV model with capsids, Journal of Difference Equations and Applications 21 (2015) 918–933.

[25] R. Mickens, A. Gumel, Numerical study of a non-standard finite-difference scheme for the Van der Pol equation [2], Journal of Sound and Vibration 250 (2002) 955–963.

[26] A. Mohsen, A simple solution of the Bratu problem, Computers & Mathematics with Applications 67 (2014) 26–33.

[27] K. C. Patidar, Nonstandard finite difference methods: recent trends and further developments, Journal of Difference Equations and Applications 22 (2016) 817–849.

[28] Q. Cui, Q. Zhang, Global stability of a discrete SIR epidemic model with vaccination and treatment, Journal of Difference Equations and Applications 21 (2015) 111–117.

[29] D. T. Dimitrov, H. V. Kojouharov, Nonstandard finite-difference schemes for general two-dimensional autonomous dynamical systems, Applied Mathematics Letters 18 (2005) 769–774.

[30] R. Anguelov, J. M.-S. Lubuma, Nonstandard finite difference method by nonlocal approximation, Mathematics and Computers in Simulation 61 (2003) 465–475.

[31] D. T. Dimitrov, H. V. Kojouharov, Positive and elementary stable nonstandard numerical methods with applications to predator–prey models, Journal of Computational and Applied Mathematics 189 (2006) 98–108.

[32] S. N. Elaydi, Discrete chaos: with applications in science and engineering, CRC Press, 2007.

[33] J. C. Strikwerda, Finite difference schemes and partial differential equations, SIAM, 2004.

[34] R. J. Plemmons, M-matrix characterizations. I—nonsingular M-matrices, Linear Algebra and its Applications 18 (1977) 175–188.

[35] L. Allen, An Introduction to Mathematical Biology (2007).

[36] H. H. Goldstine, J. Von Neumann, Numerical inverting of matrices of high order. II, Proceedings of the American Mathematical Society 2 (1951) 188–202.

[37] G. D. Smith, Numerical solution of partial differential equations: finite difference methods, Oxford University Press, 1985.

[38] G. G. O'Brien, M. A. Hyman, S. Kaplan, A study of the numerical solution of partial differential equations, Journal of Mathematics and Physics 29 (1950) 223–251.

[39] P. D. Lax, R. D. Richtmyer, Survey of the stability of linear finite difference equations, Communications on Pure and Applied Mathematics 9 (1956) 267–293.

[40] R. D. Richtmyer, Difference methods for initial-value problems, volume 4, Interscience Publishers, 1957.

[41] R. D. Richtmyer, E. Dill, Difference methods for initial-value problems, Physics Today 12 (1959) 50–50.

[42] R. E. Mickens, A nonstandard finite-difference scheme for the Lotka–Volterra system, Applied Numerical Mathematics 45 (2003) 309–314.

[43] A. Gumel, K. Patidar, R. Spiteri, Asymptotically consistent non-standard finite-difference methods for solving mathematical models arising in population biology, in: Advances in the Applications of Nonstandard Finite Difference Schemes, World Scientific, 2005, pp. 385–421.

[44] R. Anguelov, Y. Dumont, J.-S. Lubuma, M. Shillor, Dynamically consistent nonstandard finite difference schemes for epidemiological models, Journal of Computational and Applied Mathematics 255 (2014) 161–182.

[45] R. Anguelov, J. M.-S. Lubuma, M. Shillor, Dynamically consistent nonstandard finite difference schemes for continuous dynamical systems, in: Conference Publications, volume 2009, Conference Publications, 2009, pp. 34–43.

[46] R. Anguelov, J.-S. Lubuma, M. Shillor, Topological dynamic consistency of non-standard finite difference schemes for dynamical systems, Journal of Difference Equations and Applications 17 (2011) 1769–1791.

[47] J. B. Cole, High accuracy nonstandard finite-difference time-domain algorithms for computational electromagnetics: applications to optics and photonics, Advances in the Applications of Nonstandard Finite Difference Schemes (2005) 89–189.

[48] A. K. Verma, S. Kayenat, On the convergence of Mickens' type nonstandard finite difference schemes on Lane-Emden type equations, Journal of Mathematical Chemistry 56 (2018) 1667–1706.

[49] W. Dai, Nonstandard finite difference schemes for solving nonlinear micro heat transport equations in double-layered metal thin films exposed to ultrashort pulsed lasers, in: Advances in the Applications of Nonstandard Finite Difference Schemes, World Scientific, 2005, pp. 191–248.

[50] A. Appadu, Numerical solution of the 1D advection-diffusion equation using standard and nonstandard finite difference schemes, Journal of Applied Mathematics 2013 (2013).

[51] C. Tadmon, S. Foko, Modeling and mathematical analysis of an initial boundary value problem for hepatitis B virus infection, Journal of Mathematical Analysis and Applications 474 (2019) 309–350.

[52] C. Celik, Stability and Hopf bifurcation in a delayed ratio dependent Holling–Tanner type model, Applied Mathematics and Computation 255 (2015) 228–237.

[53] M. Lipsitch, M. A. Nowak, D. Ebert, R. M. May, The population dynamics of vertically and horizontally transmitted parasites, Proceedings of the Royal Society of London. Series B: Biological Sciences 260 (1995) 321–327.

[54] J. Holmes, W. Bethel, Modification of intermediate host behaviour by parasites, Behavioural Aspects of Parasite Transmission (1972).

[55] K. D. Lafferty, A. K. Morris, Altered behavior of parasitized killifish increases susceptibility to predation by bird final hosts, Ecology 77 (1996) 1390–1397.

[56] R. J. Villanueva, A. J. Arenas, G. González-Parra, et al., A nonstandard dynamically consistent numerical scheme applied to obesity dynamics, Journal of Applied Mathematics 2008 (2008).

[57] R. E. Mickens, Calculation of denominator functions for nonstandard finite difference schemes for differential equations satisfying a positivity condition, Numerical Methods for Partial Differential Equations: An International Journal 23 (2007) 672–691.

[58] R. E. Mickens, T. M. Washington, NSFD discretizations of interacting population models satisfying conservation laws, Computers & Mathematics with Applications 66 (2013) 2307–2316.

[59] K. J. O'Keefe, The evolution of virulence in pathogens with frequency-dependent transmission, Journal of Theoretical Biology 233 (2005) 55–64.

[60] T. Fayeldi, A. Suryanto, A. Widodo, Dynamical behaviors of a discrete SIR epidemic model with nonmonotone incidence rate, International Journal of Applied Mathematics and Statistics 47 (2013) 416–23.

[61] D. Xiao, S. Ruan, Global analysis of an epidemic model with nonmonotone incidence rate, Mathematical Biosciences 208 (2007) 419–429.

[62] J. Chattopadhayay, R. Sarkar, M. E. Fritzsche-Hoballah, T. C. Turlings, L.-F. Bersier, Parasitoids may determine plant fitness—a mathematical model based on experimental data, Journal of Theoretical Biology 212 (2001) 295–302.

[63] M. Yakıt Ongun, İ. Turhan, et al., A numerical comparison for a discrete HIV infection of CD4+ T-cell model derived from nonstandard numerical scheme, Journal of Applied Mathematics 2013 (2013).

[64] N. Shahid, M. A. Rehman, A. Khalid, U. Fatima, T. S. Shaikh, N. Ahmed, H. Alotaibi, M. Rafiq, I. Khan, K. S. Nisar, Mathematical analysis and numerical investigation of advection-reaction-diffusion computer virus model, Results in Physics 26 (2021) 104294.

[65] N. Ahmed, M. Rafiq, W. Adel, H. Rezazadeh, I. Khan, K. S. Nisar, Structure preserving numerical analysis of HIV and CD4+ T-cells reaction diffusion model in two space dimensions, Chaos, Solitons & Fractals 139 (2020) 110307.

[66] E. Kaslik, S. Sivasundaram, Non-existence of periodic solutions in fractional-order dynamical systems and a remarkable difference between integer and fractional-order derivatives of periodic functions, Nonlinear Analysis: Real World Applications 13 (2012) 1489–1497.

[67] H. El-Saka, E. Ahmed, M. Shehata, A. El-Sayed, On stability, persistence, and Hopf bifurcation in fractional order dynamical systems, Nonlinear Dynamics 56 (2009) 121–126.

[68] V. Volpert, S. Petrovskii, Reaction–diffusion waves in biology, Physics of Life Reviews 6 (2009) 267–310.

[69] N. Ahmed, A. Elsonbaty, A. Raza, M. Rafiq, W. Adel, Numerical simulation and stability analysis of a novel reaction–diffusion Covid-19 model, Nonlinear Dynamics 106 (2021) 1293–1310.

[70] W. E. Fitzgibbon, J. J. Morgan, B. Q. Tang, H.-M. Yin, Reaction-diffusion-advection systems with discontinuous diffusion and mass control, SIAM Journal on Mathematical Analysis 53 (2021) 6771–6803.

[71] I. R. Epstein, B. Xu, Reaction–diffusion processes at the nano-and microscales, Nature Nanotechnology 11 (2016) 312–319.

[72] B. Chakraborty, H. Baek, N. Bairagi, Diffusion-induced regular and chaotic patterns in a ratio-dependent predator–prey model with fear factor and prey refuge, Chaos: An Interdisciplinary Journal of Nonlinear Science 31 (2021).

[73] S. Chinviriyasit, W. Chinviriyasit, Numerical modelling of an SIR epidemic model with diffusion, Applied Mathematics and Computation 216 (2010) 395–409.

[74] W. Huang, M. Han, K. Liu, Dynamics of an SIS reaction-diffusion epidemic model for disease transmission, Mathematical Biosciences & Engineering 7 (2009) 51–66.

[75] T. Kuniya, J. Wang, Global dynamics of an SIR epidemic model with nonlocal diffusion, Nonlinear Analysis: Real World Applications 43 (2018) 262–282.

[76] P. Magal, G. F. Webb, Y. Wu, On the basic reproduction number of reaction-diffusion epidemic models, SIAM Journal on Applied Mathematics 79 (2019) 284–304.

[77] M. T. Hoang, A class of second-order and dynamically consistent nonstandard finite difference schemes for nonlinear Volterra's population growth model, Computational and Applied Mathematics 42 (2023) 85.

[78] P. Saha, N. Bairagi, G. N'Guerekata, Positivity and dynamics preserving discretization schemes for nonlinear evolution equations, Malaya Journal of Matematik 12 (2024) 1–20.

[79] M. E. Songolo, B. Bidégaray-Fesquet, Extending nonstandard finite difference scheme rules to systems of nonlinear ODEs with constant coefficients, Journal of Difference Equations and Applications (2024) 1–26.

[80] N. Ahmed, M. Ali, D. Baleanu, M. Rafiq, et al., Numerical analysis of diffusive susceptible-infected-recovered epidemic model in three space dimension, Chaos, Solitons & Fractals 132 (2020).

[81] S. A. Pasha, Y. Nawaz, M. S. Arif, On the nonstandard finite difference method for reaction–diffusion models, Chaos, Solitons & Fractals 166 (2023) 112929.

[82] M. A. Nowak, C. R. Bangham, Population dynamics of immune responses to persistent viruses, Science 272 (1996) 74–79.

[83] A. S. Perelson, A. U. Neumann, M. Markowitz, J. M. Leonard, D. D. Ho, HIV-1 dynamics in vivo: virion clearance rate, infected cell life-span, and viral generation time, Science 271 (1996) 1582–1586.

[84] D. D. Ho, A. U. Neumann, A. S. Perelson, W. Chen, J. M. Leonard, M. Markowitz, Rapid turnover of plasma virions and CD4 lymphocytes in HIV-1 infection, Nature 373 (1995) 123–126.

[85] D. Kirschner, G. F. Webb, A model for treatment strategy in the chemotherapy of AIDS, Bulletin of Mathematical Biology 58 (1996) 367–390.

[86] A. S. Perelson, D. E. Kirschner, R. De Boer, Dynamics of HIV infection of CD4+ T cells, Mathematical Biosciences 114 (1993) 81–125.

[87] P. K. Roy, N. Bairagi, J. Chattopadhyay, B. Chattopadhyay, HIV model with intracellular delay—a mathematical study, in: International Conference on Automation Science and Engineering, IEEE, 2009, pp. 373–378.

List of publications

Published

1. **Priyanka Saha**, Nandadulal Bairagi, and Milan Biswas. "On the dynamics of a discrete predator–prey model." *Trends in Biomathematics: Modeling, Optimization and Computational Problems, R. P. Mondaini (ed.), Springer Nature, Moscow* (2018): 219-232, https://doi.org/10.1007/978-3-319-91092-5_15.

2. **Priyanka Saha** and Nandadulal Bairagi. "Dynamics of Vertically and Horizontally Transmitted Parasites: Continuous vs Discrete Models." *International Journal of Difference Equations* (2018): vol. 13, no. 2, 139-156, http://campus.mst.edu/ijde.

3. **Priyanka Saha**, Nandadulal Bairagi, and Gaston N'Guerekata. "Positivity and dynamics preserving discretization schemes for nonlinear evolution equations." *Malaya Journal of Matematik* (2024): vol. 12, no. 1, 1-20, http://doi.org/10.26637/mjm1201/001.

Communicated

1. **Priyanka Saha** and Nandadulal Bairagi. “Nonstandard finite difference scheme for diffusion-induced ratio-dependent predator-prey model.”

2. **Priyanka Saha** and Nandadulal Bairagi. “Positivity preserving nonstandard finite difference scheme for an in-host HIV reaction-diffusion model.”